การคัดกรองแอมิโลมอลเทสกลายจาก *Corynebacterium glutamicum* เพื่อระบุกรดอะมิโนที่เกี่ยวข้องกับการสร้างไซโคลเดกซ์ทรินชนิดวงใหญ่

นายธนรัชต์ ปฐมสุนทรชัย

วิทยานิพนธ์นี้เป็นส่วนหนึ่งของการศึกษาตามหลักสูตรปริญญาวิทยาศาสตรมหาบัณฑิต
สาขาวิชาชีวเคมีและชีววิทยาโมเลกุล ภาควิชาชีวเคมี
คณะวิทยาศาสตร์ จุฬาลงกรณ์มหาวิทยาลัย
ปีการศึกษา 2558

SCREENING OF MUTATED *Corynebacterium glutamicum* AMYLOMALTASE TO IDENTIFY AMINO ACIDS INVOLVED IN LARGE-RING CYCLODEXTRIN FORMATION

Mr. Thanarat Pathomsoonthornchai

A Thesis Submitted in Partial Fulfillment of the Requirements
for the Degree of Master of Science Program in Biochemistry and Molecular Biology
Department of Biochemistry
Faculty of Science
Chulalongkorn University
Academic Year 2015

Thesis Title	SCREENING OF MUTATED *Corynebacterium glutamicum* AMYLOMALTASE TO IDENTIFY AMINO ACIDS INVOLVED IN LARGE-RING CYCLODEXTRIN FORMATION
By	Mr. Thanarat Pathomsoonthornchai
Field of Study	Biochemistry and Molecular Biology
Thesis Advisor	Assistant Professor Kuakarun Krusong, Ph.D.
Thesis Co-Advisor	Professor Piamsook Pongsawasdi, Ph.D.

Accepted by the Faculty of Science, Chulalongkorn University in Partial Fulfillment of the Requirements for the Master's Degree

.....Dean of the Faculty of Science
(Associate Professor Polkit Sangvanich, Ph.D.)

THESIS COMMITTEE

.....Chairman
(Assistant Professor Manchumas Prousoontorn, Ph.D.)
.....Thesis Advisor
(Assistant Professor Kuakarun Krusong, Ph.D.)
.....Thesis Co-Advisor
(Professor Piamsook Pongsawasdi, Ph.D.)
.....Examiner
(Assistant Professor Kanoktip Packdibamrung, Ph.D.)
.....External Examiner
(Associate Professor Jarunee Kaulpiboon, Ph.D.)

ธนรัชต์ ปฐมสุนทรชัย : การคัดกรองแอมิโลมอลเทสกลายจาก *Corynebacterium glutamicum* เพื่อระบุกรดอะมิโนที่เกี่ยวข้องกับการสร้างไซโคลเดกซ์ทรินชนิดวงใหญ่ (SCREENING OF MUTATED *Corynebacterium glutamicum* AMYLOMALTASE TO IDENTIFY AMINO ACIDS INVOLVED IN LARGE-RING CYCLODEXTRIN FORMATION) อ.ที่ปรึกษาวิทยานิพนธ์หลัก: ผศ. ดร. เกื้อการุณย์ ครูส่ง, อ.ที่ปรึกษาวิทยานิพนธ์ร่วม: ศ. ดร. เปี่ยมสุข พงษ์สวัสดิ์, 161 หน้า.

งานวิจัยนี้มีจุดมุ่งหมายในการคัดกรองแอมิโลมอลเทสกลาย เพื่อระบุกรดอะมิโนที่เกี่ยวข้องกับการสร้างไซโคลเดกซ์ทรินชนิดวงใหญ่ ในขั้นแรกทำการคัดกรองจากโคลนที่ทำการกลายยีนแบบสุ่มและการกลายยีนเฉพาะตำแหน่ง เพื่อค้นหาโคลนที่มีแอคทิวิตีของแอมิโลมอลเทสที่เหมาะสม จากนั้นจึงทำการคัดกรองโดยตรวจสอบรูปแบบผลิตภัณฑ์ไซโคลเดกซ์ทรินชนิดวงใหญ่ที่เปลี่ยนไป พบว่าแอมิโลมอลเทสกลาย 1E5, H5 และ E231Y ให้รูปแบบผลิตภัณฑ์ไซโคลเดกซ์ทรินชนิดวงใหญ่ที่เปลี่ยนไปเมื่อเทียบกับแอมิโลมอลเทสดั้งเดิม ในงานวิจัยนี้ เลือกแอมิโลมอลเทสกลาย E231Y ซึ่งกรดอะมิโนกลูทามิกที่ตำแหน่ง 231 ถูกกลายเป็นกรดอะมิโนไทโรซีน มาศึกษาต่อ โดยทำแอมิโลมอลเทสกลาย E231Y ให้บริสุทธิ์ด้วยคอลัมน์ DEAE FF™ และ Phenyl FF™ ตามลำดับ ได้ค่าแอคทิวิตีจำเพาะอยู่ที่ 29.8 ยูนิต/มิลลิกรัมโปรตีน และมีความบริสุทธิ์เพิ่มขึ้น 29.8 เท่า โดยมี %yield เป็น 5.84 แอมิโลมอลเทสกลาย E231Y มีอุณหภูมิที่เหมาะสมในการเร่งปฏิกิริยาอยู่ที่ 35 องศาเซลเซียสสำหรับปฏิกิริยา starch transglycosylation และ 45 องศาเซลเซียสสำหรับปฏิกิริยา disproportionation มี pH ที่เหมาะสมในการเร่งปฏิกิริยาอยู่ที่ pH 6.5 สำหรับทั้งสองปฏิกิริยา ในการตรวจสอบเสถียรภาพของแอมิโลมอลเทสกลาย E231Y ที่อุณหภูมิ และ pH ต่างๆ พบว่าเอนไซม์กลายมีความเสถียรที่คล้ายคลึงกับเอนไซม์ดั้งเดิม แอมิโลมอลเทสกลาย E231Y มีแอคทิวิตีของ disproportionation และ cyclization ที่สูงกว่าเอนไซม์ดั้งเดิม ในขณะที่แอคทิวิตี hydrolysis, coupling และ starch degradation ไม่ต่างจากแอมิโลมอลเทสดั้งเดิม จากการศึกษาจลนพลศาสตร์ของเอนไซม์พบว่า E231Y มีค่า k_{cat}/K_m ของปฏิกิริยา starch transglycosylation, disproportionation และ cyclization สูงกว่าแอมิโลมอลเทสดั้งเดิมทั้งหมด ในการสังเคราะห์ไซโคลเดกทรินซ์ชนิดวงใหญ่ พบว่าเมื่อใช้ปริมาณเอนไซม์และเวลาในการบ่มปฏิกิริยาเท่ากันที่ 12 ชั่วโมง แอมิโลมอลเทสกลาย E231Y ให้ผลิตภัณฑ์หลักเป็น CD22 ถึง CD24 ซึ่งมีขนาดเล็กลง เมื่อเทียบกับเอนไซม์ดั้งเดิมที่มีผลิตภัณฑ์หลักเป็น CD24 ถึง CD26 ซึ่งคาดว่าเกิดจากแอมิโลมอลเทสกลาย E231Y เร่งปฏิกิริยาการเปลี่ยนขนาดของไซโคลเดกซ์ทรินได้ในอัตราที่เร็วกว่าเอนไซม์ดั้งเดิม จากการวิเคราะห์ด้วยเทคนิค circular dichroism (CD) พบว่าโครงสร้างทุติยภูมิของแอมิโลมอลเทสกลายไม่แตกต่างไปจากแอมิโลมอลเทสดั้งเดิม จึงคาดว่ากรดอะมิโนกลูทามิกที่ตำแหน่ง 231 บนแอมิโลมอลเทสมีบทบาทในการกำหนดขนาดผลิตภัณฑ์ไซโคลเดกซ์ทรินชนิดวงใหญ่

ภาควิชา	ชีวเคมี	ลายมือชื่อนิสิต .....
สาขาวิชา	ชีวเคมีและชีววิทยาโมเลกุล	ลายมือชื่อ อ.ที่ปรึกษาหลัก .....
ปีการศึกษา	2558	ลายมือชื่อ อ.ที่ปรึกษาร่วม .....

5572816523 : MAJOR BIOCHEMISTRY AND MOLECULAR BIOLOGY
KEYWORDS: LARGE-RING CYCLODEXTRIN / AMYLOMALTASE

THANARAT PATHOMSOONTHORNCHAI: SCREENING OF MUTATED *Corynebacterium glutamicum* AMYLOMALTASE TO IDENTIFY AMINO ACIDS INVOLVED IN LARGE-RING CYCLODEXTRIN FORMATION. ADVISOR: ASST. PROF. KUAKARUN KRUSONG, Ph.D., CO-ADVISOR: PROF. PIAMSOOK PONGSAWASDI, Ph.D., 161 pp.

This research aims to screen for a mutated *Corynebacterium glutamicum* amylomaltase (*Cg*AM) with altered large-ring cyclodextrin (LR-CD) production profile in order to identify amino acid residues involved in LR-CD formation. Initially, random mutagenesis and site-directed mutagenesis clones were screened for acceptable *Cg*AM activity and subsequently screened for altered LR-CDs profiles. The result indicated that 1E5, H5 and E231Y *Cg*AMs displayed altered LR-CDs product profiles from that of the WT *Cg*AM. In this work, E231Y *Cg*AM, of which Glu-231 was substituted by Tyr, was selected for further investigation. E231Y *Cg*AM was successfully purified through DEAE FF™ and Phenyl FF™ column with the specific activity of 29.8 U/mg, purification fold of 29.8 and 5.84% yield. E231Y *Cg*AM displayed optimum temperature at 35°C and 45 °C on starch transglycosylation and disproportionation activity, respectively. The optimum pH of E231Y was pH 6.5 on both activities. Temperature and pH stability of E231Y was similar to that of the WT. In comparison to WT, E23Y *Cg*AM displayed higher disproportionation and cyclization activity but similar hydrolysis, coupling and starch degradation activity. E231Y *Cg*AM showed higher catalytic efficiency (k_{cat}/K_m) of starch transglycosylation, disproportionation and cyclization activities than WT *Cg*AM. At 12 hr incubation, E231Y *Cg*AM produced the principal CD of 22 to 24, while the principal CD of WT enzyme was 24 to 26. It seemed that E231Y was more effective on altering LR-CD product size than the WT. Circlular dichroism (CD) showed that there was no change in secondary structure of E231Y *Cg*AM. These results suggested that Glu-231 may play a role in LR-CDs formation.

Department:	Biochemistry	Student's Signature	.....
Field of Study:	Biochemistry and Molecular Biology	Advisor's Signature	.....
		Co-Advisor's Signature	.....
Academic Year:	2015		

ACKNOWLEDGEMENTS

Although I am responsible for this thesis in its entirety, without any helps from my thesis advisor, Assistant Professor Kuakarun Krusong, Ph.D., this thesis would not have been completed. All compositions of this thesis including its content, approach, possible shortcoming and effective guidance throughout the project, were brought under her careful attention in every single detail in this thesis. My thanks also extend to my thesis co-advisor, Professor Piamsook Pongsawasdi, Ph.D., for her kind assistance and effective encouragement.

My deep appreciation would go to the Department of Biochemistry, Faculty of Science, Chulalongkorn University and particularly to those of my colleagues, 705 members, 618 members and all alliances of the department who have advised me beneficial suggestions to improve and develop my knowledge, skills and background in Biochemistry and other related fields.

I would like to thank all those members serving as thesis committee; Assistant Professor Manchumas Prousoontorn, Assistant Professor Kanoktip Packdibamrung and Associate Professor Jarunee Kaulpiboon for their contributions on comments or any recommendations to this thesis.

Finally, my last deepest gratitude was dedicated to my family who makes me driven to be successful in my life. Their understanding, helping and supporting on everything will remind me to surpass amidst all those since the day I was born till the day of my graduation.

CONTENTS

Page

THAI ABSTRACT iv
ENGLISH ABSTRACT v
ACKNOWLEDGEMENTS vi
CONTENTS vii
LIST OF FIGURES xiii
LIST OF TABLES xvii
ABBREVIATIONS xviii
CHAPTER I INTRODUCTION 1
1.1 Starch and its composition 1
1.2 Overview of starch-modifying enzyme 3
1.2.1 Endo-acting enzyme 3
1.2.2 Exo-acting enzyme 4
1.3 4-α-glucanotransferase (4αCGTase); a member of α-amylase super family 7
1.4 Amylomaltase and its structure 8
1.4.1 Actions of amylomaltase 9
1.4.2 Topology of amylomaltase 11
1.4.3 Exploration of the active site 13
1.4.4 Catalytic residues 16
1.4.5 Secondary binding site 17
1.4.6 Unique 250s loop of AM 18
1.5 Large-ring cyclodextrins and their contemporary applications 22
1.6 Objectives 26
CHAPTER II MATERIALS AND METHODS 27
2.3.2 Disproportionation activity assay 32
2.3.3 Expression of WT and mutated *Cg*AM from library screening 32
2.3.4 Partial purification of *Cg*AM 33
2.3.4.1 Partial purification of WT CgAM 33

Page

2.3.4.2 Partial purification of mutated CgAM from library screening 34
2.3.5 LR-CDs synthesis 34
2.3.6 Analysis of LR-CDs product profile by High Performance Anion Exchange Chromatography with Pulse Amperometric Detection (HPAEC-PAD) 35
2.4 Screening for mutants with altered LR-CDs profiles from site-directed mutagenesis mutants 35
2.4.1 Expression of WT and mutated *Cg*AM constructed by site-directed mutagenesis 35
2.4.2 Partial purification of WT and mutated *Cg*AM 36
2.4.3 Synthesis of LR-CDs and Profile analysis 36
2.5 Identification of mutated amino acid residues involved in LR-CDs formation 37
2.5.1 Cell cultivating and *Cg*AM plasmid extraction 37
2.5.2 Restriction enzyme digestion 38
2.5.3 Agarose gel electrophoresis 38
2.5.4 Nucleotide sequencing 39
2.6 Optimization of mutated *CgAM* gene expression 39
2.7 Purification of WT and mutated *Cg*AM 40
2.7.1 Purification of WT *Cg*AM 40
2.7.2 Purification of mutated *Cg*AM 41
2.8 Enzyme assay 41
2.8.1 Starch transglycosylation activity 41
2.8.2 Starch degrading activity 42
2.8.3 Disproportionation activity 42
2.8.4 Cyclization activity 43
2.8.5 Hydrolysis activity 43
2.8.6 Coupling activity 44
2.9 Determination of protein concentration 45

Page

2.10 Polyacrylamide gel electrophoresis (PAGE) 45
2.10.1 SDS-Polyacrylamide gel electrophoresis (SDS-PAGE) 45
2.10.2 Staining with coomassie blue 45
2.11 Characterization of WT and mutated *Cg*AM 46
2.11.1 Effect of temperature on *Cg*AM activity 46
2.11.2 Effect of pH on *Cg*AM activity 46
2.11.3 Temperature stability of *Cg*AM 46
2.11.4 pH stability of *Cg*AM 47
2.11.5 Substrate specificity on disproportionation activity of *Cg*AM 47
2.11.6 Kinetic studies of *Cg*AM 48
2.11.6.1 Kinetic study of starch transglycosylation activity 48
2.11.6.2 Kinetic study of disproportionation activity 48
2.11.6.3 Kinetic study of cyclization activity 48
2.11.7 Effect of incubation time and unit of enzyme on LR-CDs production 49
2.11.7.1 Effect of incubation time 49
2.11.7.2 Effect of unit of enzyme 49
2.11.8 Secondary structure analysis by Circular dichroism (CD) spectrometer 50
CHAPTER III RESULTS 52
3.1 Screening for mutants with altered LR-CD profiles from random mutagenesis library 52
3.1.1 Disproportionation activity assay 52
3.1.2 Expression of selected *Cg*AMs 53
3.1.3 Partial purification of *Cg*AM 53
3.1.4 LR-CDs profiles by HPAEC-PAD 54
3.1.5 Identification of mutated amino acid residues 61
3.1.5.1 Extraction and restriction enzyme digestion of recombinant WT and mutated CgAM plasmid 61
3.1.5.2 Nucleotide sequencing 61

Page

3.2 Screening for mutants with altered LR-CD profiles from site-directed mutagenesis mutants 64
3.2.1 Expression and crude extract preparation of E231Y *Cg*AM 64
3.2.2 Partial purification of E231Y *Cg*AM 64
3.2.3 LR-CDs profile by HPAEC-PAD analysis 67
3.2.4.1 Extraction and restriction enzyme digestion of recombinant E231Y plasmid 69
3.2.4.2 Nucleotide sequencing 69
3.3 Expression and purification of WT and E231Y mutant 72
3.3.1 Optimization of E231Y *CgAM* gene expression 72
3.3.1.1 Expression of CgAM gene with 0.4 mM IPTG induction at 37°C 72
3.3.1.2 Expression of CgAM gene with 0.4 mM IPTG induction at 16°C 72
3.3.2 Scale-up of WT and E231Y *Cg*AM production and preparation of crude extracts 76
3.3.3 Partial purification of WT and E231Y *Cg*AM by DEAE FF™ column chromatography 76
3.3.4 Purification of *Cg*AMs by Phenyl FF™ column chromatography 77
3.3.4.1 Purification of WT CgAM 77
3.3.4.2 Purification of E231Y CgAM 77
3.3.5 Determination of enzyme purity of *Cg*AMs 78
3.4 Characterization of E231Y *Cg*AM 83
3.4.1 Effect of temperature on *Cg*AM activity 83
3.4.2 Effect of pH on *Cg*AM activity 85
3.4.3 Temperature stability of *Cg*AM 88
3.4.4 pH stability of *Cg*AM 88
3.4.5 Activities of *Cg*AM 90
3.4.5 Substrate specificity on disproportionation activity of *Cg*AM 92
3.4.6 Kinetic studies of *Cg*AM 94

Page

3.4.6.1 Kinetic study of starch transglycosylation activity 94
3.4.6.2 Kinetic study of disproportionation activity 94
3.4.6.3 Kinetic study of cyclization activity 95
3.4.7 Effect of incubation time and unit of enzyme on LR-CDs production 99
3.4.7.1 Effect of incubation time 99
3.4.7.2 Effect of unit of enzyme 100
3.4.8 Secondary structure analysis by Circular dichroism (CD) spectrometry 107
CHAPTER IV DISCUSSION 109
4.1 Screening for mutant with altered LR-CDs profile from random mutagenesis library 110
4.1.1 Screening by disproportionation activity assay 110
4.1.2 Expression and partial purification of WT and selected *Cg*AMs 110
4.1.3 Analysis of LR-CDs profiles 112
4.2 Screening for mutant with altered LR-CDs profiles from site-directed mutagenesis clones 113
4.2.1 Expression and purification of E231Y *Cg*AM 113
4.2.2 Analysis of LR-CDs profile of E231Y *Cg*AM 114
4.3 Expression and purification of WT and E231Y *Cg*AM 114
4.3.1 Optimization of E231Y *CgAM* gene expression 114
4.3.2 Purification of WT and E231Y *Cg*AMs 115
4.4 Characterization of E231Y *Cg*AM 117
4.4.1 Effect of temperature and pH on *Cg*AM activities 117
4.4.2 Effect of temperature and pH on *Cg*AM stability 117
4.4.3 *Cg*AM activities 118
4.4.4 Substrate specificity on disproportionation activity 119
4.4.5 Kinetic studies on *Cg*AM activities 120
4.4.6 Secondary structure of *Cg*AMs 120

Page

4.6.7 The influence of incubation time and unit of enzyme on LR-CDs production 121
CHAPTER V CONCLUSIONS 126
REFERENCES 129
APPENDICES 142
APPENDIX 1 Preparation of SDS-polyacrylamide gel electrophoresis (SDS-PAGE) 143
APPENDIX 2 Preparation of buffer for crude enzyme preparation 146
APPENDIX 3 Preparation of purification buffer 148
APPENDIX 4 Preparation of iodine solution 150
APPENDIX 5 Preparation of Bradford's solution 151
APPENDIX 6 Preparation of bicinchoninic acid reagent 152
APPENDIX 7 Preparation of DNS reagent 153
APPENDIX 8 Restriction map of pET-17b vector 154
APPENDIX 9 Standard curve for protein determination by Bradford's assay 155
APPENDIX 10 Standard curve for starch degradation activity assay 156
APPENDIX 11 Standard curve for glucose determination by glucose oxidase assay 157
APPENDIX 12 Standard curve for glucose determination by bicinchoninic acid assay 158
APPENDIX 13 Abbreviations (three letters and one letter) of amino acid residues found in protein 159
APPENDIX 14 Example of typical HPAEC profile 160
VITA 161

LIST OF FIGURES

Figure 1 Structures of amylose and amylopectin 2

Figure 2 Summary of starch-modifying enzymes 6

Figure 3 Four main actions of amylomaltase 10

Figure 4 Fold of amylomaltase from *Thermus aquaticus* 12

Figure 5 Schematic representation of the interaction of acarbose bound to the active site 14

Figure 6 Stereo images of structures representing different states during reaction cycle of amylomaltase 15

Figure 7 Superimposition of amylomaltase-acarbose complex 16

Figure 8 Schematic representation of the interactions of acarbose bound to the secondary binding site 18

Figure 9 Molecular surface of amylomaltase. The two acarbose molecules are shown in addition to two putative binding paths 20

Figure 10 Molecular surfaces of α-amylase isozyme, CGTase and amylomaltase.. 21

Figure 11 Structure of CD26 24

Figure 12 Purification profile of WT *Cg*AM by DEAE FF™ column chromatography 56

Figure 13 Purification profile of H5 *Cg*AM by DEAE FF™ column chromatography 57

Figure 14 Purification profile of 1E5 *Cg*AM by DEAE FF™ column chromatography 58

Figure 15 7.5% SDS-PAGE of crude and partially purified CgAMs. 59

Figure 16 LR-CDs production profile of WT, 1E5 and H5 amylomaltases, analyzed by HPAEC 60

Figure 17 Agarose gel electrophoresis of recombinant 1E5 and H5 plasmids 62

Figure 18 Amino acid sequence alignment of 1E5 and WT CgAMs using ClustalW tool 63

Figure 19 Purification profile of E231Y *Cg*AM by DEAE FF™ column chromatography 66

Figure 20 LR-CDs production profile of WT and E231Y *Cg*AMs, analyzed by HPAEC 68

Figure 21 Agarose gel electrophoresis of recombinant E231Y plasmids 70

Figure 22 Amino acid sequence alignment of E231Y and WT *Cg*AMs using ClustalW tool 71

Figure 23 7.5% SDS-PAGE of crude E231Y *Cg*AM obtained from 37°C cultivation, 0.4 mM IPTG induction at various times 74

Figure 24 7.5% SDS-PAGE of crude E231Y *Cg*AM obtained from 16°C cultivation, 0.4 mM IPTG induction at various times 75

Figure 25 Purification profile of WT *Cg*AM by Phenyl FF™ column chromatography 79

Figure 26 Purification profile of E231Y *Cg*AM by Phenyl FF™ column chromatography … 80

Figure 27 SDS-PAGE analysis of WT and E231Y *Cg*AM from each purification step 81

Figure 28 Effect of temperature on starch transglycosylation activity 84

Figure 29 Effect of temperature on disproportionation activity 84

Figure 30 Effect of pH on starch transglycosylation activity of E231Y *Cg*AM 86

Figure 31 Effect of pH on starch transglycosylation activity of WT *Cg*AM 86

Figure 32 Effect of pH on E231Y *Cg*AM disproportionation activity 87

Figure 33 Effect of pH on WT *Cg*AM disproportionation activity 87

Figure 34 Effect of temperature on E231Y *Cg*AM stability 89

Figure 35 Effect of pH on E231Y *Cg*AM stability 89

Figure 36 Substrate specificity of WT and E231Y *Cg*AMs on disproportionation activity 93

Figure 37 Lineweaver-Burk plot of WT and E231Y *Cg*AMs on starch transglycosylation activity 96

Figure 38 Lineweaver-Burk plot of WT and E231Y *Cg*AMs on disproportionation activity 97

Figure 39 Lineweaver-Burk plot of WT and E231Y *Cg*AMs on cyclization activity 98

Figure 40 HPAEC analysis of WT and E231Y LR-CDs profiles at different incubation times. 101

Figure 41 HPAEC analysis of LR-CDs profiles obtained by *Cg*AMs with 0.05, 0.1 and 0.15U of starch degradation activity 104

Figure 42 Circular dichroism (CD) spectra of WT and E231Y *Cg*AMs 108

Figure 43 Superimposition of *C. glutamicum* (*Cg*AM) and *T. aquaticus* (*Ta*AM) 124

Figure 44 Stereo views of the amylomaltase–acarbose complexs 125

LIST OF TABLES

Table 1 Applications of inclusion complex of LR-CDs to various guest compounds 25

Table 2 Summary of mutated amylomaltase clones, screened by glucose oxidase assay 53

Table 3 Purification Table of WT, 1E5 and H5 *Cg*AMs 55

Table 4 Purification Table of WT and E231Y *Cg*AMs 65

Table 5 Purification Table of WT and E231Y *Cg*AMs (optimized expression) ... 82

Table 6 Specific activities of WT and E231Y *Cg*AMs 91

Table 7 Summary of kinetic parameters of WT and E231Y *Cg*AMs on starch transglycosylation activity using glucose (G1) as receptor. 96

Table 8 Summary of kinetic parameters of WT and E231Y *Cg*AMs on disproportionation activity using maltotriose (G3) as substrate. 97

Table 9 Summary of kinetic parameters of WT and E231Y *Cg*AMs on cyclization activity using pea starch as substrate. 98

Table 10 Summary of principal CDs obtained under varying incubation times by *Cg*AMs carrying 0.05 U starch degradation activity 106

Table 11 Summary of principal CDs obtained under varying the amount of enzyme 106

Table 12 Estimation of *Cg*AMs' secondary structure composition, calculated by K2D3 program. 108

ABBREVIATIONS

A	absorbance
AM	amylomaltase
BSA	bovine serum albumin
°C	degree Celsius
CAs or CDs	cycloamyloses or cyclodextrins
Da	Dalton
DP	degree of polymerization
g	gram
4αGTase	4-α-glucanotransferase
GH	glycoside hydrolase
hr	hour
l	litre
LR-CDs	large-ring cyclodextrins
µg	microgram
µl	microlitre
M	molarity
mA	milliampere
min	minute
mg	milligram
ml	millilitre
mM	millimolar
MW	molecular weight

PAGE	polyarylamide gel electrophoresis
rpm	round per minute (revolution per minute)
SDS	sodium dodecyl sulfate
U	unit

CHAPTER I

INTRODUCTION

1.1 Starch and its composition

Starch is a naturally occurring polysaccharide that is widely distributed through many parts of plants; for instance, found in leaf, seed, fruit, stem and root. Rivaling in the amount to cellulose, starch is considered to be the second abundant on the Earth. It serves as the primary source of stored energy in living organisms. Most starch is composed of two major types of polysaccharides called 'amylose and amylopectin' (Figure 1). Amylose is a linear polymer comprised almost entirely of α-1,4-linked glucose monomers (Norisuye, 1994). Meanwhile, amylopectin, a predominant structure in most starch, is a branched polymer that contains both α-1,4-linked glucose monomers connected with α-1,6 linkage, indicating where a branch point is originated (Bertoft, 2015).

Because of 60 to 70% of the chief meal for humans made of starch, a large-scale production of starch industrial has been emerged. Starch is easily hydrolyzed to glucose and/or different oligosaccharide products by several processes and thereafter various starch-derivatized products are available in commonplace (van der Maarel *et al*., 2002). For example, a production of glucose syrups, high-fructose syrups, linear maltooligosaccharide with a wide range of average molecular weights, cyclomaltodextrins, D-sorbital and even the production of ethanol, acetic acid and other organic compounds. Nowadays, an alternative approach to modify starch is focusing on the use of starch-modifying enzyme instead (van der Maarel *et al*., 2002).

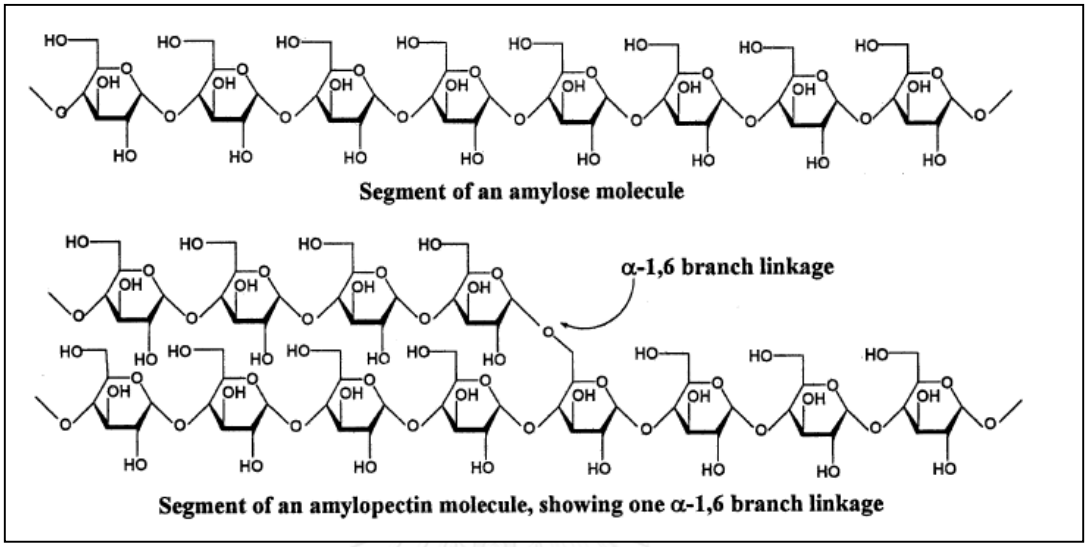

Figure 1 Structures of amylose and amylopectin (Robyt, 2008)

1.2 Overview of starch-modifying enzyme

Carbohydrate (starch) is well known to play crucial roles in myriad biological processes. The complexity of various oligosaccharide structures is derived from a rational enzymatic formation and breakdown of glycosidic bonds achieved by the action of starch degrading enzymes as shown by Figure 2 (Keeling and Myers, 2010, Horvathova *et al*., 2001, Kaper *et al*., 2004).

1.2.1 Endo-acting enzyme

The major type of enzymes that catalyzes directly on α-1,4-linkages of starch is α-amylase. This enzyme can be produced by several organisms including bacteria, fungi, plant, and animal. The α-amylase is an endo-acting enzyme, or is sometimes called liquefying enzyme, that cleaves the inside of starch polymer, resulting in a short chain of polymer. When the α-1,4-glycosidic linkages are hydrolyzed, a by-product of low molecular weight maltodextrin is usually obtained (Horvathova *et al*., 2001). A common misconception about the action of α-amylase is that it acts randomly, but this is rarely true. The major maltodextrin products are produced in uniformity of specific sizes, depending upon biological sources of the α-amylase. For instance, α-amylase of human produce maltose (G2), maltotriose (G3), maltotetraose (G4) (Dube SK. *et al*., 1962 and Robyt JF *et al*., 1967), and α-1,6-branched maltodextrins, ranging from four to seven glucose residues (Kainuma K. *et al*., 1970). Beside, another common misconception is that glucose is the major product. In fact, glucose is such a very minor product that is being produced by a slow hydrolysis of the primary products. For example, *Bacillus subtilis* α-amylase initially produces maltotriose (G3), maltohexaose (G6), and maltoheptaose (G7) as the major products. Glucose is produced via secondary

hydrolysis of the preceding G7 and G6 but not for G5 or smaller (Robyt JF *et al*., 1967). The other reports of α-amylase that are very similar to *B. subtilis* α-amylase are barley malt α-amylase (from plant) and *B. licheniformis* bacterial α-amylase (Maggregor *et al*., 1968 and Saito, 1973).

1.2.2 Exo-acting enzyme

Exo-acting enzymes exhibit unique property that is to act specifically at non-reducing end of starch, yielding maltodextrin or glucose products. A primary exo-acting amylase is β-amylase that is almost found in plants (Robyt, 1984). β-amylase catalyzes the hydrolysis of the glycosidic linkage from non-reducing-ends of starch chains, forming β-maltose. Apart from plant, β-amylases from other sources have been reported from *B. polymyxa* (Robyt, 1964) and *Streptomyces* sp., which were different in terms of products (Hikada *et al*., 1978). Glucoamylase, one of the exo-acting enzymes, hydrolyzes the first glycosidic linkage at the non-reducing end to give a glucose monomer. Glucoamylases isolated from several sources *Aspergillus niger, A. awamori, Rhizopus delemar,* and *R. niveus* have been reported (Pazur *et al*., 1959, Ueda *et al*. 1956, Savel'ev *et al*., 1982 and Hiromi *et al*., 1970). Another one is phosphorylase, which mainly involves in starch degradation in plants. Phosphorylase catalyzes on the α-1,4-linkage of the terminal glucose residue at the non-reducing to produce α-D-glucose-1-phosphate (Stetten *et al*., 1960). In case of α-1,6-glycosidic linkage, starch debranching enzyme (DE) can hydrolyze this linkage for further cleavage of the α-1,4-linkage by previously mentioned enzymes. Isoamylase also hydrolyzes the α-1,6-branch points of starch and it is first recognized in plants and first isolated from beans (Hobson et al., 1951 and Abe *et al*, 1999). *Pseudomonas amyloderamosa* isoamylase

has been characterized in the aim to study of amylopectin and related polysaccharide structure. In the past decades, starch lyase has been first discovered in red seaweeds and fungi. It functions to remove glucose residues at the non-reducing ends and subsequently converts them into 1,5-anhydro-D-fructopyranoses that are found to be a promising antioxidant and a building block for fine chemical synthesis (Anderson *et al*., 2002 and Lee *et al*., 2003).

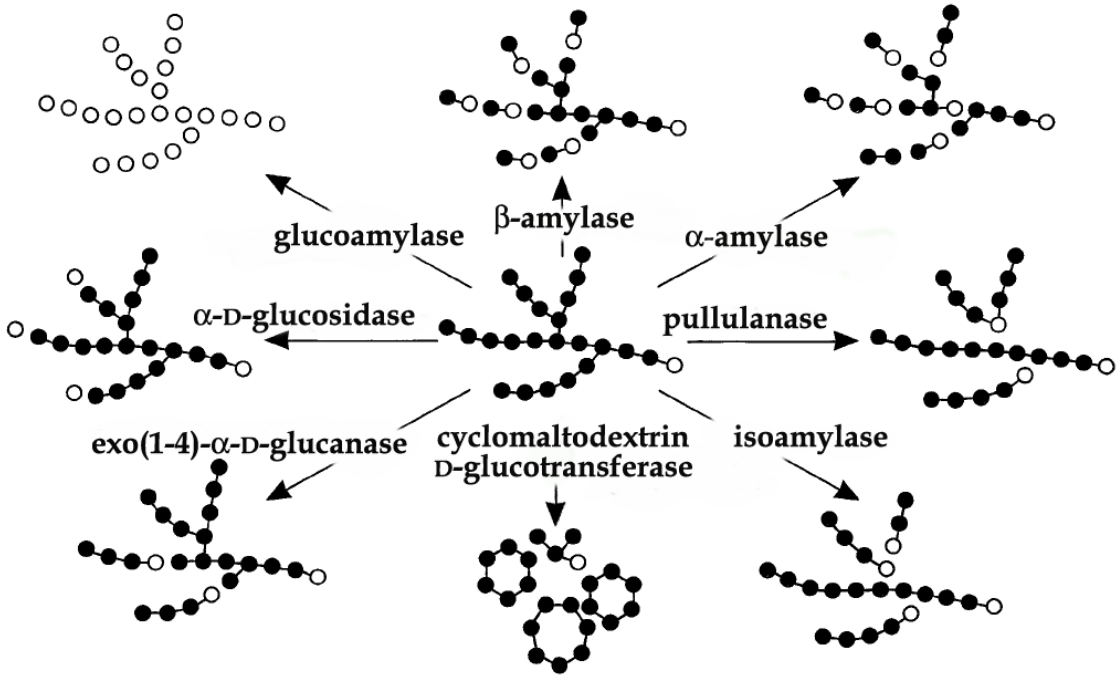

Figure 2 Summary of starch-modifying enzymes. The white and black circles represent the reducing and non-reducing sugars, respectively (Picture from Ismaya *et al*., 2012)

1.3 4-α-glucanotransferase (4αCGTase); a member of α-amylase super family

Another type of starch-modifying enzyme is a transferase group. For example, 4αCGTase, which is categorized to α-amylase super family (Henrissat, 1991, Henrissat et al., 1995), plays a role in breaking α-1,4-linkage and transferring that glucan moiety from donor to its acceptor (Takaha *et al*., 1998, Takaha and Smith, 1999, Kaper *et al*., 2005, Kaper *et al*., 2007). Transferase group can be divided into three types; (I) cyclodextrin glycosyltransferase (CGTase), (II) disproportionating enzyme (D-enzyme) or amylomaltase and (III) glycogen debranching enzyme (GDE). The major products of CGTase are cycloamyloses or cyclodextrins (CAs or CDs), a non-reducing α-1,4-linked maltodextrin, with degree of polymerization of 6 to 8. The C4–OH group of the non-reducing glucose residue of starch is attached to C1 of the sixth, seventh, and eighth glucose residues away from the non-reducing end. Several CGTases are elaborated by different species of bacteria. The first CGTase to be isolated was from *Bacillus macerans* and its major products was cyclomaltohexaose (CD6), with smaller amounts of cyclomaltoheptaose (CD7) and cyclomaltooctaose (CD8) (French *et al*., 1975). CGTases from *B. megaterium* and *B. circulans* primarily produce CD7 and *Brevibacterium* sp. CGTase produce CD8 as a major CD (Mora *et al*., 2012)

In addition, amylomaltase (AM), one type of the transferase enzymes, displays a similar reaction to CGTase but differs in terms of final products. AM forms large-ring cyclodextrins (LR-CDs) as major products while CGTase mainly produces small ring CDs (CD6 to CD8). By comparing to the CGTase, AM shows remarkably low hydrolysis activity (Takaha and Smith, 1999). In *Escherichia coli*, G3 is found to be the smallest substrate for AM while maltose (G2) has been reported as the smallest

substrate for D-enzyme (Palmer *et al*., 1976, Takaha and Smith, 1999). For detailed information on AM will be described in the next section.

1.4 Amylomaltase and its structure

AM is involved in maltodextrin transportation and utilization in *E. coli* (Monod and Torriani, 1950, Dippel and Boos, 2005). The maltodextrin-utilizing system includes phosphorylase, an enzyme that catalyze α-1,4-glycosidic linkage and related maltose transport proteins. AM initially catalyzes a conversion of short oligosaccharides to longer oligosaccharides, and thereafter phosphorylase break α-1,4-glycosidic linkage from non-reducing end of those oligosaccharides (Pugsley and Dubreuil, 1988). The constitution of maltodextrin utilization system is under *malPQ* operon. The other *MalPQ* operons are reported in *S. pneumonoae* (Nieto *et al*., 1997), *Klebsiella pneumonia*e (Kornacker *et al*., 1989) and *Clostridium butyricum* (Goda *et al*., 1997) as well. Apart from *malPQ* operon, glycogen operon is discovered in *Haemopphilus influenza* and *Aquifex aeolicus* (Fleischmann *et al*., 1995, Deckert *et al*., 1998) with the functions involved in glocogen synthesis and metabolism. The roles of AMs thus are varied depending upon organisms (Takaha and Smith, 1999).

1.4.1 Actions of amylomaltase

AM catalyzes both intermolecular and intramolecular transglycosylation reactions (Hwang *et al*., 2013). Four main reactions have been observed on AM; disproportionation, cyclization, coupling and hydrolysis activity as shown by Figure 3 (Takaha and Smith, 1999, van der Veen *et al*., 2000, Fujii *et al*., 2005, Kaper *et al*., 2005)

Disproportionation reaction is an activity to transfer a linear glucan moiety from donor to its acceptor, resulting in varying chain length oligosaccharide products.

Cyclization is an intermolecular transfer of a linear glucan to produce a cyclic oligosaccharide called ‘cyclodextrins or cyloamyloses’ (CDs or CAs).

Coupling activity is a reverse reaction of cyclization in which CDs are hydrolyzed and transferred to the acceptor, producing long linear oligosaccharides.

Hydrolysis activity refers to a hydrolysis of starch without any receptors. Notably, AM displayed a very low hydrolysis activity and coupling activity comparing to CGTase.

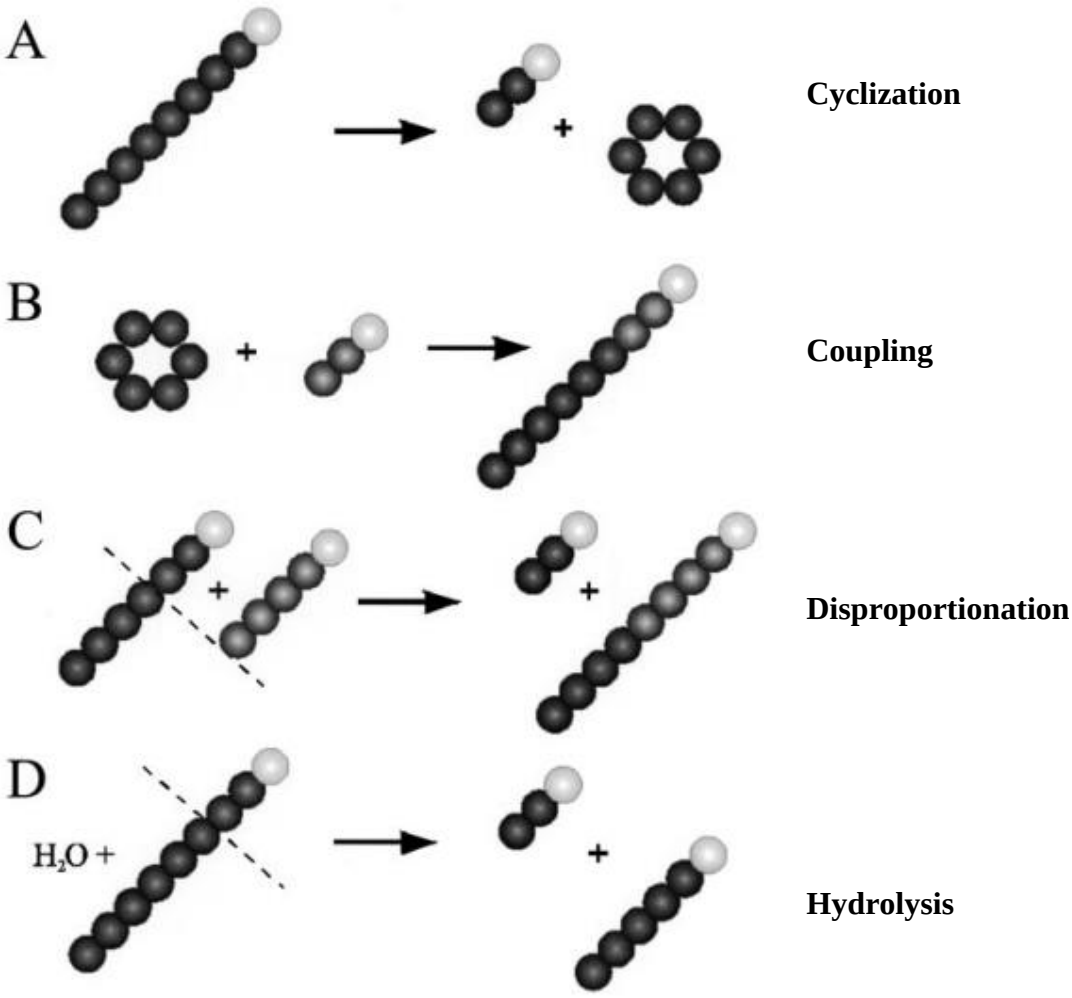

Figure 3 Four main actions of amylomaltase (van der Veen *et al*., 2000)

1.4.2 Topology of amylomaltase

AM structure comprises two major domains, ‘domain A and B’. AM contains several insertions between the core $(\alpha/\beta)_8$-barrel which is called ‘subdomain A’ (Jespersen *et al*., 1993). Notably, the substrate binding site is located nearly the insertions around C terminal side of the barrel. These insertions are subdivided into three subdomains (subdomain B1, B2 and B3), aiming to facilitate comparison among related enzymes. Subdomain B1 corresponds to domain B of related family-13 α-amylase enzymes. The core of this domain is structured by an insertion between the third and fourth barrel strand. Meanwhile, an insertion between the second and third barrel strand is observed in CGTase instead. By comparing among related enzymes, AM reveals an extra insertion between the second and third barrel strand which is called ‘subdomain B2’. Subdomain B2 is suggested to be unique in AM due to the fact that this subdomain is apparently presented in AM and D-enzyme, but not for α-amylase and CGTase. In addition, AM is absent in C-terminal domain C that is normally presented among all other members of the α-amylase superfamily. The result from superimposition of CGTase and amylase indicated that subdomain B3 of AM is located at nearly the exact position as domain C in other enzymes and may play a similar role. The structure of subdomain B3 consists of insertion linked between the first and second strand and seventh and eighth barrel strand (Przylas *et al*., 2000a, Fujii *et al.*, 2005). The topology of AM from *thermus aquaticus* is depicted as shown by Figure 4 (Przylas *et al*., 2000a)**.**

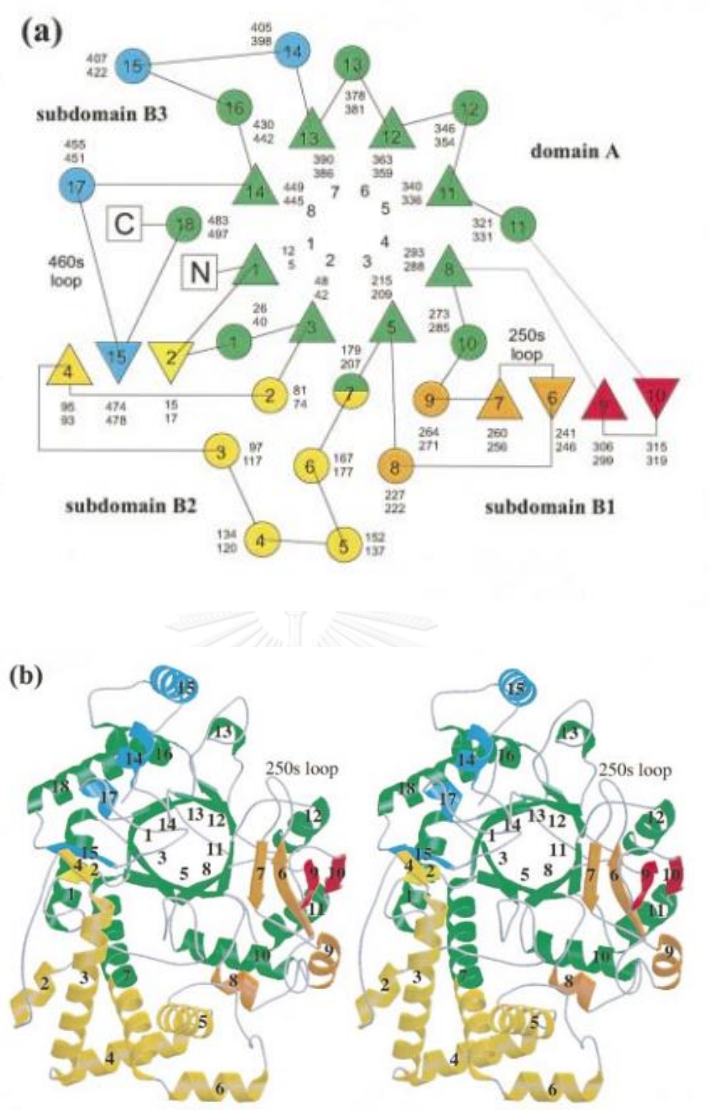

Figure 4 Fold of amylomaltase from *Thermus aquaticus*. (a) Topography diagram; β-strands are indicated by triangles, helices are marked by circles. The first and last residue numbers of each secondary structure are shown. (b) Ribbon representation; numbers (1–8) are eighth barrel strand, $(\beta/\alpha)_8$ barrel core structure (subdomain A) is coloured in green, insertions between the first and fifth strand of the barrel (subdomain B2 and B1) are painted in a gradient going from yellow to red. Additional small insertions are shown in blue (subdomain B3). (Przylas *et al*., 2000a)

1.4.3 Exploration of the active site

A striking difference from that of family-13 enzymes is that AM displays altered binding sites with acarbose (substrate analog), changing from subsite -1 and +1 to -3 to +1 (Figure 5) (Cockburn *et al*., 2014). As has been analyzed by 3D structure, there are two different observations when compared to other related enzymes. Firstly, Asp-293 of *Thermus aquaticus* AM (*Ta*AM), which functions mainly in the nucleophilic attack at C1 (carbon atom position 1) of the substrate in family-13 enzymes, is not positioned to interact with the substrate in the first time. Then, Asp-293 can form hydrogen bonding to Arg-291 and Asp-213 to promote covalent intermediate formation with acarbose (Figure 6). Secondly, Glu-340 of AM is bound to O1, O2 and O3 (oxygen atom position 1, 2 and 3) of the glucose unit at the reducing end. This residue is bound to O4 of the scissile bond of CGTase (Kuriki and Imanaka, 1999). Therefore, the positions of those two catalytic residues are not suited with respect to their catalytic functions. However, the binding mode of acarbose to subsites +1 to −3 is in agreement with the location of the cleavage sites of potato D-enzyme on maltotetraose substrate (Walker and Whelan, 1959).

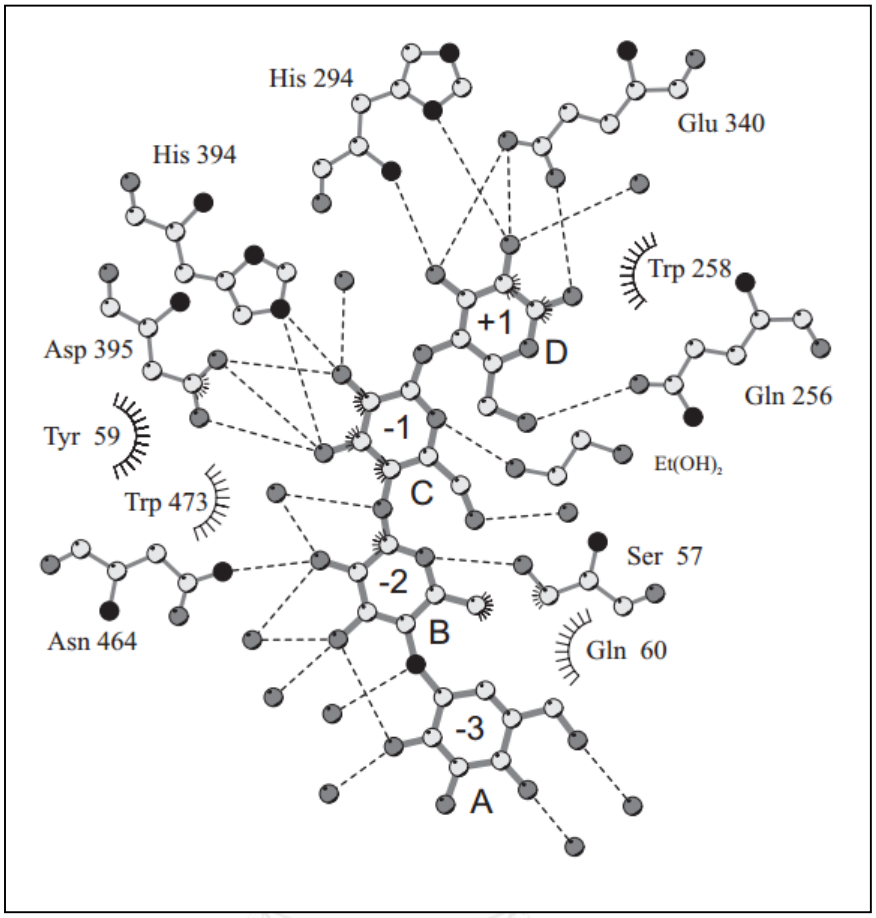

Figure 5 Schematic representation of the interaction of acarbose bound to the active site. Hydrogen bonds are represented by dash lines (picture from Strater *et al*., 2002)

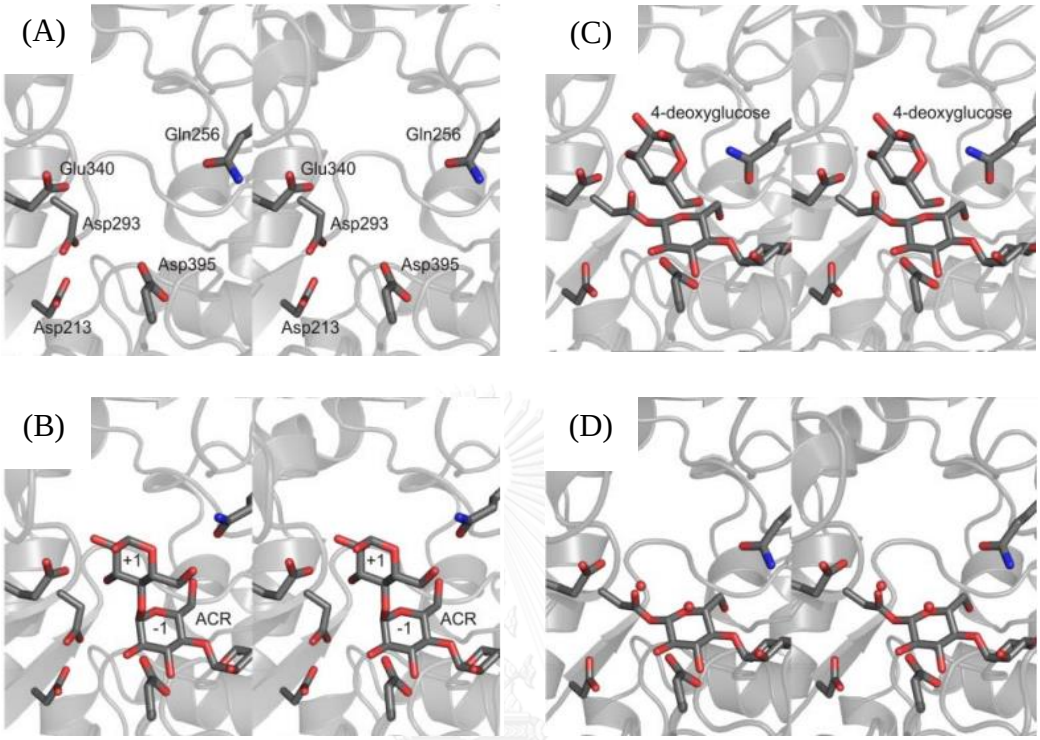

Figure 6 Stereo images of structures representing different states during reaction cycle of amylomaltase (A) An empty active site (B) Initial amylomaltase-acarbose complex (C) Covalent intermediate formation with acarbose. Asp-293 points into the active site (D) Covalent intermediate formation with acarbose. Possible hydrolytic water molecules are indicated as spheres (Barends *et al*., 2007)

1.4.4 Catalytic residues

The superimposition of the catalytic site of AM, comparing to CGTase and amylase reveals that seven residues are conserved and located under similar orientation in these superimposed structures; the three catalytic residues Asp-293, Glu-340 and Asp-395 and residues Tyr-59, Asp-213, Arg-291 and His-394. These seven residues, regardless of Tyr-59, build up the catalytic cleft of AM. Tyr-59 is the only amino acid residue that is not occurred on the four conserved motifs of family 13 (Nakamura *et al*., 1994). Based upon sequence comparisons, His-122, which is conserved among other family members, is not conserved in AM.

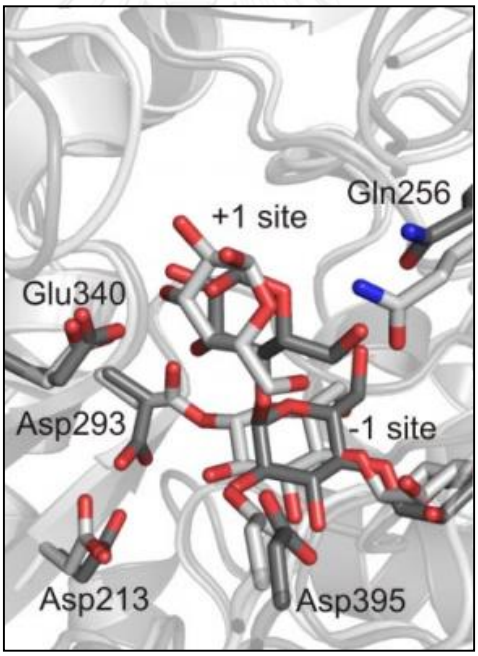

Figure 7 Superimposition of amylomaltase-acarbose complex. The pictures show three conserved catalytic residues, Asp-293, Glu-340 and Asp-395 (Barends *et al*., 2007)

1.4.5 Secondary binding site

A surprising observation on AM from *Thermus aquaticus* (*Ta*AM) is that a second acarbose molecule is found in a groove close to the active site called ‘second binding glucan site’ (Figure 8). The distance between these sites is about 14 ˚A far away the active site. Hydrophobic interaction is the main interaction that participates in the conformation and binding of the inhibitor; Tyr-54 with glucose unit B and of Tyr-101 with unit C of acarbose (Haga *et al*., 2003, Watanasatitarpa *et al*., 2014). It is observed that the second acarbose displays fewer interactions as compared to the acarbose bound to the catalytic site. In contrast to the conserved residues located within the active site, Tyr-54 and Tyr-101 are not well-conserved among reported AMs or D-enzymes. Despite unpredictably conserved residues, the amino acid sequence around Tyr-54 shows a pattern with several glycines and two conserved prolines (PLGPTGYGDSP). This secondary binding site is proposed to help the formation of cycloamylose.

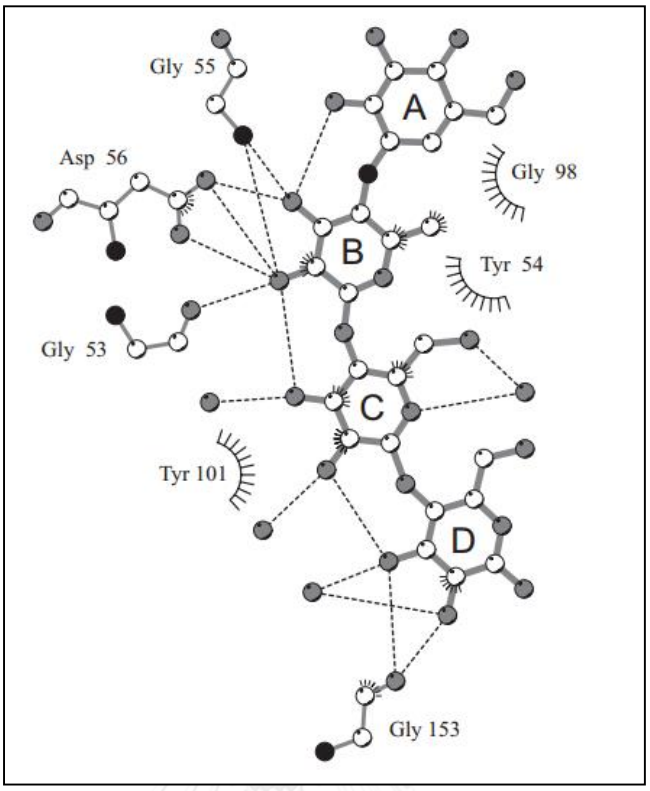

Figure 8 Schematic representation of the interactions of acarbose bound to the secondary binding site (picture from Starter *et al*., 2002).

1.4.6 Unique 250s loop of AM

The 250s loop (residue 247 to 255), a highly conserved structure of subdomain B1 in AM, is a long extended loop protruding out of a cleft covering the active site groove (Figure 9) (Jung *et al*., 2011). Two hydrophobic residues, Tyr-250 and Phe-251, are located at the tip of the loop. Those residues can maintain their flexibility of the loop both with and without acarbose. This loop is highly conserved among AMs. It mainly involves in substrate binding and dissociation of products. When LR-CDs product wraps 250s loop during cyclization activity, the ring size may be restricted to about 18 residues by this loop. In addition, the 460s loop was found and its function

was to help restrict the formation of small ring LR-CDs product (Przylas *et al*., 2000a). Molecular surfaces of α- amylase, CGTase and AM has been compared as shown by Figure 10. Alpha-amylase has a relatively open active-site cleft, which is formed by residues of domains A and B. In CGTase, domain B forms a part of the active site pocket. Tyr-195 of *Bacillus circulans* CGTase has been proposed to favor the synthesis of cyclodextrins by forming non-polar core (Nakamura *et al*., 1994, Uitdehaag *et al*., 1999). Trp258 in *Thermus brokianus* AM, proposed to be Tyr-195 in CGTase, can interact with the substrate analog bound to the active site by forming hydrophobic contacts to the glucose residue bound to subsite +1.

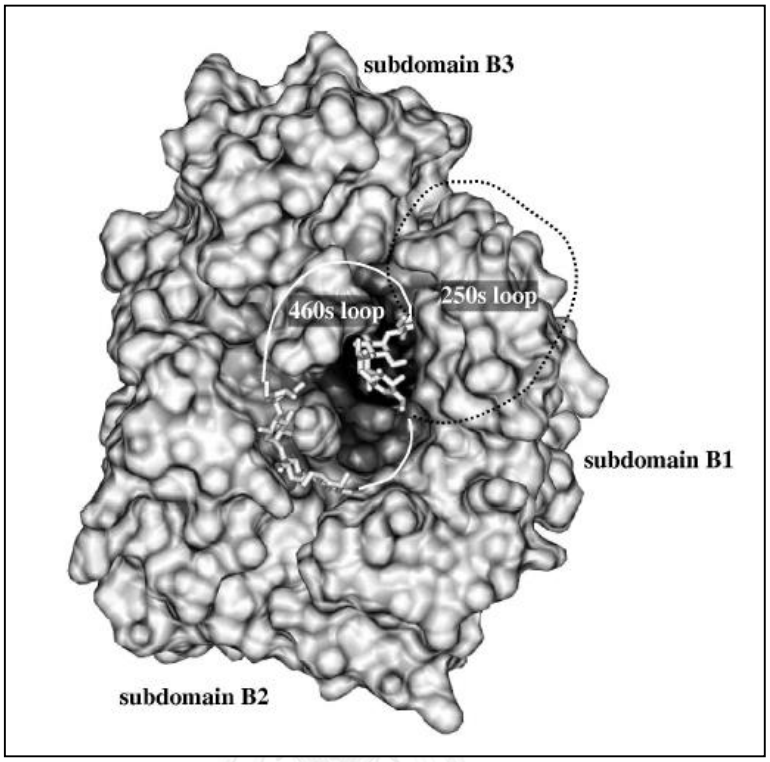

Figure 9 Molecular surface of amylomaltase. The two acarbose molecules are shown in addition to two putative binding paths (picture from Strater *et al*., 2002).

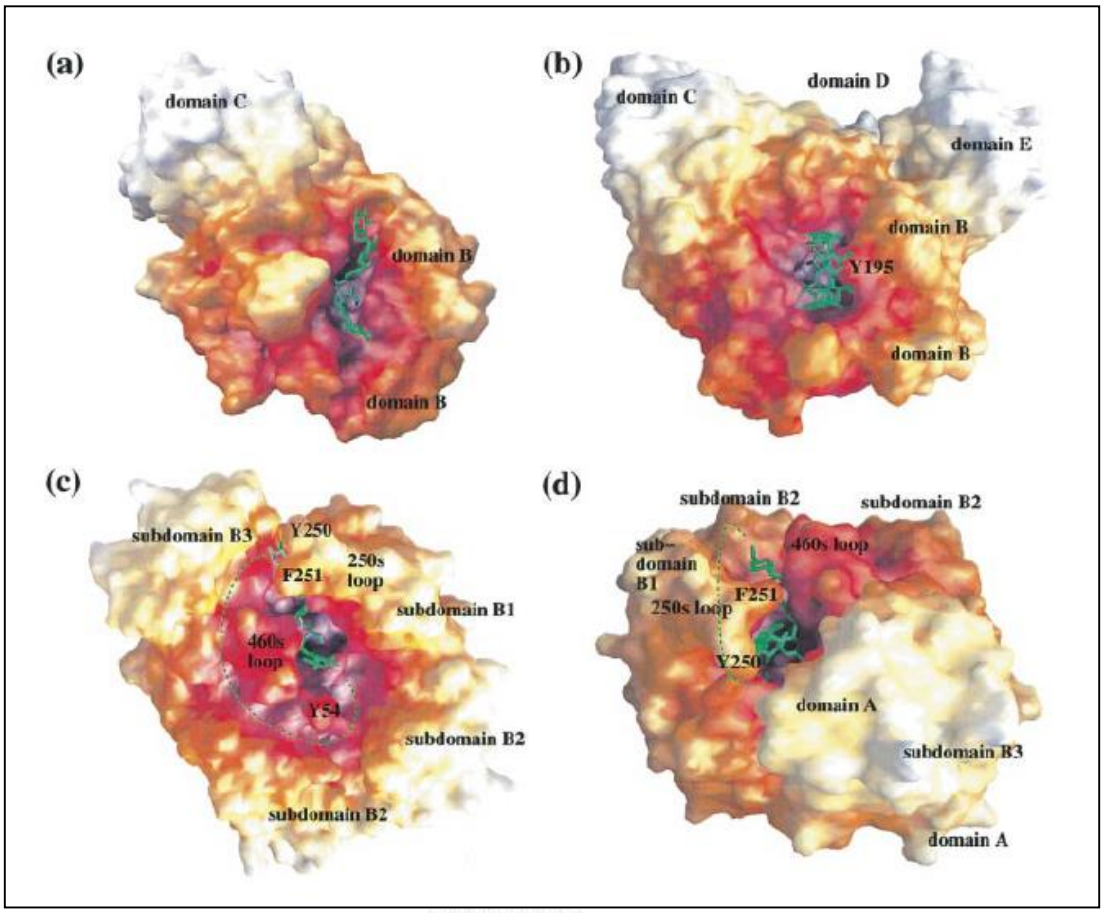

Figure 10 Molecular surfaces of (a) α-amylase isozyme II of porcine pancreas in complex with a maltohexaose (b) CGTase from *Bacillus circulans* strain 8 complexed with β-cyclodextrin (c), (d) Amylomaltase from *Thermus aquaticus* with a modeled binding mode of maltohexaose. The surfaces are colored according to the distance away from the center of mass (from red to white). The bound inhibitors are shown in green. Possible binding paths for cycloamylose production of amylomaltase are indicated as dash green lines in (c) and (d). The locations of two loops, the 250s loop and the 460s loop are also labeled. The active center of amylomaltase is located at the center of the modeled oligosaccharide in (c) and (d) (Przylas *et al*., 2000b).

1.5 Large-ring cyclodextrins and their contemporary applications

Large-ring cyclodextrins (LR-CDs) are cyclic oligosaccharides, comprising at least 9 units of glucose monomers to more than a hundred units linked by α-1,4-glycosidic linkage (Terada *et al*., 1997, Taira *et al*., 2006, Srisimarat *et al*., 2011). The degree of polymerization (DP) varies depending on the production sources. For example, the minimum DP is DP17 in *E. coli*, DP 22 in *T. aquaticus*, DP 17 in D-enzyme of plant potato and DP19 in *Corynebcterium glutamicum* (Takaha and Smith, 1999, Taira *et al*., 2006, Srisimarat *et al*., 2012). LR-CDs form a hydrophobic core that can help improve solubility and stability of various guest molecules, in particular, hardly dissolved compounds. LR-CDs also form hydrophilic outside; thus, they exhibit higher solubility in water (Przylas *et al*., 2000a, Larsen, 2002, Taira *et al*., 2006, Miyazawa *et al*., 1995). Each CD displays different shapes. For instance, a boat-shaped shape (CD9), a butterfly-like structure (CD10 and CD14) and two single helices with 13 monomer units each in antiparallel direction (CD26) (Figure 11). Due to their distinct structural features from the small CDs, LR-CDs are suggested as promising alternative compounds in molecular recognition processes (Kobayashi, 1993, Ivanov and Jaime, 2004). Because of the low yields and the difficulty in purification from CD mixtures, only a few of them have been successfully characterized (Endo *et al*., 1995)

At first, CD9 was used in pharmaceutical field, aiming to enhance solubility of drugs, spironolactone and digoxin (Miyazawa *et al*., 1995). CD9-C_{70} (Buckminster fullerene) complex is also prepared and its solubility is successfully improved. Besides, a mixture of LR-CDs has been considerably interested in recent years, since the use of LR-CD mixture (CD22 to CD45 or larger than CD50) as an artificial chaperone for protein refolding was achieved (Machida et al., 2000, Sasaki and Akiyoshi, 2010). They

are able to pull detergents out and then help refold the denatured proteins to their native states. In 2003, LR-CDs mixture successfully refolded denatured antibody to correct active structure (Machida *et al*., 2000). Tomono *et al*. evaluated the interactions between mixtures of LR-CDs (CD20 to CD50) with prednisolone, cholesterol, digoxin, digitoxin and nitroglycerin, using the solubility method (Tomono *et al*., 2002). Although nitroglycerin did not interact with the mixture of LR-CDs, the solubilities of prednisolone, cholesterol, digoxin and digitoxin were successfully improved. For enhancement of cholesterol solubility, use of LR-CDs mixture is reported as the highest effective method comparing to those previous reports on β and γ-CDs.

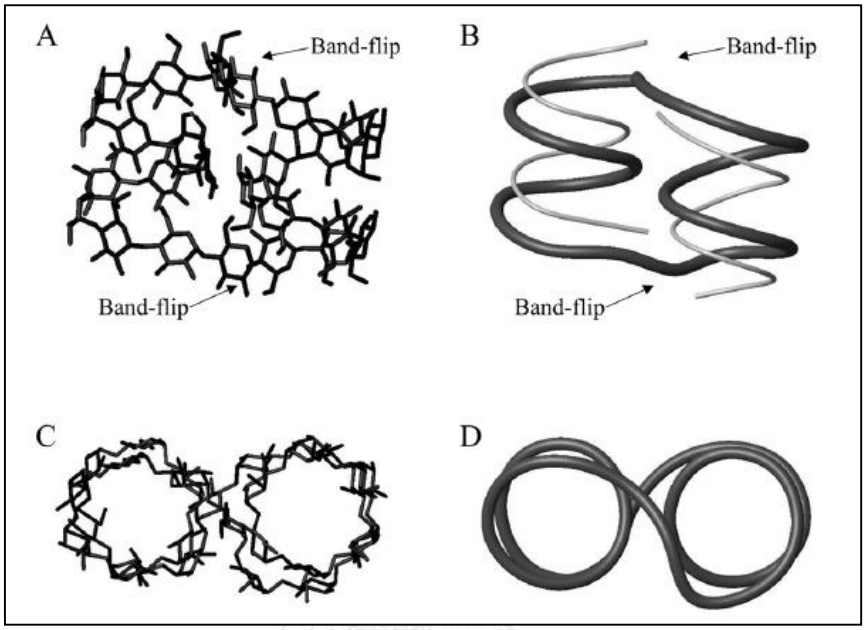

Figure 11 Structure of CD26 (A) CD26 with the band flip positions (B) CD26 represented in tube structure (C) Top view of CD26 (D) Top view of CD26 represented in tube structure (Larsen, 2002)

Table 1 Applications of inclusion complex of LR-CDs to various guest compounds

CD	Compound
CD9	Anthracene Amphotericin Ajmalicine Ajmaline Carbamazepine Digitoxin Spironolactone
CD9 – CD13	Benzoate 2-Methyl benzoate 3-Methyl benzoate 4-Methyl benzoate 2,4-Dimethyl benzoate 2,5-Dimethyl benzoate
CD14 – CD17	Salicylate 4-tert-Butyl benzoate Ibuprofen anion
CD21 – CD32	8-Anilino-1-naphthalene sulfonic acid 1-Octanol 1-Butanol

1.6 Objectives

1. To screen for mutated *corynebacterium glutamicum* amylomaltase (*Cg*AM) with altered large-ring cyclodextrins (LR-CDs) product profile from that of the wild-type

2. To identify amino acid residue involved in LR-CDs formation

3. To characterize the mutated *Cg*AM in the aim to understand the effect of mutated residue towards LR-CDs formation.

CHAPTER II

MATERIALS AND METHODS

2.1 Equipments and Instruments

Autoclave (Model H-88L, KokusanEnsinki Co., Ltd., Japan)

Autopipette (Pipetman, Gilson, France)

Centrifuge (refrigerated centrifuge) (Avanti model J30-11, Beckman Inc., USA)

Electrophoresis unit :

- Mini protein, Bio-Rad, USA
- Agarose gel electrophoresis, Bio-Rad, USA

FPLC AKTA (Amersham Pharmacia Biotech Unit, USA)

- Chromatographic columns : DEAE FF™ and HiPrep Phenyl FF™
- Detector : UPC-900
- Pump : P-920
- Fraction collector : Frac-900

Gel document (SYNGEND, England)

HPAEC DX-600 (Dionex Corp., Sunnydale, USA)

- Column : Carbopac PA-100™ 4 x 250 mm
- Pulsed Amperometry Detector (PAD) : DIONEX ED40
- Autosampler : DIONEX AS40
- Column oven : DIONEX ICS-3000 SP

Incubator :

- Model M20S, Lauda, Germany and BioChiller 2000, FOTODYNE Inc., USA

- Model ISOTEMP 210, Fisher Scientific, USA

Incubator shaker (Innova™ 4080 New Brunswick Scientific Co., Ltd., England)

Laminar flow (HT123, ISSCO, USA)

Magnetic stirrer (Model Fisherbrand, Fisher Scirntific, USA)

Membrane filter (polyethersulfone (PES), pore size 0.45 µm, Whatman, England)

Microcentrifuge (1.5 ml Eppendorf, Germany)

pH meter (Model PHM95, Radiometer Copenhagen, Denmark)

Peristaltic pump (Pump P-1, GE Healthcare Bio-Scientific AB, Sweden)

Power supply (Model POWER PAC 300, Bio-Rad, USA)

Shaking waterbath (Model G-76, New Brunswick Scientific Co., Inc., USA)

Sonicator (Bendelin, Germany)

Spectrophotometer :

- Biomate 3, Thermo scientific, USA
- DU Series 650, Beckman, USA

Vortex (Model K-550-GE, Scientific Industries, Inc., USA)

2.2 Chemicals

Acrylamide (Merck, Germany)

Agar (Merck, Germany)

Agarose (SEKEM LE Agarose. FMC Bioproducts, USA)

Ammonium persulphate (Sigma. USA)

Ammonium sulphate (Carlo EarbaReagenti, Italy)

Ampicilin (Sigma, USA)

L-aspartic acid (Fluka, Switzerland)

Bovine serum albumin (BSA) (Sigma, USA)

Boric acid (Merck, Germany)

Casein hydrolysate (Merck, Germany)

Coomassie brilliant blue G-250 (Sigma, USA)

Coomassie brilliant blue R-250 (Sigma, USA)

4,4'-Dicarboxy-2,2'-biquinoline (Sigma, USA)

Dimethyl sulfoxide (DMSO) (Merck, Germany)

di-Potassium hydrogen phosphate anhydrous (Carlo Earba Reagenti, Italy)

1 kb DNA ladder™ (New England BioLabs Inc., USA and Fermentus, Canada)

Ethidium bromide (Sigma, USA)

Ethylene diaminetetraacetic acid (EDTA) (Merck, Germany)

Glacial acetic acid (Carlo Earba Reagenti, Italy)

Glucose (BDH, England)

Glucose liquicolor (Glucose oxidase kit) (Humana, Germany)

Glycerol (Merck, Germany)

Glycine (Sigma, USA)

Hydrochloric acid (Carlo Earba Reagenti, Italy)

Iodine (Baker chemical, USA)

Isopropyl β-D-1-thiogalactopyranoside (IPTG) (Sigma, USA)

Maltoheptaose (Wako Pure Chemical Industries, Japan)

Maltohexaose (Wako Pure Chemical Industries, Japan)

Maltopentaose (Wako Pure Chemical Industries, Japan)

Maltose (BDH, England)

Maltotetraose (Wako Pure Chemical Industries, Japan)

Maltotriose (Wako Pure Chemical Industries, Japan)

β-Mercaptoethanol (Fluka, Switzerland)

N,N'-Methylene-bis-acrylamide (Sigma, USA)

N,N,N',N'-Tetramethyl-1,2-diaminoethane (TEMED) (Carlo Earba Reagenti, Italy)

Pea starch (Emsland-Starke GmbH, Germany)

Peptone (Scharlau microbiology, Spain)

Phenol (Fisher Scientific, England)

Phenylmethylsulfonyl fluoride (PMSF) (Sigma, USA)

Plasmid mini kit (Geneaids Biotech Ltd., Taiwan)

Potassium iodide (Mallinckrodt, USA)

Potassium phosphate monobasic (Carlo Earba Reagenti, Italy)

Sodium acetate (Merck, Germany)

Sodium carbonate anhydrous (Carlo EarbaReagenti, Italy)

Sodium chloride (Carlo EarbaReagenti, Italy)

Sodium citrate (Carlo EarbaReagenti, Italy)

Sodium dodecyl sulfate (Sigma, USA)

Sodium hydroxide (Merck, USA)

Soluble starch (Potato) (Scharlau microbiology, Spain)

Standard LR-CDs (Ezaki Glico Co., Ltd., Japan)

Standard protein marker (Amersham Pharmacia Biotech Inc., USA)

Tris (hydroxymethyl)-aminomethane (Carlo EarbaReagenti, Italy)

Tryptone (Scharlau microbiology, Spain)

Yeast extract (Scharlau microbiology, Spain)

2.3 Screening for mutants with altered LR-CDs profiles from random mutagenesis library

2.3.1 Cell cultivation and crude extract preparation of WT and mutated *Cg*AM from random mutagenesis library

A single colony of wild-type (WT) and mutated *Cg*AM clones, constructed by PCR-mediated random mutagenesis, were cultured in 500 µl LB medium (1% (w/v) tryptone, 0.5% (w/v) yeast extract and 0.5% (w/v) sodium chloride) containing 100 µg/ml of ampicilin at 37 °C with 250 rpm shaking for overnight (16-18 hr). One percent (v/v) starter inoculum was transferred into 3 ml of LB medium with 100 µg/ml of ampicilin and cultivated further until OD_{600} reached 0.4 to 0.6. After that, IPTG was added to the final concentration of 0.4 mM. Cells were harvested after 2 hr IPTG induction via centrifugation at 6,000 x g for 10 min. Cells were washed by 0.85% NaCl and extraction buffer (50 mM potassium phosphate buffer, pH 7.4 containing 0.1 mM PMSF, 0.01% β-mercaptoethanol and 1.0 mM EDTA), and then resuspended (1 g per 2.5 ml) with the same extraction buffer. Crude extracts were obtained after cell disruption via sonication (21% power for 1 min with pulse-on 1 sec and pulse-off 2 sec, repeated for 2 cycles). Removal of cell debris was performed by centrifugation at 12,000 x g for 10 min. The supernatant was ready for disproportionation activity assay.

2.3.2 Disproportionation activity assay

Disproportionation activity was determined by glucose oxidase assay, measuring the amount of free glucose in the reaction (Sols and De La Fuente, 1957, Sols and De La Fuente, 1958). This assay was an enzymatic oxidation to determine glucose content from the reaction

$$\text{glucose} + O_2 + H_2O \rightarrow \text{gluconic acid} + H_2O_2$$

$$2H_2O_2 + \text{4-aminophenazone} \rightarrow \text{quinoneimine} + 4H_2O$$

When glucoses were presented, the reaction color became dark pink. Twenty microliters of crude enzyme was incubated with 30 µl of 5% maltotriose (G3) at 40°C for 10 min and terminated by adding 30 µl of 1 N HCl. After that, 920 µl of glucose oxidase reagent was added and incubated for 10 minutes at 30°C. The reaction mixture was suddenly measured at A_{505}. The mutated clones that contained residual disproportionation activity at least 80% of the wild-type enzyme's, were selected for further experiment.

2.3.3 Expression of WT and mutated *Cg*AM from library screening

Single isolated colonies of WT and the mutants that harbored acceptable disproportionation activity from section 2.3.2 were cultivated overnight (16-18 hr) in 5 ml of LB medium supplemented with 100 µg/ml ampicilin at 37°C, 250 rpm shaking. Five milliliters of overnight culture was transferred into 500 ml of LB medium containing 100 µg/ml of ampicilin and continued shaking at 37°C, 250 rpm shaking. Expression of WT or mutated *Cg*AM was induced by adding IPTG to the final concentration of 0.4 mM. When OD_{600} of cell culture reached 0.4 to 0.6, cells were

collected at 2 hr after IPTG induction, and then washed with 0.85% NaCl and extraction buffer, respectively. Harvested cells were resuspended with the same extraction buffer and then subjected to cell disruption. Sonication was performed with the power of 30% for 1 min, pulse-on 1 sec and pulse-off 2 sec, repeated for 10 cycles. Cell debris was removed via centrifugation at 12,000 x g for 1 hr to obtain the crude extract. The supernatant was first dialyzed against 50 mM phosphate buffer pH 7.4 and then subjected to enzyme partial purification.

2.3.4 Partial purification of *Cg*AM

2.3.4.1 Partial purification of WT *Cg*AM

Crude extract from section 2.3.3 was partially purified by DEAE FF™ column chromatography, an anion exchanger, using FPLC AKTA instrument. Before applying the crude extract onto DEAE FF™ column. DEAE FF™ column was first equilibrated with 50 mM phosphate buffer pH 7.4 containing 0.01% β-mercaptoethanol with the constant flow rate of 1 ml/min for at least 5 column volumes. Crude enzyme was loaded onto the column and the column was washed with the same buffer until A_{280} reached the baseline level. Bound proteins were eluted by a step gradient of 0.2 M, 0.3 M and 1.0 M of NaCl in 50 mM phosphate buffer pH 7.4. Fractions of 2 ml were collected throughout elution steps. The fractions carrying starch transglycosylation activity (as described in section 2.8.1) were pooled and dialyzed against 50 mM phosphate buffer pH 7.4.

2.3.4.2 Partial purification of mutated *Cg*AM from library screening

Column was equilibrated as described in section 2.3.4.1. A linear gradient in a range of 0 to 1.0 M of NaCl was applied onto the column and fractions of 2 ml were collected. The fractions that contained starch transglycosylation activity of amylomaltase (assay described in section 2.8.1) were pooled and dialyzed against 50 mM phosphate buffer. When an appropriate NaCl concentration required for mutated *Cg*AM elution was determined, a step-wise elution was also done instead of a linear gradient elution.

2.3.5 LR-CDs synthesis

LR-CDs synthesis was performed in 1 ml of reaction mixture comprising 100 µl of 0.2% pea starch, 0.05 U starch degrading activity (mean of assay can be seen in section 2.8.2) of partially purified enzyme from section 2.3.4and the rest was 50 mM phosphate buffer pH 6.0. The reaction was incubated at 30°C with150 rpm of shaking for 6 hr. The reaction was stopped by boiling for 10 min. To assure that the residual linear oligosaccharides were completely digested, 4 U of glucoamylase (Fluka, Switzerland) was added to the reaction mixture and incubated overnight at 40°C, and inactivated by boiling for 10 min. LR-CDs profiles were analyzed by High Performance Anion Exchange Chromatography with Pulse Amperometric Detection (HPAEC-PAD) analysis.

2.3.6 Analysis of LR-CDs product profile by High Performance Anion Exchange Chromatography with Pulse Amperometric Detection (HPAEC-PAD)

LR-CDs products were analyzed by HPAEC-PAD (Koizumi *et al*., 1999). The model instrument ICS 3000 system (DIONEX, USA) was used with Carbopac-PA 100 column (4 x 250 mm). Column was first equilibrated with 150 mM sodium hydroxide. A sample of 110 µl was injected into the column and it was then performed a linear gradient elution of 200 mM sodium nitrate with the constant flow rate of 1 ml/min under these following steps (Srisimarat *et al*. 2011); (1) 0-2 min, increasing from 4% to 8% sodium nitrate; (2) 2-10 min, increasing from 8% to 18% sodium nitrate; (3) 10-20 min, increasing from 18% to 28% sodium nitrate; (4) 20-40 min, increasing from 28% to 35% sodium nitrate; (5) 40-55 min, increasing from 35% to 45% sodium nitrate, and (6) 55-60 min, increasing from 45% to 63% sodium nitrate

The size of LR-CDs was determined by comparing to the standard LR-CDs (Ezaki, Japan). If a mutant carried altered LR-CDs profile according to a criterion for mutant candidates, then that mutant was selected for further experiment.

2.4 Screening for mutants with altered LR-CDs profiles from site-directed mutagenesis mutants

2.4.1 Expression of WT and mutated *Cg*AM constructed by site-directed mutagenesis

A single colony, both WT and mutant clone, was cultured overnight (16-18 hr) in 5 ml of LB medium containing 100 µg/ml ampicilin at 37°C, 250 rpm shaking. One percent (v/v) inoculum of overnight culture was transferred into 500 ml of LB medium

containing 100 µg/ml of ampicilin and cell cultivating was continued at 37°C, 250 rpm shaking. When OD_{600} of cell culture reached 0.4 to 0.6, IPTG was introduced to the final concentration of 0.4 mM to induce an expression of *Cg*AM. Cells were collected at 2 hr after IPTG induction, and then washed with 0.85% NaCl and extraction buffer, respectively. Cells were resuspended with the same extraction buffer. Cell Sonication was performed with 30% power for 1 min - pulse-on 1 sec and pulse-off 2 sec - repeated for 10 cycles. The debris was removed via centrifugation at 12,000 x g for 1 hr. The supernatant was then dialyzed against 50 mM phosphate buffer pH 7.4 before subjecting to enzyme partial purification.

2.4.2 Partial purification of WT and mutated *Cg*AM

Crude extract of WT and mutated *Cg*AM prepared from section 2.4.1 were subjected to partial purification prior to use for LR-CDs synthesis. Partial purification approach could be followed as described in section 2.3.4.1 for WT *Cg*AM and section 2.3.4.2 for mutated *Cg*AM. Those partially purified enzymes were dialyzed against 50 mM phosphate buffer pH 7.4.

2.4.3 Synthesis of LR-CDs and Profile analysis

LR-CDs products were synthesized by mean of method from section 2.3.5 using the dialyzed proteins obtained from section 2.4.2. Then, the LR-CDs mixture was analyzed by HPAEC-PAD, process described in section 2.3.6, in order to investigate the LR-CDs profiles. If the mutated *Cg*AM exemplified an altered LR-CDs product

pattern, it was then subjected to identify amino acid residue which was considered to be a key residue in determining LR-CDs product pattern.

2.5 Identification of mutated amino acid residues involved in LR-CDs formation

2.5.1 Cell cultivating and *Cg*AM plasmid extraction

A single colony of recombinant *E. coli* BL21 (DE3), a clone possessed mutated *Cg*AM that was capable of producing altered LR-CDs profile from that of the WT enzyme was cultured in 5 ml LB medium with 100 µg/ml ampicilin at 37°C, 250 rpm shaking for overnight (16-18 hr). Cells were harvested via centrifugation at 6,000 x g for 10 min. Plasmid Mini Kit (Geneaids, Taiwan) was used to extract the recombinant plasmid harboring mutated *CgAM* gene. In order to determine the purity and concentration of the plasmid, A_{260} and the ratio of A_{260}/A_{280} value was detected by spectrophotometric method and examined by agarose gel electrophoresis as well.

Double stranded DNA (dsDNA) concentration was estimated by the following equation

Concentration (µg/ml) = A_{260} x dilution factor x 50 µg/ml

*A_{260} of 1.0 referred to a concentration of 50 µg/ml of pure dsDNA

To evaluate the DNA purity, the ratio of A_{260}/A_{280} nearly or above 1.8 would be an appropriate DNA quality.

2.5.2 Restriction enzyme digestion

The recombinant plasmid extracted from section 2.5.1 was digested with the two restriction enzymes, *Nde* I and *Xho* I (FastDigest™). Reaction mixture of 15 µl contained 20 ng of DNA sample, 0.5 µl for each of *Nde* I and *Xho* I restriction enzymes, 1.5 µl of buffer 4 (10x) and adjusted the final volume to be 15 µl with ultrapure (UP) water. The reaction was incubated at 37°C for10 min.

2.5.3 Agarose gel electrophoresis

An agarose gel was prepared by providing 0.8% (w/v) agarose into 100 ml of electrophoresis buffer (89 mM Tris-HCl, 8.9 mM boric acid and 2.5 mM EDTA, pH 8.0) in 250 ml Erlenmeyer flask. The mixture was melted by a microwave oven until the homogeneous solution could be clearly seen. Letting the melted solution cooled down; then, it was poured into the electrophoresis tray. One-fifth volume of DNA-loading dye (0.025% bromophenol blue, 40% ficoll 400 and 0.5% SDS) was mixed with the DNA sample before loading into the well of the agarose gel. A constant voltage of 10 volt/cm was applied during the running process. Once the migration of dye front (bromophenol blue) was found to be approximately 1 cm away from the bottom of the gel, the running was stopped and the gel was stained with 2.5 µg/ml ethidium bromide for 5 min, and subsequently destained in distilled water for 15 min. DNA sample in the gel was visualized under an excitation of a long wavelength UV light and photographed by Gel document. The size of DNA sample was estimated by comparing to the standard 1 kb DNA ladder™ (Fermentus, Canada).

2.5.4 Nucleotide sequencing

At least 100 ng of recombinant plasmid from section 2.5.1 was required for automated DNA sequencing (Ward Medic Co., Ltd.). *CgAM* gene sequencing was performed using two universal primers, T7 promoter for 5'-terminus sequencing and T7 terminator for 3'-terminus sequencing. To obtain full-length *CgAM* gene, f2CGAM and r2CGAM primers were designed for sequencing a middle of *CgAM* gene. The sequences of two primers were shown as follows

f2CGAM : 5'-TCT ACT CTG TGC GTT CCA CGT TG-3'

r2CGAM : 5'-CCT GCG AGT TCT GCT TAT AGG-3'

Ten micromolar of primers was required at least 10 µl per reaction. The DNA sequencing results were edited and analyzed using bioinformatic tools. ExPASy tool (http://web.expasy.org/translate/) was used to translate DNA sequence into amino acid sequence. ClustalW tool (http://www.ebi.ac.uk/Tools/msa/clustalo/) was used for amino sequence alignment to point where the mutation on *Cg*AM was located.

2.6 Optimization of mutated *CgAM* gene expression

E. coli BL21 (DE3) harboring recombinant plasmid *CgAM* was grown overnight at 37°C, 250 rpm shaking in 4 ml LB medium containing 100 µg/ml. One percent (v/v) of overnight culture was transferred to 100 ml LB medium supplemented with 100 µg/ml. The cells were continued to culture at 37°C until the optical density at 600 nm was approximately 0.4 to 0.6. Then, *Cg*AM production was triggered by IPTG induction at a final concentration of 0.4 mM. After IPTG induction, the cells were collectedat various time points including 0, 1, 2, 3, 4, 5, 6 hr. Each of cell pellets was

resuspended with 200 µl of extraction buffer. Cell disruption was performed by sonication with 21% power under alternating step of pulse-on 1 sec and pulse-off 2 sec for 1 min, repeated for 2 cycles. Removal of cell debris was done by centrifugation at 12,000 x g for 30 min. The expression pattern of *Cg*AM was analyzed by 7.5% sodium dodecyl sulfate polyacrylamide gel electrophoresis (SDS-PAGE). SDS-PAGE preparation was described in section 2.10. If there was less production of *Cg*AM in soluble form, experiment was conducted again but performed at 16°C instead.

2.7 Purification of WT and mutated *Cg*AM

2.7.1 Purification of WT *Cg*AM

To obtain a purified enzyme, two-step purification was performed. First, crude enzyme was initially performed partial purification using DEAE FF™ column chromatography as described in section 2.3.4. Subsequently, it was subjected to high sub Phenyl FF™ column chromatography, a hydrophobic interaction chromatography (HIC). The Phenyl FF™ column was equilibrated by at least 5 times column volume of 50 mM phosphate buffer pH 7.4 containing 1 M ammonium sulfate and 0.01% β-mercaptoethanol with a flow rate of 1 ml/min. Ammonium sulfate was gradually added to the dialyzed protein to the final concentration of 1M.Then, the dialyzed protein with 1 M ammonium sulfate was applied to the Phenyl FF™ column. The column was washed with the same buffer until A_{280} of sample decreased to baseline. Fractions of 2 ml were collected during all purification steps. Bound proteins were eluted in 2 steps by 0.2 M and 0 M ammonium sulfate, respectively. The purified fractions carrying

starch transglycosylation activity (assay explained in section 2.8.1) were pooled together before investigating enzyme purity and enzyme assay.

2.7.2 Purification of mutated *Cg*AM

Partially purified *Cg*AM was prepared as described in section 2.3.4 and Phenyl FF™ column equilibrating was performed using the same process as described in section 2.7.1. In the step of elution, a linear gradient elution, decreasing from1.0 to 0 M of ammonium sulfate, was used to follow the elution profile of the mutated *Cg*AM. The fractions that contained starch transglycosylation activity (assay explained in section 2.8.1) of amylomaltase were pooled. If the enzyme could not be eluted with 0 M of ammonium sulfate, the enzyme must be dialyzed against 50 mM phosphate buffer pH 7.4 prior to use. Purity of purified enzyme was determined by SDS-PAGE as described in section 2.10.

2.8 Enzyme assay

2.8.1 Starch transglycosylation activity

Starch transglycosylation activity was an activity to transfer a part of glycosyl group from starch donor to maltose acceptor. The measurement of this activity aimed to measure the residual starch in the reaction by iodine method (modified from Park et al. 2007).

The reaction mixture included 100 µl of enzyme, 250 µl of 0.2% (w/v) soluble potato starch, 50 µl of 1% (w/v) maltose and 600 µl of 50 mM phosphate buffer pH 6.0. Incubation was at 30°C for10 min, reaction was then terminated by boiling for 10 min.

A hundred microliter of aliquot was withdrawn and mixed with 1 ml of iodine solution (0.02% (w/v) I_2 in 0.2% (w/v) KI). The absorbance at 600 nm was measured.

One unit of starch transglycosylation activity was defined as the amount of enzyme required for producing 1% decrease in the intensity of starch-iodine complex per min under described condition.

2.8.2 Starch degrading activity

Starch degrading activity was assayed by measuring the amount of degraded starch in the reaction, determined by iodine method (Srisimarat *et al*, 2012). The reaction mixture consisted of 100 µl of 0.75% (w/v) of soluble potato starch, 50 µl of enzyme and 100 µl of 50 mM phosphate buffer pH 6.0. Reaction mixture was incubated at 30°C for 10 min before inactivating by adding 500 µl of 1 N HCl. A hundred microliter of reaction mixture was transferred and mixed with 900 µl of iodine solution (0.005% (w/v) I_2 in 0.05% (w/v) KI). The absorbance at 660 nm was measured.

One unit of starch degrading activity was defined as the amount of enzyme that could degrade 1 mg/ml of starch per min under the assay condition performed.

2.8.3 Disproportionation activity

Disproportionation activity determined the amount of free glucose released as a by-product from catalyzing a substrate maltotriose (G3). The assay was measured by glucose oxidase method (Berham et al 1972).A mean of assay was already described in section 2.3.2.

One unit of disproportionation activity was defined as the amount of enzyme that produced 1 µmol of glucose per min under described condition.

2.8.4 Cyclization activity

Cyclization activity was well-known as a reaction that linear oligosaccharide was used to produce a cyclic polymer called cyclodextrin (CD). Cyclization activity was determined by HPAEC-PAD analysis (Srisimarat, 2012). The reaction mixture was composed of 150 µl of 2% pea starch, 50 µl of enzyme and 1,300 µl of 50 mM phosphate buffer pH 6.0. The reaction was incubated at 30°C for 90 min. Reaction was stopped by boiling for 10 min. Reaction was then treated overnight with 8 U glucoamylase (Fluka, Switzerland) at 40°C in order to digest linear oligosaccharides, and inactivated by boiling for 10 min. Analysis of LR-CDs profile was done by HPAEC-PAD. An approach to obtain LR-CDs profiles was well-described in section 2.3.6.

One unit of cyclization was defined as the amount of enzyme required for the production of 1 nC of CD34 per min under assayed condition.

2.8.5 Hydrolysis activity

Bicinchoninic acid (BCA) reagent was used to test hydrolysis activity (Sinner and Puls, 1978). Ten microliters of enzyme was provided into a mixture containing 30 µl of 0.5 mg/ml LR-CDs and 10 µl of 50 mM phosphate buffer pH 6.0 and incubated at 30°C for 10 min. Reaction was stopped by adding 30 µl of 1N HCl. 950 µl of BCA reagent was added into the mixture and transferred to incubate at 80°C for 25 min. To

inactivate the reaction, incubated reaction was transferred on ice for 5 min and suddenly taken out to measure A_{562}.

One unit of hydrolysis activity was defined as the amount of enzyme used for producing 1µmol of reducing sugar per min under described condition.

2.8.6 Coupling activity

Coupling activity reflected a reversible reaction of cyclization activity. This reaction could be examined by several methods, for instance, DNS reagent, bicinchoninic acid assay, and glucose oxidase method.

For determining of coupling activity by glucose oxidase method (Miwa et al. 1972), 100 µl of reaction mixture was prepared as follows: 20 µl of 3 mg/ml LR-CDs, 20 µl of 1 mg/ml cellobiose, 20 µl of enzyme and 40 µl of 50 mM phosphate buffer pH 6.0. Reaction was incubated at 30°C for 10 min and stopped by boiling. Subsequently, 8 U of glucoamylase (Fluka, Switzerland) was added to the reaction mixture and further incubated at 40°C for 30 min, then terminated by boiling. Glucose oxidase reagent was added to the final volume of 1 ml, incubated at 30°C for 10 min and measured at A_{505}.

One unit of coupling activity was defined as the amount of enzyme that produced 1 µmol of glucose per min under described condition.

2.9 Determination of protein concentration

Protein concentration was determined by mean of Bradford's assay (1976). Standard curve for determining the protein concentration was constructed using 1 mg/ml of bovine serum albumin as a standard protein. A hundred microlitre of protein sample was mixed with 1 ml of Bradford working reagent and let the reaction stand for 2 min before measuring at A_{595}.

2.10 Polyacrylamide gel electrophoresis (PAGE)

2.10.1 SDS-Polyacrylamide gel electrophoresis (SDS-PAGE)

Denaturing gel was prepared by 5% (w/v) stacking gel and 7.5% (w/v) separating gel containing 0.1% (w/v) SDS. Electrophoresis was carried out by Mini-Gel electrophoresis (Bio-Rad, Hercules, MA, USA). Sample buffer with SDS-loading dye was mixed to the protein sample by one-fifth of the sample volume and boiled for 5 min before loading into the gel. During a run of electrophoresis, a constant current of 20 mA (per gel slab) was set. After a complete run, the gel was subjected to coomassie blue staining solution for visualizing the protein bands

2.10.2 Staining with coomassie blue

The gel was stained with coomassie blue R-250 staining solution (1% Coomassie blue r-250, 45% methanol and 10% glacial acetic acid) for 2 hr shaking at room temperature. The gel was then destained with destaining solution (10% methanol and 10% glacial acetic acid) for several times till protein bands could be clearly seen without a disruptive background.

2.11 Characterization of WT and mutated *Cg*AM

2.11.1 Effect of temperature on *Cg*AM activity

The effect of temperature on *Cg*AM activity was carried out on two activities; starch transglycosylation activity and disproportionation activity. Assay conditions were performed in 50 mM phosphate buffer pH 6.0 at various temperatures in a range of 20°C to 70°C. The activity assay was done as described in section 2.8.1 and 2.8.3. The results were shown as a plot of relative activity (%) against temperature. The temperature at which the maximum activity was given was set to be 100%.

2.11.2 Effect of pH on *Cg*AM activity

The effect of pH on *Cg*AM activity was observed on starch transglycosylation activity and disproportionation activity. Assay conditions were performed under optimum temperature from section 2.11.1 but varied in pH ranging from pH 4.0 to 9.0. Three separated buffer systems were used as follows; 50 mM acetate buffer pH 4.0 to 6.0, 50 mM phosphate buffer pH 6.0 to pH 8.0 and 50 mM Tris-HCl pH 7.0 to 9.0. The activities were examined as previously explained in section 2.8.1 and 2.8.3. The results were shown as a plot of relative activity (%) against temperature. The highest activity observed was set as 100%.

2.11.3 Temperature stability of *Cg*AM

For temperature stability, the assay aimed to measure the remaining activity of starch transglycosylation after the enzyme was pre-incubated at each temperature. The enzyme was incubated at various temperatures for 0 up to 180 min before withdrawn

to perform activity assay. Method of starch transglycosylation activity assay was described in section 2.8.1. The results were illustrated as a percentage of relative activity.

2.11.4 pH stability of *Cg*AM

The effect of pH on *Cg*AM stability was determined at various pHs. The enzyme was pre-incubated with buffers of different pHs at the optimum temperature for 0 to180 min before determining starch transglycosylation activity as described in section 2.8.1. The buffer systems for the experiment were followed by the same systems used in section 2.11.2.The results were illustrated as a percentage of relative activity over a period of time.

2.11.5 Substrate specificity on disproportionation activity of *Cg*AM

An ability of *Cg*AM to catalyze different maltooligosaccharides was investigated on disproportionation activity. Maltose (G2) to maltoheptaose (G7) was used as substrates. The enzyme carrying 0.2 U of starch transglycosylation activity in 50 mM phosphate buffer pH 6.0 was added to 50 mM of substrate and then incubated at the optimum temperature of disproportionation activity for 10 min. The amount of free glucose was determined by glucose oxidase method, described in details in section 2.8.3.

2.11.6 Kinetic studies of *Cg*AM

2.11.6.1 Kinetic study of starch transglycosylation activity

To obtain starch transglycosylation kinetic parameters, experiment was conducted by incubating purified *Cg*AM in 50 mM phosphate buffer pH 6.0 with various concentrations of glucose acceptor, ranging from 0 to 10 mM. Incubation was continued for 10 min and stopped by boiling for 10 min. The amount of degraded starch was detected by iodine method (see section 2.8.1 for method). The kinetic parameters K_m and V_{max} were calculated from Lineweaver-Burk plot. Besides, turnover number of enzyme (k_{cat}) and catalytic efficiency (k_{cat}/K_m) were also determined.

2.11.6.2 Kinetic study of disproportionation activity

Kinetic parameters on disproportionation activity of *Cg*AM were investigated by incubating *Cg*AM in 50 mM phosphate buffer with various concentrations of maltotriose (G3), preferable substrate of *Cg*AM, in a range of 0 to 200 mM for 10 min at 40°C. After that, the reaction was terminated by boiling 10 min. The amount of free glucose was detected by glucose oxidase method (well-described in section 2.3.2 and 2.8.3). All kinetic parameters including K_m,V_{max}, k_{cat} and k_{cat}/K_m were calculated.

2.11.6.3 Kinetic study of cyclization activity

Determination of kinetic parameters on *Cg*AM cyclization activity was investigated. The purified *Cg*AM of 0.05 U starch degrading activity was incubated in 50 mM phosphate buffer pH 6.0 under varying a concentration of pea starch, 0 to 0.5% (w/v) at 30°C for 60 min, then stopped by boiling for 10 min. 8 U of glucoamylase

(Fluka, Switzerland) was introduced into the reaction and incubated overnight at 40°C, and inactivated by boiling for 10 min. LR-CDs mixture was subjected to HPAEC-PAD analysis and the activity of cyclization was determined as described in section 2.8.4. The kinetic parameters K_m and V_{max} were calculated from Lineweaver-Burk plot. Besides, turnover number of enzyme (k_{cat}) and catalytic efficiency (k_{cat}/K_m) of the enzyme were investigated as well.

2.11.7 Effect of incubation time and unit of enzyme on LR-CDs production

Two important parameters, incubation time and unit of enzyme that possessed immense effects on LR-CDs production were investigated.

2.11.7.1 Effect of incubation time

The reaction mixture that included 0.2% (w/v) pea starch and 0.05 U starch degrading activity *Cg*AM in 50 mM phosphate buffer pH 6.0 was incubated at 30°C for each time point: 1, 2, 3, 6, 12 and 24 hr. Reaction was terminated by boiling. Then the reaction was treated with 8 U of glucoamylase (Fluka, Switzerland) and incubated at 40°C for overnight, and inactivated by boiling. LR-CDs products were analyzed by HPAEC-PAD analysis. The method of HPAEC-PAD analysis was described in section 2.3.6.

2.11.7.2 Effect of unit of enzyme

LR-CDs were synthesized by using 0.2% (w/v) pea starch as substrate but varied in the amount of enzyme. Enzymes with 0.05, 0.1 and 0.15 U of starch degrading

activity were used to synthesize LR-CDs separately under incubation at 30°C at a fixed time point of 6 hr. The reactions were stopped by boiling and subsequently added with 8 U glucoamylase (Fluka, Switzerland) and further incubated at 40°C for overnight. The reactions were stopped by 10 min boiling before subjecting to LR-CDs profiling by HPAEC-PAD as described in section 2.3.6.

2.11.8 Secondary structure analysis by Circular dichroism (CD) spectrometer

The spectra of WT and mutated *Cg*AM were generated by CD spectrometer (J-815, Jasco, Japan). A purified protein sample with the concentration of 0.2 mg/ml was required for the measurement. Wavelength excitation was done in the range of 190 to 250 nm at 25°C. The actual CD spectrum was constructed by the average result of three scans from CD spectrometer. To calculate the Mean Residue Weight (MRW) of CD spectrum, method of Kelly (Kelly et al. 2015) was used to interpret the data. MRW was defined as an average of molecular weight of amino acids in whichthe protein contained. For this method, MRW was often used in place of the molecular weight.The calculation was given by the following equation

$$MRW = \frac{M}{N-1}$$

M = the molecular weight of polypeptide chain (Da)

N = the number of amino acid residues in the polypeptide chain

Thus, N-1 indicated the number of peptide bonds found in the protein. Using Mean Residue Ellipticity (MRE) facilitated comparing the CD of proteins of different

molecular weight; use of this normalized CD was important in study of protein structure.

MRE could be calculated by this given equation

$$[\theta]mrw,\lambda = \frac{MRW\ x\ \theta\lambda}{10\ x\ dc}$$

Where $\theta\lambda$ = ellipticity (degrees) at each wavelength of λ

d = path length of the cuvette (cm)

c = protein concentration (g/ml)

The secondary structure of protein was predicted using K2D3 server program (http://cbdm-01.zdv.uni-mainz.de/~andrade/k2d3//).

CHAPTER III

RESULTS

3.1 Screening for mutants with altered LR-CD profiles from random mutagenesis library

Random mutagenesis clones of *CgAM* gene, constructed by PCR-mediated random mutagenesis technique, were given by Asst. Prof. Kuakarun Krusong, Ph.D. These clones were used to screen for mutated *Cg*AM that possessed altered LR-CDs profile in order to determine the key amino acid residue involved in LR-CDs formation.

3.1.1 Disproportionation activity assay

In the first step, five batches (about 90 clones each) of mutated clones were screened by disproportionation activity as described in section 2.3.2. Crude enzymes of WT and mutants were incubated with maltotriose (G3) at 40°C. Glucose oxidase reagent was added to the reaction, aiming to detect the amount of free glucose in the reaction. Mutants that displayed disproportionation activity at least 80% of wild-type (WT) enzyme activity were selected. Table 2 showed the summary of mutated clones screened by glucose oxidase method. In this work, H5 and 1E5 were candidate mutants selected from disproportionation activity screening.

Table 2 Summary of mutated amylomaltase clones, screened by glucose oxidase assay

	lower than 80% of WT activity	80 - 100% of WT activity	More than 100% of WT activity
Number of clones	90	7	3

3.1.2 Expression of selected *Cg*AMs

E. coli BL21 (DE3) harboring *CgAM* gene was cultured in 1.5 liters of LB broth containing 100 µg/ml of ampicilin. The expression condition was to induce with 0.4 mM IPTG and further cultured for 2 hr. For crude extract preparation of WT, 1E5 and H5 *Cg*AMs, cell wet weight of 3.8 g, 4.2 and 4.3 g were obtained and resuspended in extraction buffer (1 g per 2.5 ml), and then disrupted by sonication. The supernatants were assayed by starch transglycosylation activity as described in section 2.8.1. Total proteins in crude extract of WT, 1E5 and H5 *Cg*AMs were 255, 268 and 344.8 mg with 583.1, 477 and 537.9 U of starch transglycosylation, respectively. The specific activities of WT, H5 and 1E5 crude extracts were 2.29, 1.56 and 1.78 U/mg (Table 3).

3.1.3 Partial purification of *Cg*AM

Crude enzyme was applied onto DEAE FF™ column. Column was equilibrated as explained in section 2.3.4. The purification profiles of WT and mutated *Cg*AMs were shown in Figure 12 to 14. For WT *Cg*AM purification, bound proteins were eluted with three steps of NaCl concentrations at 0.2 M, 0.3 M and 1 M, respectively. Protein fractions eluted by 0.3 M NaCl displayed higher starch transglycosylation activity in comparison to 0.2 M NaCl elution fractions. Therefore, 0.3 M NaCl elution fractions

were pooled and dialyzed against 50 mM phosphate buffer pH 7.4. The specific activity of WT enzyme at this step was 15.1 U/mg. For H5 and 1E5 *Cg*AM purification, those bound *Cg*AMs were eluted at the same concentration of NaCl as WT *Cg*AM did. The specific activities of partially purified 1E5 and H5 enzymes were 7.59 and 8.18 U/mg, respectively. Purification Table of all *Cg*AMs was shown in Table 3.

Crude and partially purified *Cg*AMs were analyzed by SDS-PAGE (Figure 15). Fifteen micrograms of crude and eight micrograms were used for crude and partially purified *Cg*AM, respectively. The protein patterns showed less protein bands after partially purified through DEAE FF™ column when compared to the crude extract. Apparent molecular mass of amylomaltases were detected at a size of 84 kDa. This indicated that the enzymes could be partially purified by anion exchange chromatography.

3.1.4 LR-CDs profiles by HPAEC-PAD

Production of LR-CDs was carried out as described in section 2.3.5. To compare the LR-CDs product pattern, *Cg*AMs with 0.05 U starch degradation activity were incubated with 0.2% (w/v) pea starch at 30°C for 6 hr incubation time. LR-CDs mixture was analyzed by HPAEC-PAD. The size of LR-CDs was determined by comparing with the standard LR-CDs (Ezaki Glico, Japan). Figure 16 represented merged *Cg*AMs' profiles. CD27 (cyclodextrin with 27 glucose monomers) to CD29 were principal CDs product of WT *Cg*AM. 1E5 enzyme showed the same LR-CDs profile as WT enzyme but produced higher amount of CD26 to CD35 while principal CDs of H5 enzyme were shifted to CD30 to CD32 and CD34 to CD36.

Table 3 Purification Table of WT, 1E5 and H5 *Cg*AMs

Purification step	Total protein (mg)	Total activity* (U)	Specific activity* (U/mg)	Purification fold	Yield (%)
WT crude extract	255	583	2.29	1	100
WT DEAE FF^{TM}	11.9	180	15.1	6.60	30.8
1E5 crude extract	268	477	1.78	1	100
1E5 DEAE FF^{TM}	14.1	107	7.59	4.26	22.4
H5 crude extract	345	538	1.56	1	100
H5 DEAE FF^{TM}	13.2	108	8.18	5.24	20.1

**activity assay was performed by starch transglycosylation assay*

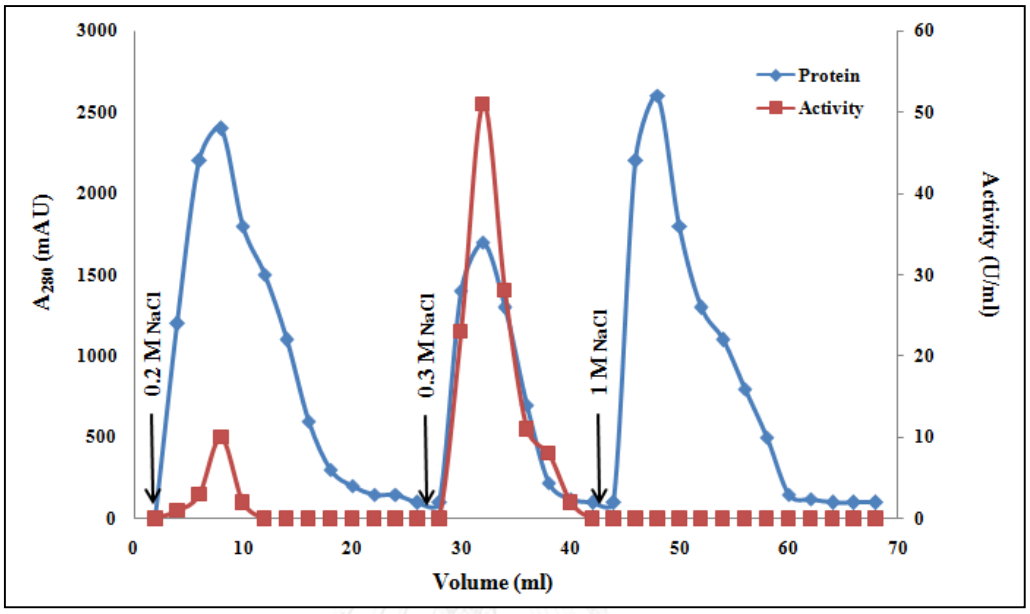

Figure 12 Purification profile of WT *Cg*AM by DEAE FF™ column chromatography. The column was equilibrated with 50 mM phosphate buffer pH 7.4. Bound proteins were eluted by 0.2 M, 0.3 M and 1 M NaCl in the same buffer. Fraction size was 2 ml. The arrows indicated the point at which a stepwise elution was performed. *Cg*AM activity was followed by starch transglycosylation assay.

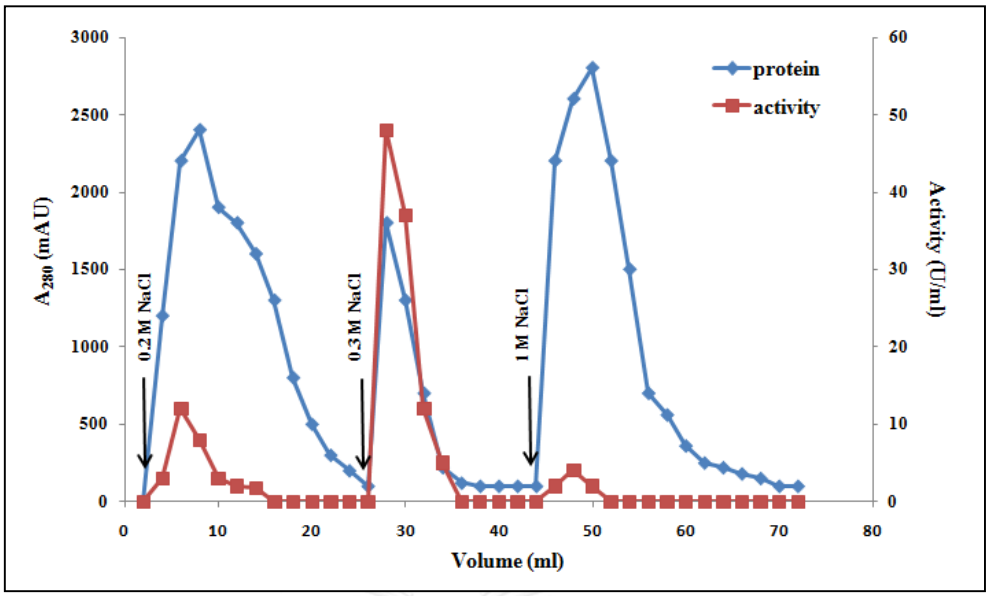

Figure 13 Purification profile of H5 *Cg*AM by DEAE FF™ column chromatography. The column was equilibrated with 50 mM phosphate buffer pH 7.4. Bound proteins were eluted by 0.2 M, 0.3 M and 1 M NaCl in the same buffer. Fraction size was 2 ml. The arrows indicated the point at which a stepwise elution was performed. *Cg*AM activity was followed by starch transglycosylation assay.

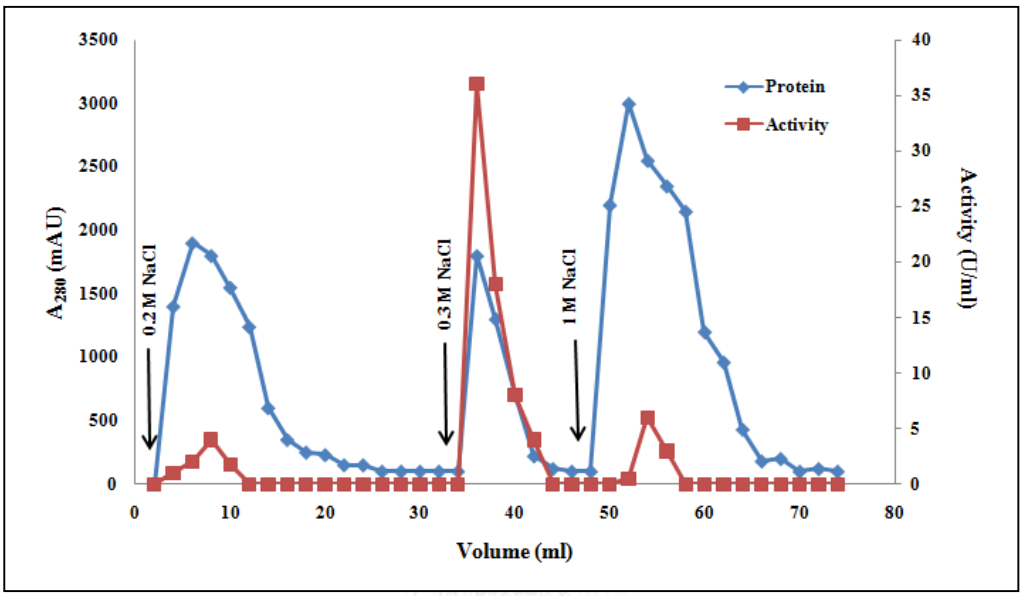

Figure 14 Purification profile of 1E5 *Cg*AM by DEAE FF™ column chromatography. The column was equilibrated with 50 mM phosphate buffer pH 7.4. Bound proteins were eluted by 0.2 M, 0.3 M and 1 M NaCl in the same buffer. Fraction size was 2 ml. The arrows indicated the point at which a stepwise elution was performed. *Cg*AM activity was followed by starch transglycosylation assay.

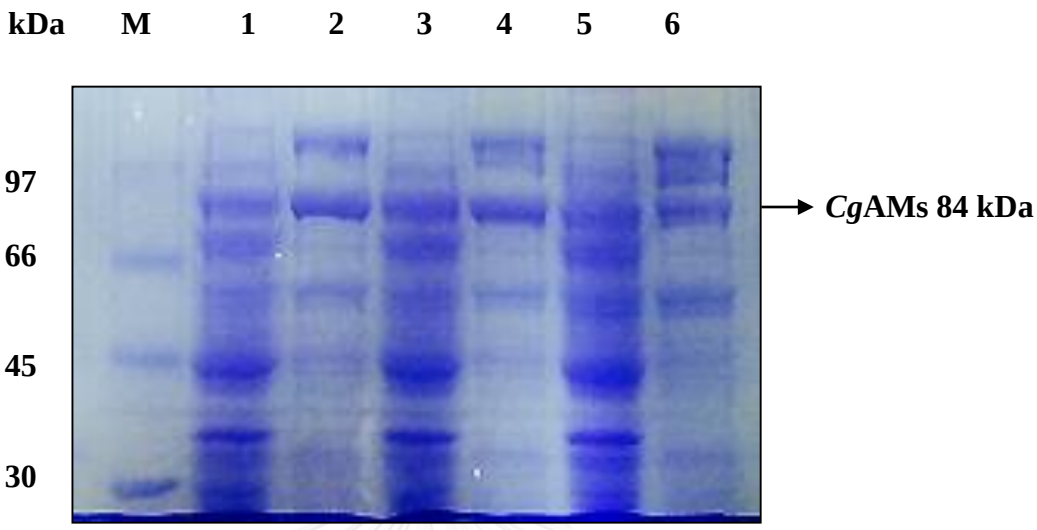

Figure 15 7.5% SDS-PAGE of crude and partially purified *Cg*AMs.

Lane M = low molecular weight protein marker (Amersham, USA)

Lane 1 = crude WT *Cg*AM

Lane 2 = partially purified WT *Cg*AM

Lane 3 = crude 1E5 *Cg*AM

Lane 4 = partially purified 1E5 *Cg*AM

Lane 5 = crude H5 *Cg*AM

Lane 6 = partially purified H5 *Cg*AM

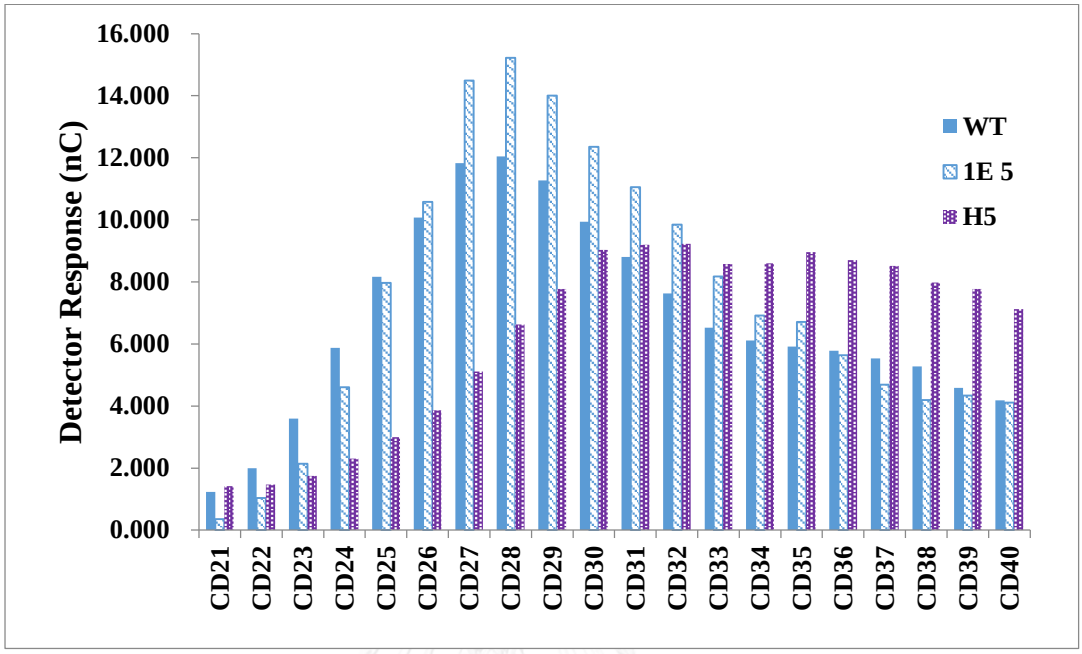

Figure 16 LR-CDs production profile of WT, 1E5 and H5 amylomaltases, analyzed by HPAEC. LR-CDs synthesis was performed using 0.05U starch degradation activity of *Cg*AM and 0.2% (w/v) pea starch in 50 mM phosphate buffer pH 6.0 at 30°C for 6 hr under 150 rpm shaking. Each CD number represented glucose monomers. Amount of CDs were determined by an electrocatalytic oxidation (nC) by HPAEC detector.

3.1.5 Identification of mutated amino acid residues

3.1.5.1 Extraction and restriction enzyme digestion of recombinant WT and mutated *Cg*AM plasmid

The recombinant H5 and 1E5 plasmids were extracted and analyzed by agarose gel electrophoresis. Restriction enzymes *Nde* I and *Xho* I were used to double digest the recombinant plasmids. Two bands were obtained after restriction enzyme digestion as indicated by Figure 17. The size of pET-17b vector and *CgAM* gene were found to be approximately 3.3 kb and 2.1 kb, respectively.

3.1.5.2 Nucleotide sequencing

To investigate a mutation on *CgAM* gene, the recombinant plasmids were subjected to DNA sequencing. T7 promoter and T7 terminator primers were used to sequence the 5'-terminus and 3'-terminus, respectively. The residual sequence of the gene was extended by two primer pairs of f2CGAM and r2CGAM (sequences shown in section 2.5.4). It was found that the nucleotide sequences of 1E5 *CgAM* gene were found to be 2,121 bps which could be deduced into 706 amino acids. The nucleotide sequence of H5 *CgAM* gene was 2,123 bps. This led to a frameshift mutation occurred on the gene. Deduced amino acid sequence of 1E5 *Cg*AM was then compared to the WT sequence using ClustalW program. The result revealed three mutations occurred on 1E5 *CgAM* gene. Amino acid residues at 9, 265 and 697 were changed from Glu (E) to Pro (P), Asp (D) to His (H) and His (H) to Gln (Q), respectively.

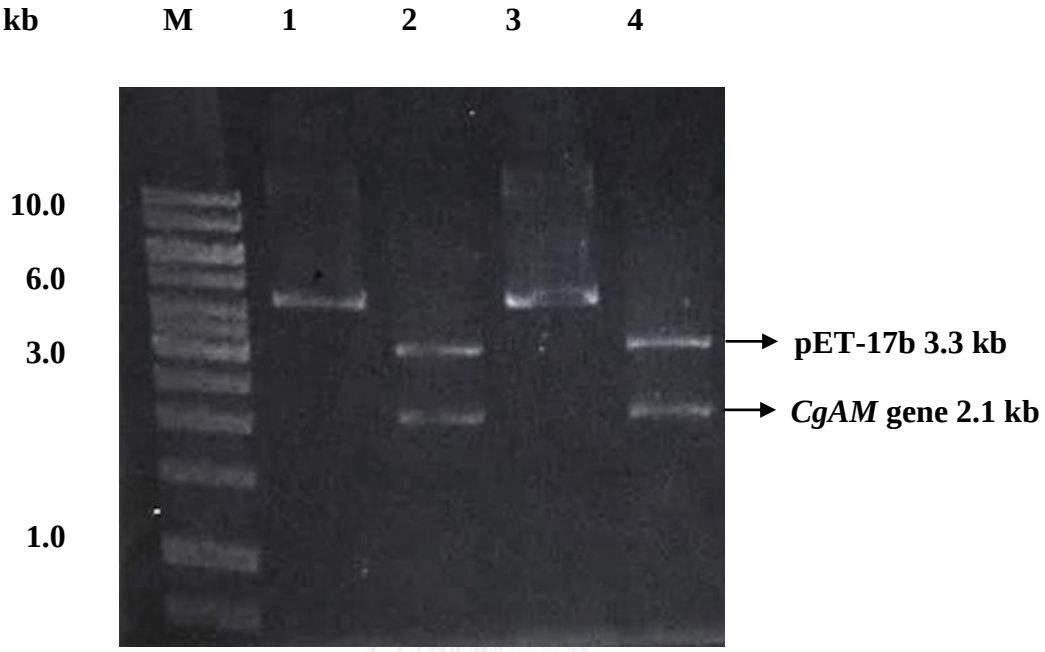

Figure 17 Agarose gel electrophoresis of recombinant 1E5 and H5 plasmids. DNA samples were separated on 0.8% agarose gel and visualized by ethidium bromide staining.

Lane M = DNA marker 1 kb (Fermentus, Canada)

Lane 1 = recombinant 1E5 plasmid

Lane 2 = recombinant 1E5 plasmid digested with *Xho* I and *Nde* I

Lane 3 = recombinant H5 plasmid

Lane 4 = recombinant H5 plasmid digested with *Xho* I and *Nde*

```
WT                1 MTARRFLNELADLYGVATSYTDYKGAHIEVSDDTLVKILRALGVNLDTSN     50
                    ||||||||.||||||||||||||||||||||||||||||||||||||||
1E5               1 MTARRFLNPLADLYGVATSYTDYKGAHIEVSDDTLVKILRALGVNLDTSN     50

WT               51 LPNDDAIQRQIALFHDREFTRPLPPSVVAVEGDELVFPVHVHDGSPADVH    100
                    ||||||||||||||||||||||||||||||||||||||||||||||||||||
1E5              51 LPNDDAIQRQIALFHDREFTRPLPPSVVAVEGDELVFPVHVHDGSPADVH    100

WT              101 IELEDGTQRDVSQVENWTAPREIDGIRWGEASFKIPGDLPLGWHKLHLKS    150
                    ||||||||||||||||||||||||||||||||||||||||||||||||||||
1E5             101 IELEDGTQRDVSQVENWTAPREIDGIRWGEASFKIPGDLPLGWHKLHLKS    150

WT              151 NERSAECGLIITPARLSTADKYLDSPRSGVMAQIYSVRSTLSWGMGDFND    200
                    ||||||||||||||||||||||||||||||||||||||||||||||||||||
1E5             151 NERSAECGLIITPARLSTADKYLDSPRSGVMAQIYSVRSTLSWGMGDFND    200

WT              201 LGNLASVVAQDGADFLLINPMHAAEPLPPTEDSPYLPTTRRFINPIYIRV    250
                    ||||||||||||||||||||||||||||||||||||||||||||||||||||
1E5             201 LGNLASVVAQDGADFLLINPMHAAEPLPPTEDSPYLPTTRRFINPIYIRV    250

WT              251 EDIPEFNQLEIDLRDDIAEMAAEFRERNLTSDIIERNDVYAAKLQVLRAI    300
                    ||||||||||||||.||||||||||||||||||||||||||||||||||||
1E5             251 EDIPEFNQLEIDLRHDIAEMAAEFRERNLTSDIIERNDVYAAKLQVLRAI    300

WT              301 FEMPRSSEREANFVSFVQREGQGLIDFATWCADRETAQSESVHGTEPDRD    350
                    ||||||||||||||||||||||||||||||||||||||||||||||||||||
1E5             301 FEMPRSSEREANFVSFVQREGQGLIDFATWCADRETAQSESVHGTEPDRD    350

WT              351 ELTMFYMWLQWLCDEQLAAAQKRAVDAGMSIGIMADLAVGVHPGGADAQN    400
                    ||||||||||||||||||||||||||||||||||||||||||||||||||||
1E5             351 ELTMFYMWLQWLCDEQLAAAQKRAVDAGMSIGIMADLAVGVHPGGADAQN    400

WT              401 LSHVLAPDASVGAPPDGYNQQGQDWSQPPWHPVRLAEEGYIPWRNLLRTV    450
                    ||||||||||||||||||||||||||||||||||||||||||||||||||||
1E5             401 LSHVLAPDASVGAPPDGYNQQGQDWSQPPWHPVRLAEEGYIPWRNLLRTV    450

WT              451 LRHSGGIRVDHVLGLFRLFVMPRMQSPATGTYIRFDHNALVGILALEAEL    500
                    ||||||||||||||||||||||||||||||||||||||||||||||||||||
1E5             451 LRHSGGIRVDHVLGLFRLFVMPRMQSPATGTYIRFDHNALVGILALEAEL    500

WT              501 AGAVVIGEDLGTFEPWVQDALAQRGIMGTSILWFEHSPSQPGPRRQEEYR    550
                    ||||||||||||||||||||||||||||||||||||||||||||||||||||
1E5             501 AGAVVIGEDLGTFEPWVQDALAQRGIMGTSILWFEHSPSQPGPRRQEEYR    550

WT              551 PLALTTVTTHDLPPTAGYLEGEHIALRERLGVLNTDPAAELAEDLQWQAE    600
                    ||||||||||||||||||||||||||||||||||||||||||||||||||||
1E5             551 PLALTTVTTHDLPPTAGYLEGEHIALRERLGVLNTDPAAELAEDLQWQAE    600

WT              601 ILDVAASANALPAREYVGLERDQRGELAELLEGLHTFVAKTPSALTCVCL    650
                    ||||||||||||||||||||||||||||||||||||||||||||||||||||
1E5             601 ILDVAASANALPAREYVGLERDQRGELAELLEGLHTFVAKTPSALTCVCL    650

WT              651 VDMVGEKRAQNQPGTTRDMYPNWCIPLCDSEGNSVLIESLRENELYHRVA    700
                    ||||||||||||||||||||||||||||||||||||||||||||||||.|||
1E5             651 VDMVGEKRAQNQPGTTRDMYPNWCIPLCDSEGNSVLIESLRENELYQRVA    700

WT              701 KASKRD   706
                    ||||||
1E5             701 KASKRD   706
```

Figure 18 Amino acid sequence alignment of 1E5 and WT *Cg*AMs using ClustalW tool. The highlights indicated where the mutations located (E9P, D265H and H697Q).

3.2 Screening for mutants with altered LR-CD profiles from site-directed mutagenesis mutants

Site-directed mutagenesis clones were from Asst. Prof. Kuakarun Krusong, Ph.D. Among these, E231Y mutant by which the amino acid residue Glu (E) at position 231 on *Cg*AM was changed to Tyr (Y), was selected for this study.

3.2.1 Expression and crude extract preparation of E231Y *Cg*AM

E. coli BL21 (DE3) carrying *CgAM* gene was cultured in 1.5 liters of LB medium containing 100 µg/ml of ampicilin. WT *Cg*AM expression condition was 2 hr after 0.4 mM IPTG induction while 4 hr after 0.4 mM IPTG induction was done in E231Y *Cg*AM expression. The harvested cells of 4 and 5.8 g were resuspended in extraction buffer (1 g per 2.5 ml) and then disrupted by sonication. The crude supernatants were assayed by starch transglycosylation activity as described in section 2.8.1. The specific activities of WT and E231Y crude extracts were 2.20 and 0.85 U/mg (Table 4).

3.2.2 Partial purification of E231Y *Cg*AM

Crude *Cg*AM enzymes obtained from section 3.2.1 were partially purified by DEAE FF™ column. Column was equilibrated as described in section 2.3.4.1. The purification step of WT *Cg*AM was explained in section 3.1.3. The chromatographic profile of E231Y *Cg*AM was shown in Figure 19. Proteins eluted by 0.3 M NaCl carried higher starch transglycosylation activity, comparing to other elution steps. Thus, those protein fractions were pooled and dialyzed against 50 mM phosphate buffer pH 7.4.

The specific activities of WT and E231Y *Cg*AMs were 12.3 and 4.84 U/mg with % recovery of 27.0 and 20.5 (Table 4).

Table 4 Purification Table of WT and E231Y *Cg*AMs

Purification step	Total protein (mg)	Total activity* (U)	Specific activity* (U/mg)	Purification fold	Yield (%)
WT crude extract	245	538	2.20	1	100
WT DEAE FF™	11.8	145	12.3	5.60	27.0
E231Y crude extract	518	440	0.85	1	100
E231Y DEAE FF™	18.6	90.0	4.84	5.69	20.5

**activity assay was performed by starch transglycosylation assay*

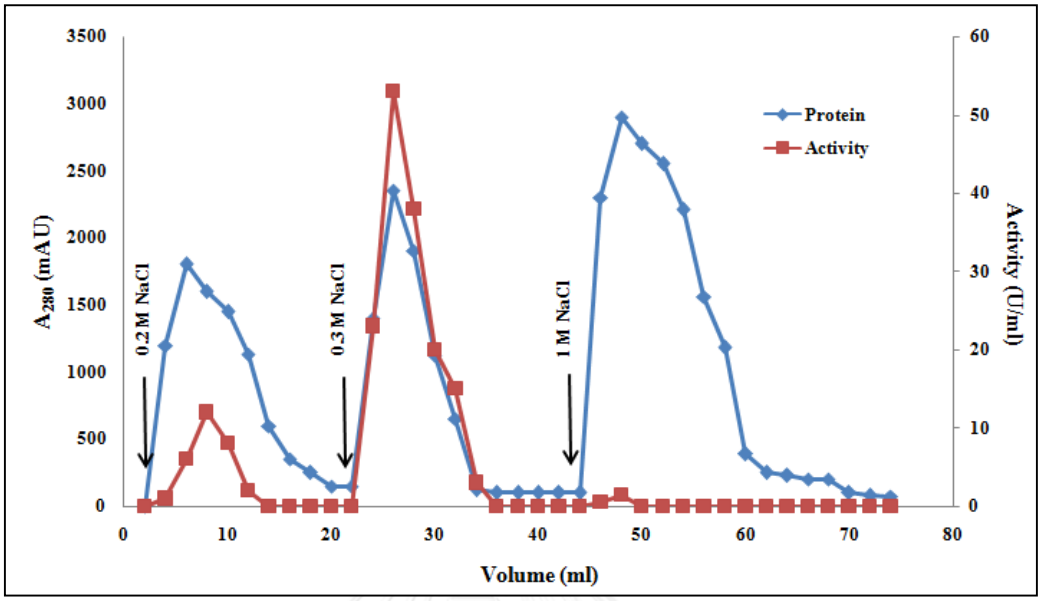

Figure 19 Purification profile of E231Y *Cg*AM by DEAE FF™ column chromatography. The column was equilibrated with 50 mM phosphate buffer pH 7.4. Bound proteins were eluted by 0.2 M, 0.3 M and 1 M NaCl in the same buffer. Fraction size was 2 ml. The arrows indicated the point at which a stepwise elution was performed. *Cg*AM activity was followed by starch transglycosylation assay.

3.2.3 LR-CDs profile by HPAEC-PAD analysis

LR-CDs synthesis was followed by section 2.3.5. Partially purified *Cg*AMs with 0.05 U starch degradation activities were used to incubated with 0.2% (w/v) pea starch at 30°C under 6 hr incubation time. LR-CDs product patterns were analyzed by HPAEC-PAD. The size of LR-CDs was determined by comparing with the standard LR-CDs (Ezaki Glico, Japan). The overlay of *Cg*AMs' LR-CD profiles was shown in Figure 20. When compared the principal CDs, CD42 to CD44 were found to be the principal CDs of E231Y whereas the WT's was CD27 to CD29. As could be seen, partially purified E231Y *Cg*AM tended to produce higher amount of larger CDs (more than CD37) while produced little amount of CD20 to CD36; on the contrary, WT *Cg*AM produced higher amount of CD23 to 36 with little amount of CD37 and larger CDs.

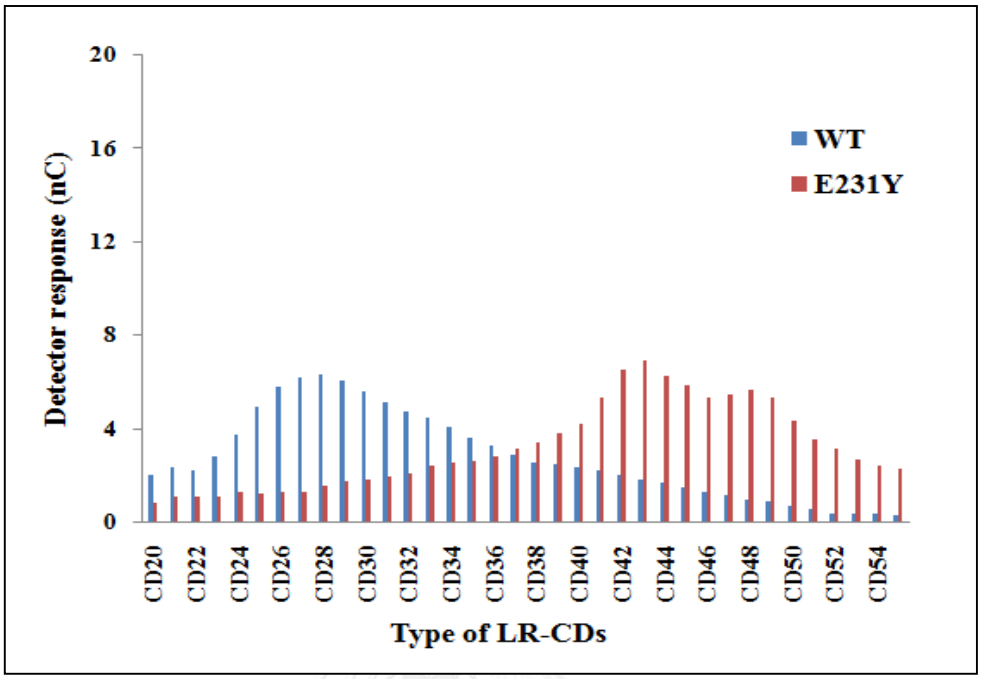

Figure 20 LR-CDs production profile of WT and E231Y *Cg*AMs, analyzed by HPAEC. LR-CDs synthesis was performed using 0.05U starch degradation activity of *Cg*AM and 0.2% (w/v) pea starch in 50 mM phosphate buffer pH 6.0 at 30°C for 6 hr under 150 rpm shaking. Each CD number represented glucose monomers. Amount of CDs were determined by an electrocatalytic oxidation (nC) by HPAEC detector.

3.2.4 Confirmation of E231Y mutation

3.2.4.1 Extraction and restriction enzyme digestion of recombinant E231Y plasmid

The pET-17b vector harboring E231Y *CgAM* gene was extracted and checked by agarose gel electrophoresis. Restriction enzymes *Nde* I and *Xho* I were used to double digest the recombinant plasmids. The results showed that the size of pET17b vector and E231Y *CgAM* gene were around 3.3 kb and 2.1 kb, respectively.

3.2.4.2 Nucleotide sequencing

Full length of E231Y *CgAM* gene was obtained by DNA sequencing. For this gene, T7 promoter and T7 terminator primers were used to sequence the 5'-terminus and 3'-terminus, respectively. A middle of the E231Y *CgAM* gene was sequenced by f2CGAM and r2CGAM primers (sequences shown in section 2.5.4). It was found that the nucleotide sequences of E231Y *CgAM* gene contained an open reading frame (ORF) of 2,121 bps which could be deduced into amino acid sequence of 706 residues. Deduced E231Y *Cg*AM amino acid sequence was subjected to amino acid sequence alignment, comparing to the WT sequence. The result from Figure 3.11 revealed that amino acid residue 231 was changed from Glu (E) to Tyr (Y). This confirmed that a single point mutation at E231Y on *CgAM* gene was obtained.

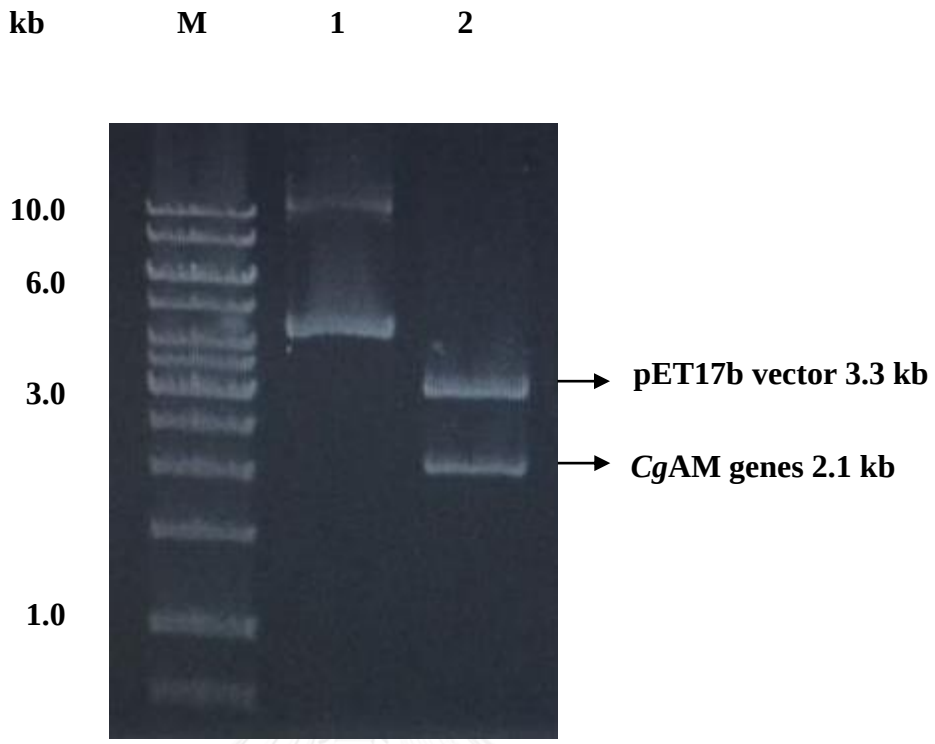

Figure 21 Agarose gel electrophoresis of recombinant E231Y plasmids. DNA samples were separated on 0.8% agarose gel and visualized by ethidium bromide staining.

Lane M = DNA marker 1 kb (Fermentus, Canada)

Lane 1 = recombinant E231Y plasmid

Lane 2 = recombinant E231Y plasmid digested with *Xho* I and *Nde* I

```
WT                1 MTARRFLNELADLYGVATSYTDYKGAHIEVSDDTLVKILRALGVNLDTSN     50
                    ||||||||||||||||||||||||||||||||||||||||||||||||||
1E5               1 MTARRFLNELADLYGVATSYTDYKGAHIEVSDDTLVKILRALGVNLDTSN     50

WT               51 LPNDDAIQRQIALFHDREFTRPLPPSVVAVEGDELVFPVHVHDGSPADVH    100
                    ||||||||||||||||||||||||||||||||||||||||||||||||||
1E5              51 LPNDDAIQRQIALFHDREFTRPLPPSVVAVEGDELVFPVHVHDGSPADVH    100

WT              101 IELEDGTQRDVSQVENWTAPREIDGIRWGEASFKIPGDLPLGWHKLHLKS    150
                    ||||||||||||||||||||||||||||||||||||||||||||||||||
1E5             101 IELEDGTQRDVSQVENWTAPREIDGIRWGEASFKIPGDLPLGWHKLHLKS    150

WT              151 NERSAECGLIITPARLSTADKYLDSPRSGVMAQIYSVRSTLSWGMGDFND    200
                    ||||||||||||||||||||||||||||||||||||||||||||||||||
1E5             151 NERSAECGLIITPARLSTADKYLDSPRSGVMAQIYSVRSTLSWGMGDFND    200

WT              201 LGNLASVVAQDGADFLLINPMHAAEPLPPTEDSPYLPTTRRFINPIYIRV    250
                    ||||||||||||||||||||||||||||||||||||||||||||||||||
1E5             201 LGNLASVVAQDGADFLLINPMHAAEPLPPTYDSPYLPTTRRFINPIYIRV    250

WT              251 EDIPEFNQLEIDLRDDIAEMAAEFRERNLTSDIIERNDVYAAKLQVLRAI    300
                    ||||||||||||||||||||||||||||||||||||||||||||||||||
1E5             251 EDIPEFNQLEIDLRDDIAEMAAEFRERNLTSDIIERNDVYAAKLQVLRAI    300

WT              301 FEMPRSSEREANFVSFVQREGQGLIDFATWCADRETAQSESVHGTEPDRD    350
                    ||||||||||||||||||||||||||||||||||||||||||||||||||
1E5             301 FEMPRSSEREANFVSFVQREGQGLIDFATWCADRETAQSESVHGTEPDRD    350

WT              351 ELTMFYMWLQWLCDEQLAAAQKRAVDAGMSIGIMADLAVGVHPGGADAQN    400
                    ||||||||||||||||||||||||||||||||||||||||||||||||||
1E5             351 ELTMFYMWLQWLCDEQLAAAQKRAVDAGMSIGIMADLAVGVHPGGADAQN    400

WT              401 LSHVLAPDASVGAPPDGYNQQGQDWSQPPWHPVRLAEEGYIPWRNLLRTV    450
                    ||||||||||||||||||||||||||||||||||||||||||||||||||
1E5             401 LSHVLAPDASVGAPPDGYNQQGQDWSQPPWHPVRLAEEGYIPWRNLLRTV    450

WT              451 LRHSGGIRVDHVLGLFRLFVMPRMQSPATGTYIRFDHNALVGILALEAEL    500
                    ||||||||||||||||||||||||||||||||||||||||||||||||||
1E5             451 LRHSGGIRVDHVLGLFRLFVMPRMQSPATGTYIRFDHNALVGILALEAEL    500

WT              501 AGAVVIGEDLGTFEPWVQDALAQRGIMGTSILWFEHSPSQPGPRRQEEYR    550
                    ||||||||||||||||||||||||||||||||||||||||||||||||||
1E5             501 AGAVVIGEDLGTFEPWVQDALAQRGIMGTSILWFEHSPSQPGPRRQEEYR    550

WT              551 PLALTTVTTHDLPPTAGYLEGEHIALRERLGVLNTDPAAELAEDLQWQAE    600
                    ||||||||||||||||||||||||||||||||||||||||||||||||||
1E5             551 PLALTTVTTHDLPPTAGYLEGEHIALRERLGVLNTDPAAELAEDLQWQAE    600

WT              601 ILDVAASANALPAREYVGLERDQRGELAELLEGLHTFVAKTPSALTCVCL    650
                    ||||||||||||||||||||||||||||||||||||||||||||||||||
1E5             601 ILDVAASANALPAREYVGLERDQRGELAELLEGLHTFVAKTPSALTCVCL    650

WT              651 VDMVGEKRAQNQPGTTRDMYPNWCIPLCDSEGNSVLIESLRENELYHRVA    700
                    ||||||||||||||||||||||||||||||||||||||||||||||||||
1E5             651 VDMVGEKRAQNQPGTTRDMYPNWCIPLCDSEGNSVLIESLRENELYHRVA    700

WT              701 KASKRD   706
                    ||||||
1E5             701 KASKRD   706
```

Figure 22 Amino acid sequence alignment of E231Y and WT *Cg*AMs using ClustalW tool. The highlights indicated where the mutations located (E231Y)

3.3 Expression and purification of WT and E231Y mutant

From overall screening results, E231Y *Cg*AM was selected to study enzyme characteristics in comparison to the WT enzyme in order to determine the importance of this residue towards *Cg*AM activity, stability and LR-CDs formation.

3.3.1 Optimization of E231Y *CgAM* gene expression

3.3.1.1 Expression of *CgAM* gene with 0.4 mM IPTG induction at 37°C

A single colony of *E. coli* BL21 (DE3) harboring recombinant E231Y plasmid was cultured in LB medium with 100 µg/ml of ampicilin at 37°C, 250 rpm shaking. To induce E231Y *CgAM* gene expression, IPTG was added to the final concentration of 0.4 mM and the cells were harvested at 0, 2, 3, 4 and 5 hr after IPTG induction. Crude extracts at each time point were prepared by sonication as described in section 2.6. Protein patterns of crude extracts and pellets were followed by electrophoresis on 7.5% separating SDS-polyacrylmide gel as shown in Figure 23. The results showed that there was no production of E231Y *Cg*AM in soluble form at 0 hr after IPTG induction while little production was found in inclusion body. At 4 hr after IPTG induction, E231Y *Cg*AM was expressed in soluble form and higher expressed at 5 hr after IPTG induction. However, there was a high production of E231Y *Cg*AM in inclusion body.

3.3.1.2 Expression of *Cg*AM gene with 0.4 mM IPTG induction at 16°C

E. coli BL21 (DE3) carrying E231Y *CgAM* gene was cultivated in 100 ml LB medium containing 100 µg/ml of ampicilin. IPTG was introduced to the final concentration of 0.4 mM and cultured at 16°C. The cells at various times after IPTG

induction were harvested. Crude extracts were obtained via sonication (described in section 2.6). Fifteen micrograms of crude extracts and pellets were subjected to electrophoresis on 7.5% separating SDS-polyacrylmide gel. SDS-PAGE of E231Y *Cg*AM protein patterns at 16°C was shown in Figure 24. The results revealed that there was no production of E231Y *Cg*AM in soluble form at 0 hr after IPTG induction while little was produced as inclusion body. At 2 hr after IPTG induction, E231Y *Cg*AM was primarily expressed in soluble form. E231Y *Cg*AM seemed to be expressed higher with later hr after IPTG induction. At 16 hr after IPTG induction, E231Y *Cg*AM was highly expressed in soluble form. Less inclusion body production was observed under expression at 16°C. It could be clearly seen that the amount of E231Y *Cg*AM produced in soluble was increased when compared to the expression at 37°C. Thus, the cultivation at 16°C for 16 hr with 0.4 mM IPTG induction was chosen for enzyme production by further experiments.

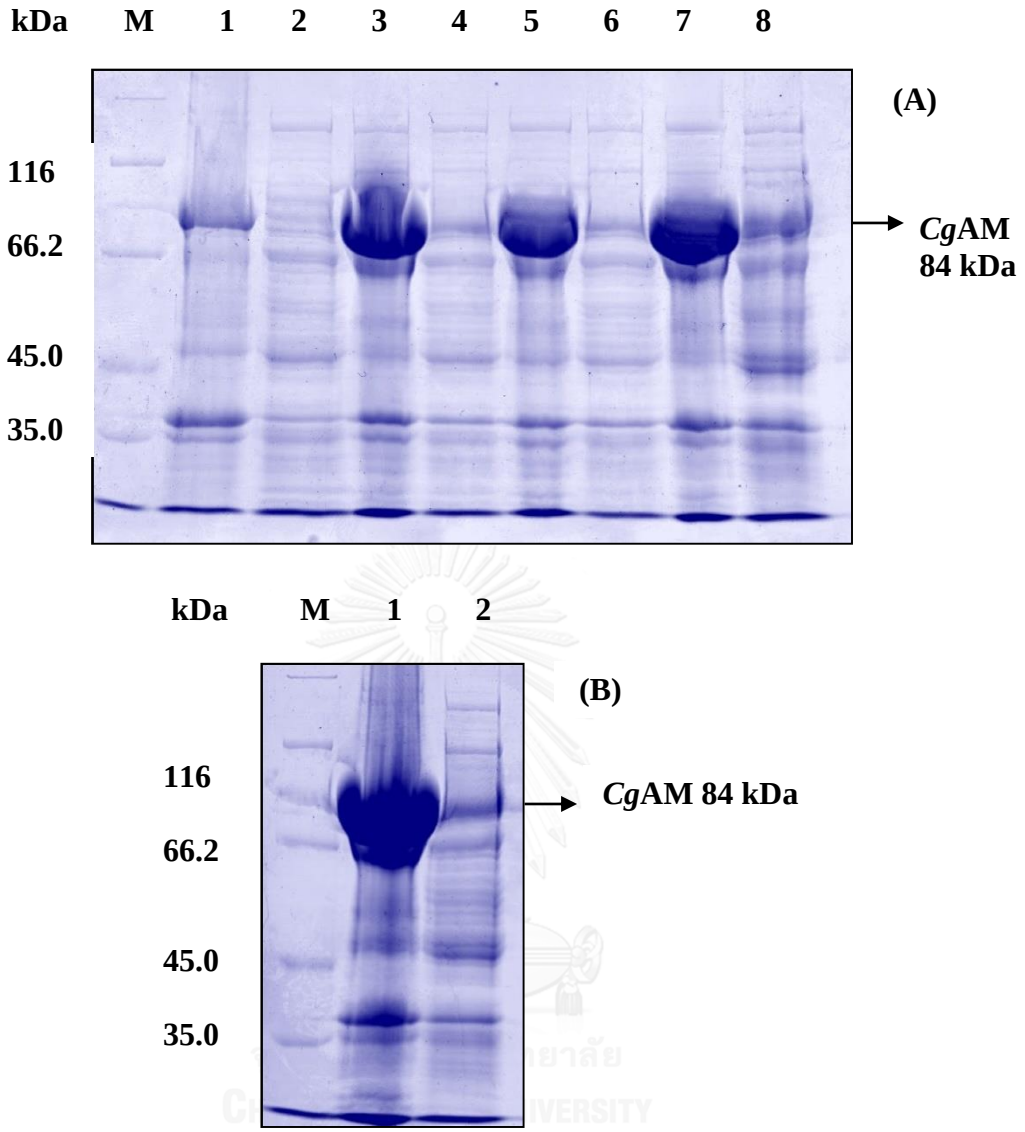

Figure 23 (A) 7.5% SDS-PAGE of crude E231Y *Cg*AM obtained from 37°C cultivation, 0.4 mM IPTG induction at 0 to 4 hr. (B) crude E231Y *Cg*AM obtained from 37°C cultivation, 0.4 mM IPTG induction at 5 hr

Lane M (A and B) = protein marker (Bio Basic, Canada)

Lane 1, 3, 5 and 7 (A) = cell pellets at 0, 2, 3 and 4 hr, respectively

Lane 2, 4, 6 and 8 (A) = supernatant at 0, 2, 3 and 4 hr, respectively

Lane 1 (B) = cell pellets at 5 hr Lane 2 (B) = supernatant 5 hr

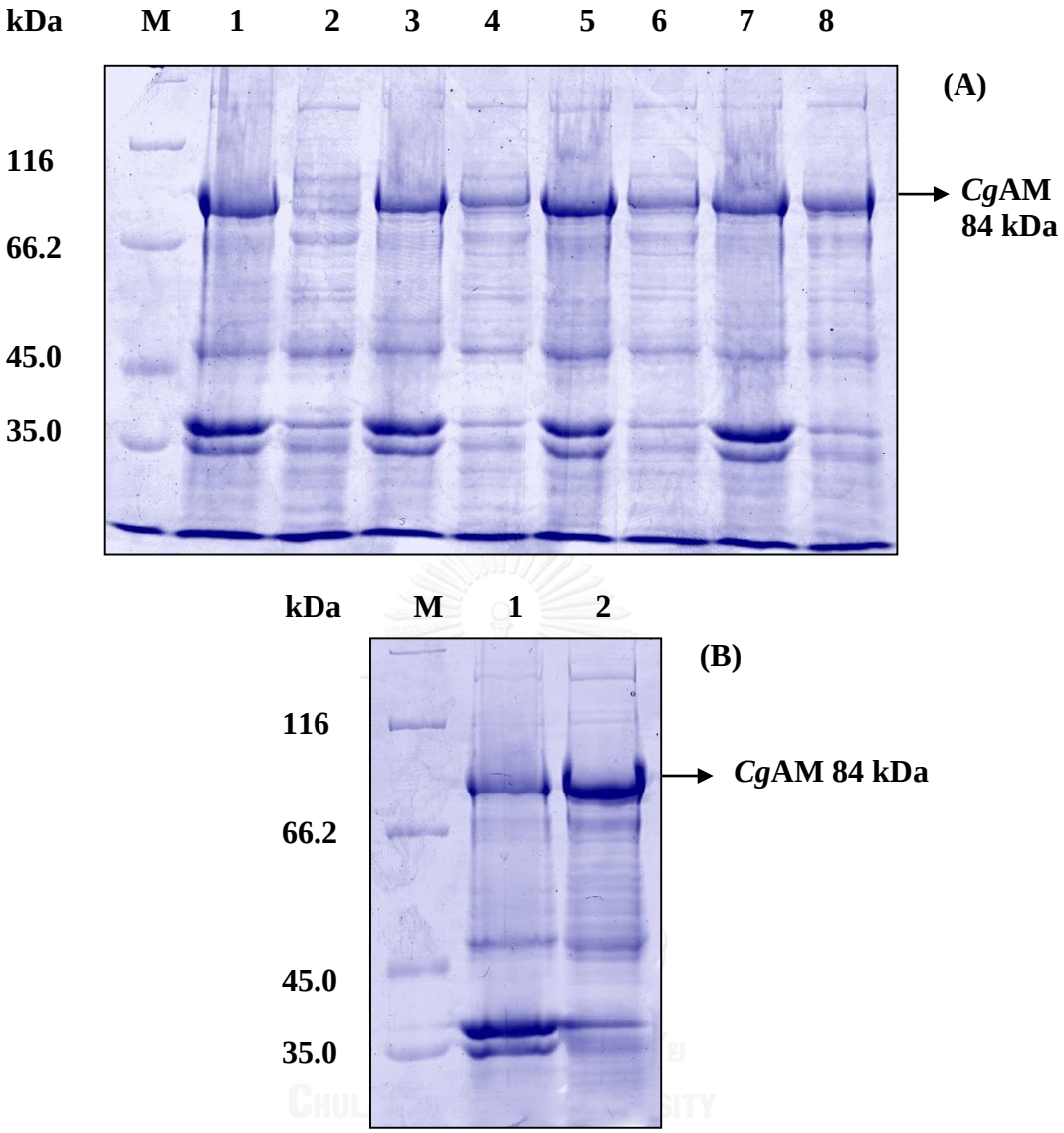

Figure 24 (A) 7.5% SDS-PAGE of crude E231Y *Cg*AM obtained from 16°C cultivation, 0.4 mM IPTG induction at 0 to 6 hr. (B) crude E231Y *Cg*AM obtained from 16°C cultivation, 0.4 mM IPTG induction at 16 hr.

Lane M (A and B) = protein marker (Bio Basic, Canada)

Lane 1, 3, 5 and 7 (A) = cell pellets at 0, 2, 4 and 6 hr, respectively

Lane 2, 4, 6 and 8 (A) = supernatant at 0, 2, 4 and 6 hr, respectively

Lane 1 (B) = cell pellets at 16 hr Lane 2 (B) = supernatant 16 hr

3.3.2 Scale-up of WT and E231Y *Cg*AM production and preparation of crude extracts

E. coli BL21 (DE3) harboring recombinant *CgAM* plasmid was cultured in 3 liters of LB medium supplemented with 100 µg/ml ampicilin. The expression condition of WT enzyme was well-described in section 2.3.3 or 2.4.1. The expression of E231Y enzyme was followed by the condition obtained from section 3.3.1.2. Fifteen milliliters of crude WT enzyme and seventeen milliliters of crude E231Y enzyme were obtained. The specific activity of crude WT and E231Y enzyme were 2.12 and 2.03 U/mg, respectively (Table 5)

3.3.3 Partial purification of WT and E231Y *Cg*AM by DEAE FF™ column chromatography

Crude *Cg*AM extracts were applied onto DEAE FF column as described in section 2.3.4. The elution steps and purification profiles of both *Cg*AMs were similar as previously shown in section 3.1.3, Figure 12 and 19. Partially purified WT and E231Y *Cg*AMs contained specific activities of 22.4 and 11.7 U/mg with 38.6% and 32.0% recovery (Table 5), and were dialyzed against 50 mM phosphate buffer pH 7.4 prior to perform the next purification step.

3.3.4 Purification of *Cg*AMs by Phenyl FF™ column chromatography

3.3.4.1 Purification of WT *Cg*AM

Partially purified WT *Cg*AM was loaded onto Phenyl FF™ column as described in section 2.7.1. The chromatographic profile was shown in Figure 25. Bound proteins were eluted by 2 following steps; 0.2 M ammonium sulfate and 0 M ammonium sulfate elution. There was no starch transglycosylation activity detected in 0.2 M ammonium sulfate eluted fractions. Higher starch transglycosylation activity was detected at 0 M ammonium sulfate eluted fractions. Those fractions were pooled and the specific activity was 41.8 U/mg. The WT *Cg*AM was purified by 19.7 fold with 10.0% recovery (Table 5).

3.3.4.2 Purification of E231Y *Cg*AM

Phenyl FF™ column was equilibrated with 50 mM phosphate buffer pH 7.4 containing 1 M ammonium sulfate as described in section 2.7.2. Partially purified E231Y *Cg*AM was then applied onto Phenyl FF™ column. The purification profile was shown in Figure 26. To elute bound E231Y *Cg*AM, three elution steps were performed as followed; 0.2 M and 0.1 M ammonium sulfate to elute other bound proteins, and 0 M ammonium sulfate to elute bound E231Y *Cg*AM. Fractions eluted by 0.2 M and 0.1 M ammonium sulfate showed no starch transglycosylation activity. Eluted proteins gained from 0 M ammonium sulfate elution step exhibited high starch transglycosylation activity. The active fractions were pooled and the specific activity was 29.8 U/mg. The E231Y *Cg*AM was purified by 14.7 fold with 5.84% recovery.

Purification Table of WT and E231Y *Cg*AMs after purified through two-step purification was shown in Table 5.

3.3.5 Determination of enzyme purity of *Cg*AMs

The purity of *Cg*AMs from each purification step was examined by SDS-PAGE (Figure 27). A single protein band at 84 kDa was observed on both purified *Cg*AMs. This suggested that WT and E231Y *Cg*AMs were successfully purified by two-step purification as previously mentioned.

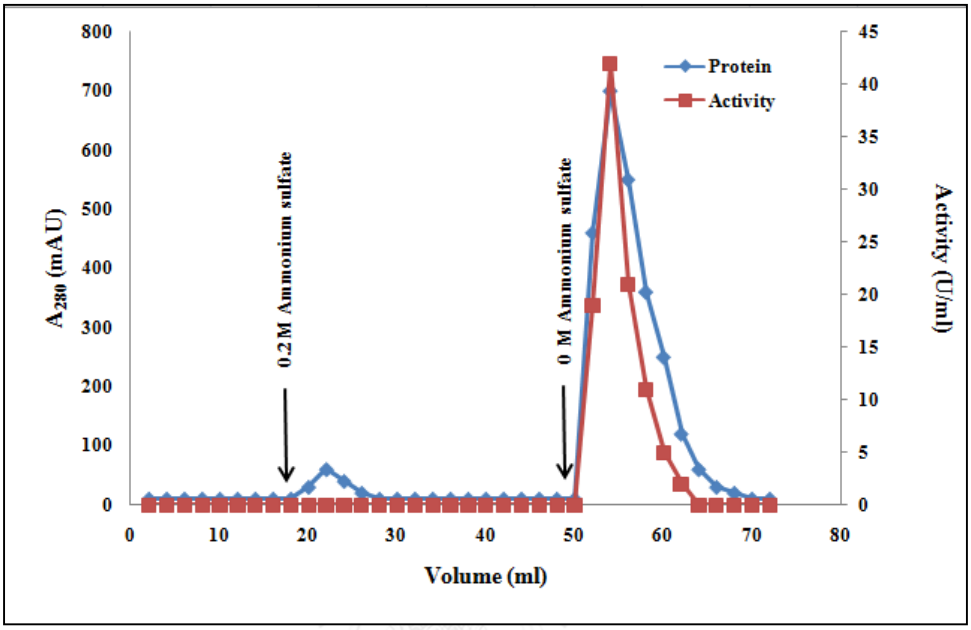

Figure 25 Purification profile of WT by Phenyl FF™ column chromatography. The column was equilibrated with 50 mM phosphate buffer pH 7.4 containing 1 M ammonium sulfate. Bound proteins were eluted by 0.2 M and 0 M ammonium sulfate in the same buffer. Fraction size was 2 ml. The arrows indicated the point at which a stepwise elution was performed. *Cg*AM activity was followed by starch transglycosylation activity assay.

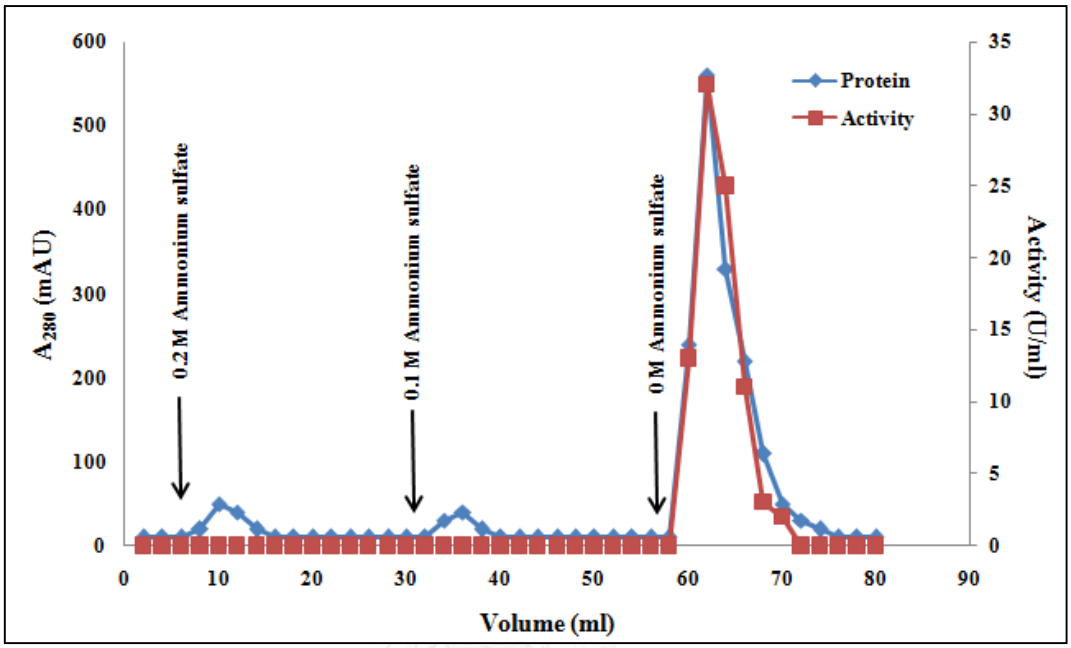

Figure 26 Purification profile of E231Y by Phenyl FF™ column chromatography. The column was equilibrated with 50 mM phosphate buffer pH 7.4 containing 1 M ammonium sulfate. Bound proteins were eluted by 0.2 M, 0.1 M and 0 M ammonium sulfate in the same buffer. Fraction size was 2 ml. The arrows indicated the point at which a stepwise elution was performed. *Cg*AM activity was followed by starch transglycosylation activity assay.

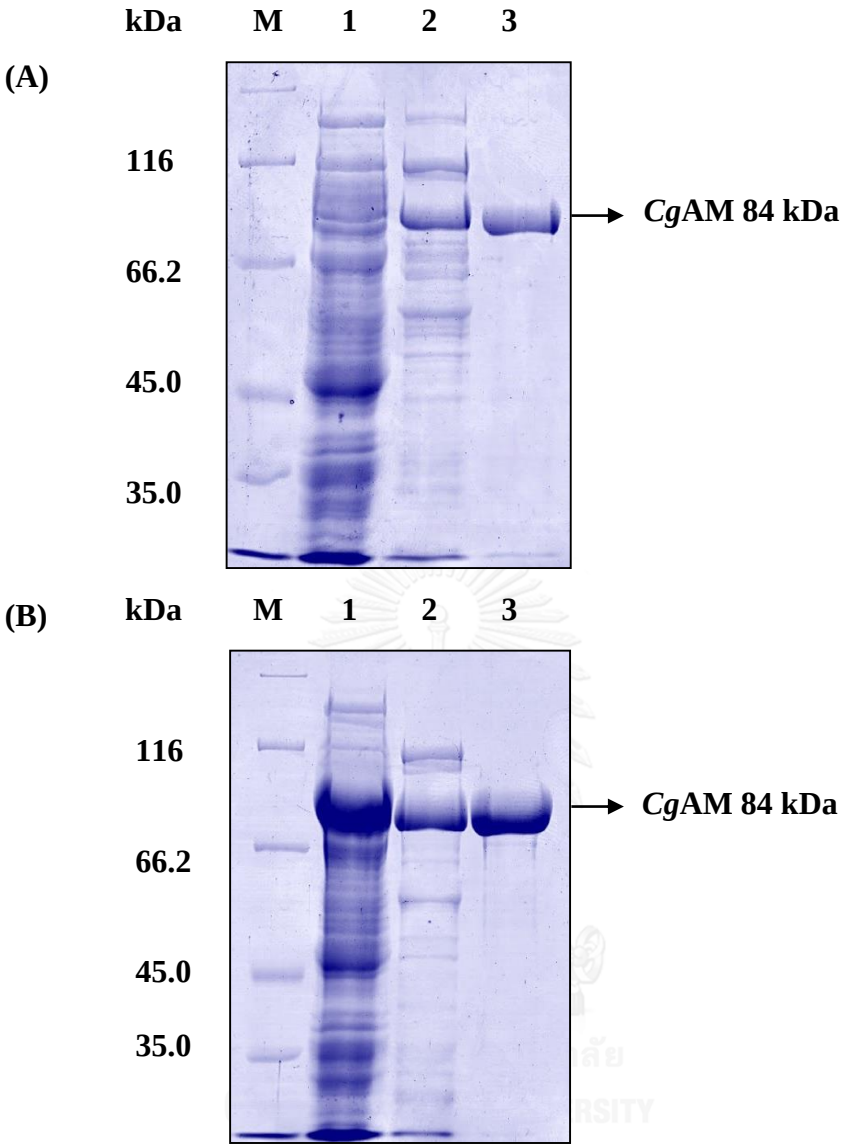

Figure 27 (A) SDS-PAGE analysis of WT *Cg*AM from each purification step (B) SDS-PAGE analysis of E231Y *Cg*AM from each purification step

Lane M (A and B) = protein marker (Bio Basic, Canada)

Lane 1 (A) = crude WT *Cg*AM Lane 2 (A) = partially purified WT *Cg*AM

Lane 3 (A) = purified WT *Cg*AM

Lane 1 (B) = crude E231Y *Cg*AM Lane 2 (B) = partially purified E231Y *Cg*AM

Lane 3 (B) = purified E231Y *Cg*AM

Table 5 Purification Table of WT and E231Y *Cg*AMs

Purification step	Total protein (mg)	Total activity* (U)	Specific activity* (U/mg)	Purification fold	Yield (%)
WT crude extract	404	856	2.12	1	100
WT DEAE FF	14.7	330	22.4	10.6	38.6
WT Phenyl FF™	2.05	85.7	41.8	19.7	10.0
E231Y crude extract	352	714	2.03	1	100
E231Y DEAE FF™	19.5	229	11.7	5.76	32.0
E231Y Phenyl FF	1.4	41.7	29.8	14.7	5.84

**activity assay was performed by starch transglycosylation assay*

3.4 Characterization of E231Y *Cg*AM

3.4.1 Effect of temperature on *Cg*AM activity

Optimum temperatures of starch transglycosylation and disproportionation activity of *Cg*AM were determined as described in section 2.11. The temperatures were observed in range of 20°C to 70°C. For starch transglycosylation activity, the optimum temperatures of WT and E321Y enzyme were found to be 30°C and 35°C, respectively (as shown in Figure 28). WT *Cg*AM could maintain its activity beyond 80% in range of 30°C to 40°C whereas E231Y *Cg*AM displayed 80% of activity in range of 30°C to 35°C. At 50°C and higher, the starch transglycosylation activities of WT and E231Y enzymes were dramatically dropped.

In case of disproportionation activity, the increase of 5°C of the optimum temperature was observed in E231Y *Cg*AM as could be seen in Figure 29. The optimum temperatures were 40°C and 45°C for WT and E231Y *Cg*AMs, respectively. Eighty percent of disproportionation activity could be retained in range of 20°C to 50°C for WT *Cg*AM and 30°C to 45°C for E231Y *Cg*AM.

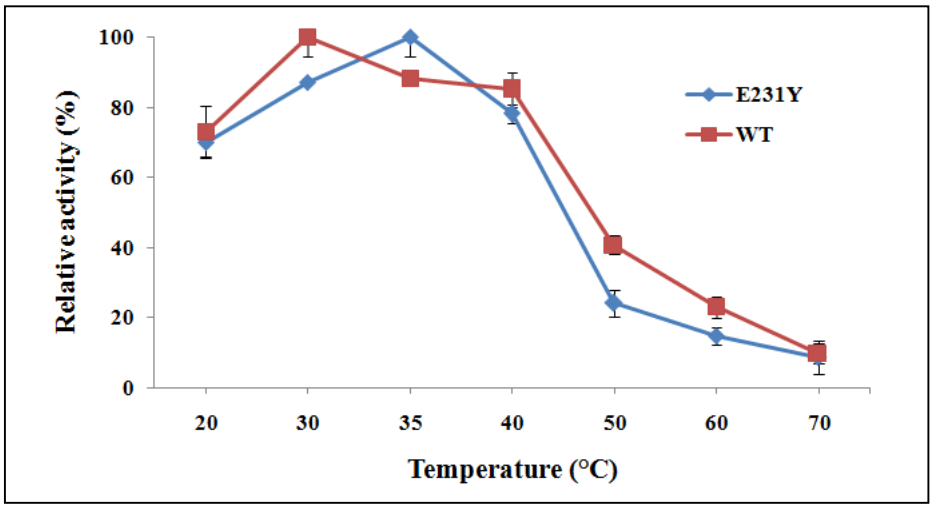

Figure 28 Effect of temperature on starch transglycosylation activity. Purified *Cg*AMs were incubated with 0.2% soluble starch and 1% (w/v) maltose in phosphate buffer pH 6.0 (WT) or pH 6.5 (E231Y) for 10 min at various temperatures. Residual starch was detected by iodine method, measuring at A_{600}.

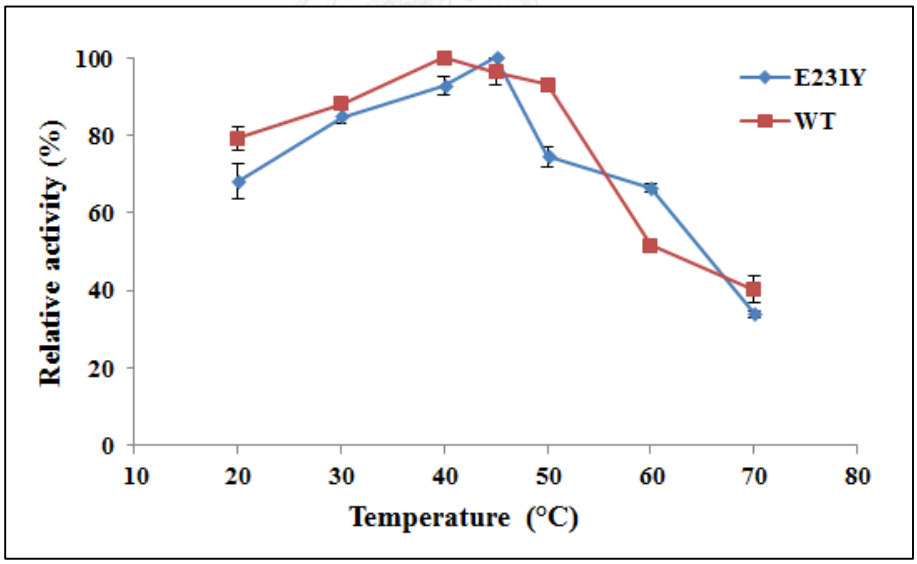

Figure 29 Effect of temperature on disproportionation activity. Purified *Cg*AMs were incubated with 5% (w/v) maltotriose for 10 min at various temperatures. Free glucose, by-product of the reaction, was detected by glucose oxidase method, measuring at A_{505}.

3.4.2 Effect of pH on *Cg*AM activity

The effect of pH was examined on starch transglycosylation and disproportionation activity. Assay conditions and buffer systems were described in section 2.11.2. Figure 30 and 31 showed that the optimum pHs of WT and E231Y CgAMs on starch transglycosylation activity were pH 6.0 and pH 6.5 of phosphate buffer, respectively. At pH 5.0, Both *Cg*AMs shared similarity in 80% or 90% loss of activity and they completely lost their activities at pH 4.0. Phosphate buffer pH range of 6.0 to 8.0 could retain *Cg*AM activity higher than 80%.

As illustrated by Figure 32 and 33 the optimum pHs of disproportionation activity were pH 6.0 and 6.5 of phosphate buffer in WT and E231Y *Cg*AM, respectively. Optimum temperature was shifted 0.5 pH unit upward for E231Y *Cg*AM. Lower acidic pH value (pH 5.0 or below) showed a massively negative effect on disproportionation activity. E231Y *Cg*AM maintained 80% of its activity in phosphate buffer ranging from pH 6.0 to pH 8.0 as same as the WT *Cg*AM did.

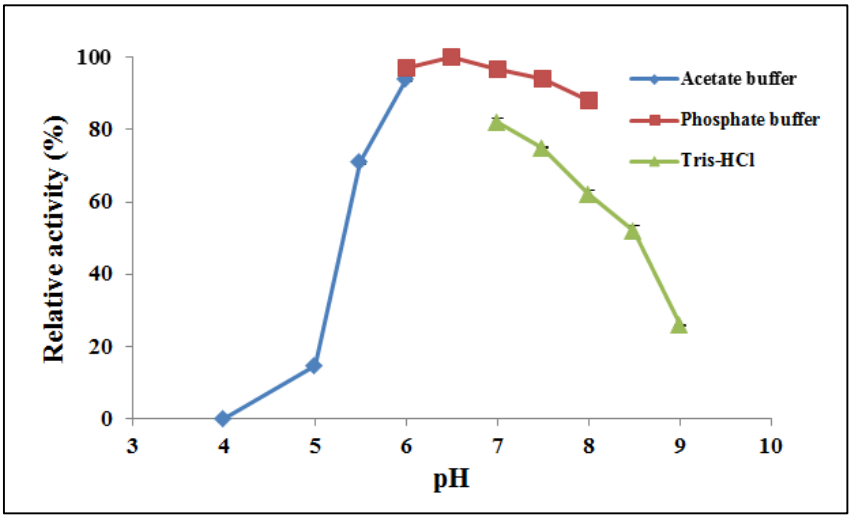

Figure 30 Effect of pH on starch transglycosylation activity of E231Y *Cg*AM. E231Y *Cg*AM was incubated with 0.2% soluble starch and 1% (w/v) maltose at 35°C for 10 min under various pHs. Degraded starch was detected by iodine method, measuring at A_{600}.

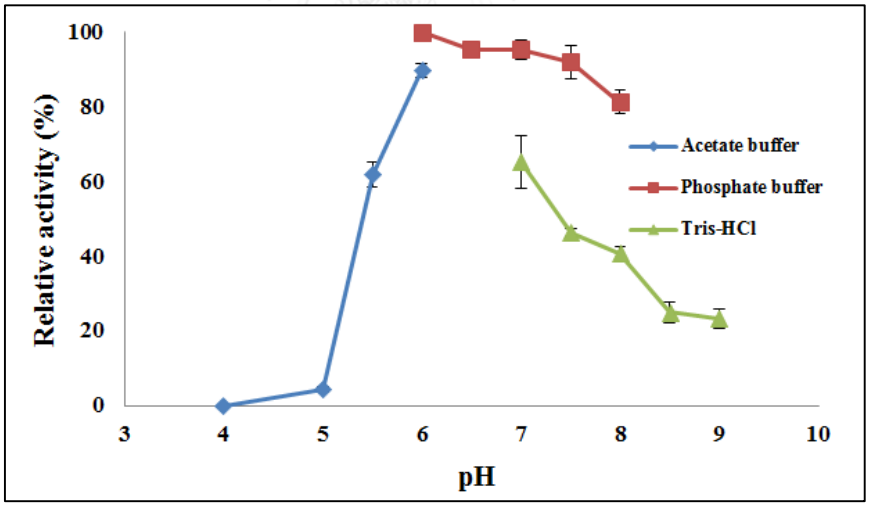

Figure 31 Effect of pH on starch transglycosylation activity of WT *Cg*AM. WT *Cg*AM was incubated with 0.2% soluble starch and 1% (w/v) maltose at 30°C for 10 min under various pHs. Degraded starch was detected by iodine method, measuring at A_{600}.

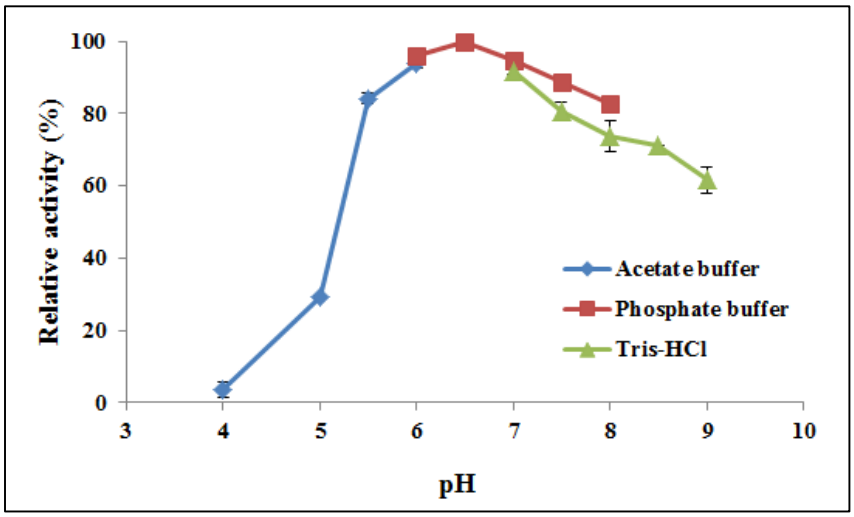

Figure 32 Effect of pH on E231Y *Cg*AM disproportionation activity. E231Y *Cg*AM was incubated with 5% (w/v) maltotriose for 10 min at 45°C under various pHs. Free glucose, by-product of the reaction, was detected by glucose oxidase method, measuring at A_{505}.

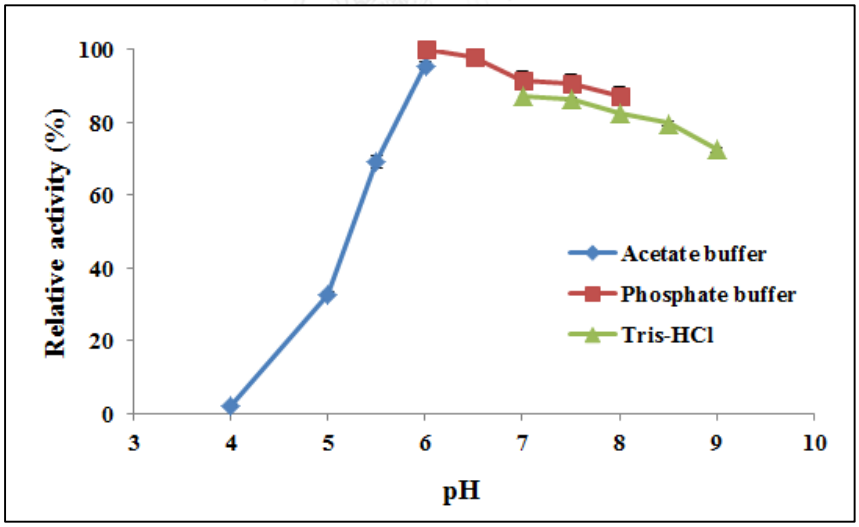

Figure 33 Effect of pH on WT *Cg*AM disproportionation activity. WT *Cg*AM was incubated with 5% (w/v) maltotriose for 10 min at 40°C under various pHs. Free glucose, by-product of the reaction, was detected by glucose oxidase method, measuring at A_{505}.

3.4.3 Temperature stability of *Cg*AM

Temperature stability was observed on starch transglycosylation activity. E231Y *Cg*AM was pre-incubated at various temperatures, ranging from 20°C to 50°C for 0 up to 180 min as described in section 2.113. As can be seen from Figure 34, E231Y *Cg*AM well maintained its activity at the temperature of 20°C and 30°C for 120 min, and lost about 60% after 180 min. At 35°C, E231Y enzyme kept its activity nearly 100% in short incubation time of 10 min. For 20 min up to 60 min incubation time, the remaining activity was around 80%. The residual activity was approximately 60% at 90 to 120 min, and 30% for 180 min. At 40°C, E231Y *Cg*AM marginally lost its activity up to about 80% at 180 min incubation time. At 50°C, the activity was dramatically dropped to 5% in 20 min incubation time, and then distinctly showed no activity after 30 min of incubation.

3.4.4 pH stability of *Cg*AM

The pH stability of starch transglycosylation was followed as described in section 2.11.4. The result was shown in Figure 35. Ninety percent of E231Y *Cg*AM's activity was maintained over the pH range of 5.5 to 8.5: under acetate buffer pH 5.5 to 6.0, under phosphate buffer pH 6.0 to 8.0, and Tris-HCl pH 7.0 to 8.5. At pH 9.0, the residual activity was 85%. The enzyme showed no activity at pH 4.0 and 15% remaining activity at pH 5.0.

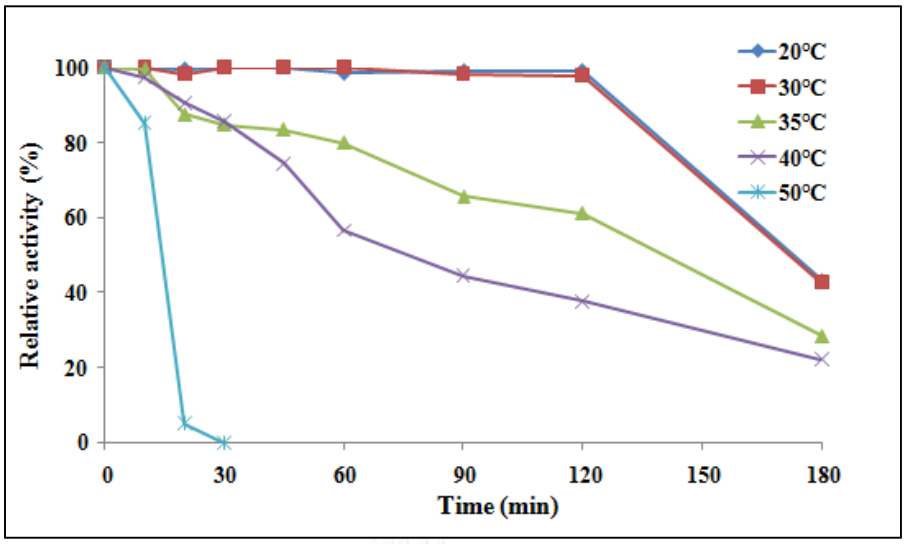

Figure 34 Effect of temperature on E231Y *Cg*AM stability. E231Y *Cg*AM was pre-incubated at various temperatures for 0 to 180 min. Pre-incubated enzyme was subjected to starch transglycosylation activity assay, measuring the amount of residual starch at A_{600}.

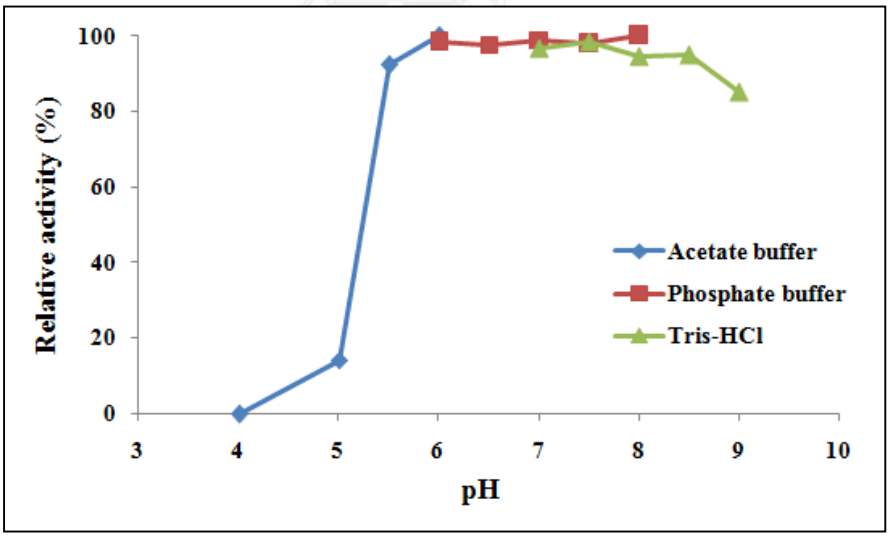

Figure 35 Effect of pH on E231Y *Cg*AM stability. Purified enzyme was pre-incubated at different pHs for 60 min. Pre-incubated enzyme was subjected to starch transglycosylation activity assay, measuring the amount of residual starch at A_{600}.

3.4.5 Activities of *Cg*AM

The effect of E231Y mutation on six *Cg*AM activities was examined as described in section 2.8. The summary of specific activitiy values on various CgAM activities were shown in Table 6. While E231Y *Cg*AM displayed lower specific activity for starch transglycosylation about 1.58 fold than the WT *Cg*AM, it showed higher specific activity of 1.38 fold on disproportionation activity and of 2.75 fold on cyclization activity. It was noticed that there were no differences in the specific activity of starch degradation, coupling and hydrolysis observed on both WT and E231Y enzyme. This could be summarized that E231Y enzyme displayed higher activity of disproportionation and cyclization that those of the WT enzyme.

Table 6 Specific activities of WT and E231Y *Cg*AMs

*Cg*AM activity	Specific activity (U/mg protein)	
	WT *Cg*AM	E231Y *Cg*AM
Starch transglycosylation	66.2	41.8
Disproportionation	52.9	72.6
Starch degradation	1.13	1.13
Cyclization	0.60	1.65
Coupling	0.03	0.03
Hydrolysis	0.02	0.02

3.4.5 Substrate specificity on disproportionation activity of *Cg*AM

An ability of *Cg*AMs to catalyze different substrates (G2 to G7) was observed on disproportionation activity. The procedure was well-described in section 2.11.5. Among all substrates, maltotriose (G3) was the best preferable substrate for both WT and E231Y *Cg*AMs. In contrast, maltose (G2) was found to be the least preferable substrate for both *Cg*AMs. The order of preferable substrate of E231Y *Cg*AM was G3 >> G4 > G5 > G6 ~ G7 > G2 while WT *Cg*AM showed the order of G3 >> G4 > G5 > G6 > G7 ~ G2. This indicated that E231Y enzyme could catalyze G7 better than the WT enzyme. Thus, maltotriose (G3) was used in the assay of disproportionation activity in further experiment.

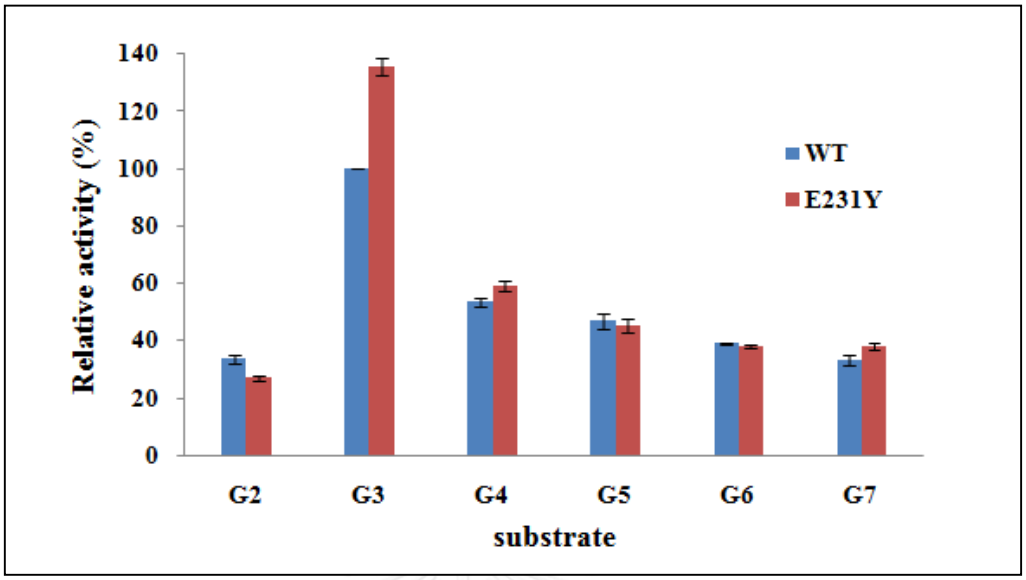

Figure 36 Substrate specificity of WT and E231Y *Cg*AMs on disproportionation activity. *Cg*AMs were incubated at 40°C for WT or 45°C for E231Y under varying substrates (maltose (G2) to maltoheptaose (G7)) for 10 min. The specific activity of WT on G3 substrate was set to 100%.

3.4.6 Kinetic studies of *Cg*AM

3.4.6.1 Kinetic study of starch transglycosylation activity

Kinetic study on starch transglycosylation of E231Y *Cg*AM was investigated in the aim to determine the amount of degraded starch. The residual starch was detected by iodine method as described in section 2.8.1. Lineweaver-Burk plot was constructed using nonlinear least square regression analysis as shown by Figure 37. All kinetic parameters were summarized in Table 7. The result showed that the K_m value of E231Y enzyme was lower than the WT about 8-fold. The turnover numbers (k_{cat}) were 0.43 and 0.18 min^{-1} for WT and E231Y *Cg*AM, respectively. The catalytic efficiency (k_{cat}/K_m) increased 3.3 times than that of the WT.

3.4.6.2 Kinetic study of disproportionation activity

Disproportionation activity was an activity in which a maltosyl group of maltotriose (G3) was transferred to the acceptor and released free glucose to the reaction. The free glucose was detected by glucose oxidase method as described in section 2.8.2. Lineweaver-burk plot of WT and E231Y *Cg*AMs was shown in Figure 38. The summary of kinetic parameters could be seen in Table 3.6. The K_m of E231Y and WT enzyme were 30.3 and 21.7 mM, respectively. The k_{cat} of E231Y *Cg*AM was 1.5-fold increased than that of the WT *Cg*AM. This indicated that the reaction rate of the enzyme to release the products was increased. The catalytic efficiency (k_{cat}/K_m) was 227and 242 $min^{-1}mM^{-1}$ for WT and E231Y *Cg*AM, respectively.

3.4.6.3 Kinetic study of cyclization activity

Kinetic study of E231Y *Cg*AM on cyclization activity, a reaction that produced cyclic oligosaccharide, was performed as described in section 2.11.6.3. The LR-CDs products were analyzed by HPAEC-PAD. Figure 39 represented Lineweaver-burk plot of *Cg*AMs. All kinetic parameters were calculated as shown by Table 9. The K_m value of E231Y *Cg*AM was about 1.5 times lower than WT *Cg*AM, indicating higher affinity towards pea starch. The k_{cat} and k_{cat}/K_m of E231Y *Cg*AMs were approximately 2 and 3-fold greater than those of the WT enzyme.

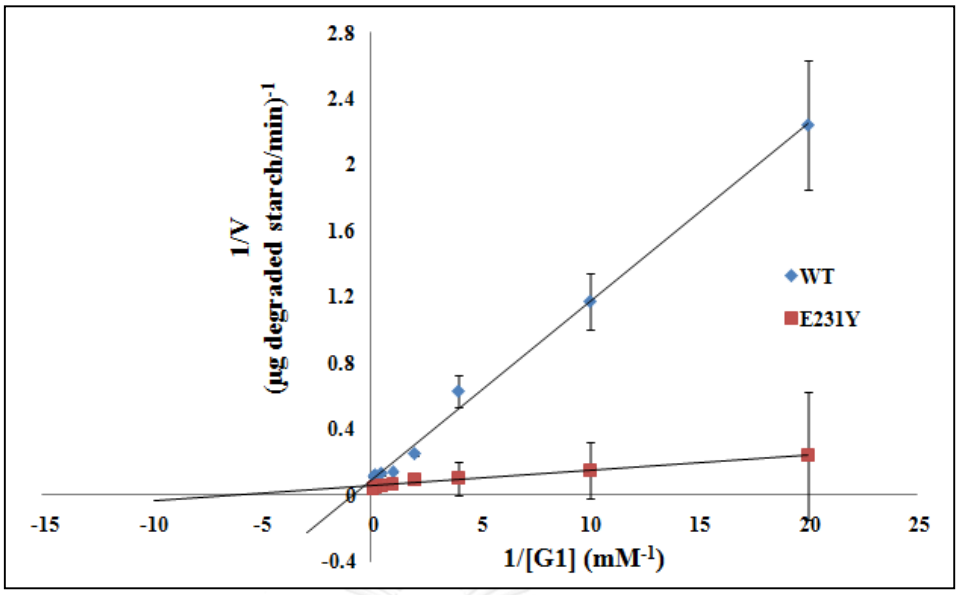

Figure 37 Lineweaver-Burk plot of WT and E231Y *Cg*AMs on starch transglycosylation activity. *Cg*AMs were incubated with 0.2% (w/v) soluble starch at 30°C for WT or 35°C for E231Y under varying acceptor (G1) concentrations. Iodine method was used to determine the residual starch.

Table 7 Summary of kinetic parameters of WT and E231Y *Cg*AMs on starch transglycosylation activity using glucose (G1) as receptor.

*Cg*AM	K_m (mM)	V_{max} (µg degraded starch/min)	k_{cat} (min^{-1})	k_{cat}/K_m ($min^{-1}mM^{-1}$)
WT	1.26	11.6	0.43	0.34
E231Y	0.16	18.2	0.18	1.13

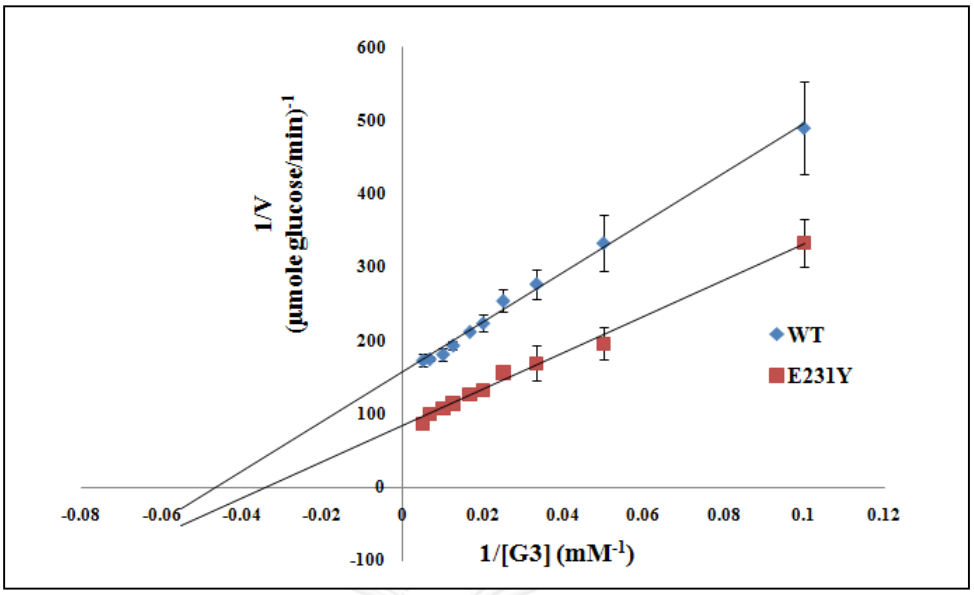

Figure 38 Lineweaver-Burk plot of WT and E231Y *Cg*AMs on disproportionation activity. *Cg*AMs were incubated at 40°C for WT or 45°C for E231Y under varying maltotriose (G3) concentrations. Glucose oxidase method was used to determine the amount of free glucose produced during the reaction.

Table 8 Summary of kinetic parameters of WT and E231Y *Cg*AMs on disproportionation activity using maltotriose (G3) as substrate.

*Cg*AM	K_m (mM)	V_{max} (µmole glucose/min)	k_{cat} (min^{-1})	k_{cat}/K_m ($min^{-1}mM^{-1}$)
WT	21.7	6.39×10^{-3}	4,917	227
E231Y	30.3	12.0×10^{-3}	7,342	242

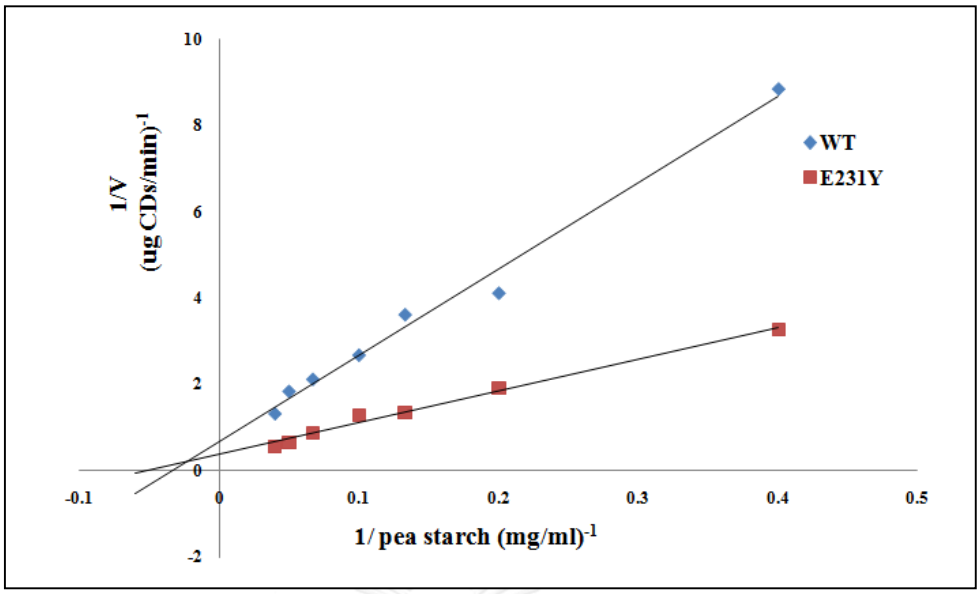

Figure 39 Lineweaver-Burk plot of WT and E231Y *Cg*AMs on cyclization activity. *Cg*AMs with 0.05 U starch degradation activity were incubated with varying concentrations (w/v) of pea starch at 30°C for 60 min. LR-CDs products were analyzed by HPAEC-PAD.

Table 9 Summary of kinetic parameters of WT and E231Y *Cg*AMs on cyclization activity using pea starch as substrate.

*Cg*AM	K_m (mg/ml)	V_{max} (µg CDs/min)	k_{cat} (min^{-1})	k_{cat}/K_m (ml/mg·min)
WT	30.3	1.49	0.03	0.99×10^{-4}
E231Y	20.0	2.70	0.06	3.00×10^{-3}

3.4.7 Effect of incubation time and unit of enzyme on LR-CDs production

3.4.7.1 Effect of incubation time

Effect of incubation time on LR-CDs production was carried out as described in section 2.11.7.1. To compare the LR-CDs product patterns of WT and E231Y, *Cg*AMs carrying 0.05 U of starch degradation were used. LR-CDs profiles were then analyzed by HPAEC-PAD (Figure 40). It was clearly found that the amount of LR-CDs produced by E231Y *Cg*AM was significantly higher than the product of WT through almost every incubation time as followed; CD21 to CD45 at 1 and 3 hr, CD17 to CD37 at 6 hr, CD16 to CD36 at 12 hr. At 1 and 3 hr incubation time, the product patterns of both *Cg*AMs were similar, and their principal CDs were CD27 to CD29. At 6 hr incubation time, the principal CDs of E231Y were shifted downward to CD26 to CD28 while they were maintained in WT (CD27 to CD29). Under incubation time of 12 hr, the principal products of WT and E231Y *Cg*AMs were shifted to CD26 to CD28 and CD24 to CD26, respectively. At 24 hr, CD24 to CD26 and CD22 to CD24 were principal CDs for WT and E231Y *Cg*AMs. Under this incubation time, it was observed that CD27 to CD45 were produced by WT *Cg*AM in higher amount than those of E231Y *Cg*AM. Throughout 24 hr on LR-CDs synthesis, it was noticed that E231Y *Cg*AM showed the faster rate in changing LR-CDs products from larger to smaller ring size. The summary of principal CDs obtained at various incubation times was shown in Table 10.

3.4.7.2 Effect of unit of enzyme

To observe the influence of unit of enzyme on LR-CDs formation, 0.05 U, 0.1 U and 0.15 U starch degradation activities of enzymes were used. The result showed that the increase of unit of enzyme resulted in a shift of the principal CDs products to smaller sizes as presented by Table 11 and Figure 41. At 6 hr incubation time, the amount of larger CDs (CD28 to CD45) produced by 0.05 U of E231Y *Cg*AM was higher than those produced by 0.1 and 0.15 U enzyme. The higher amount of smaller CDs was obtained when the higher unit of enzyme was used: increase of CD17 to CD26 for 0.1 U and CD16 to CD24 for 0.15 U. LR-CDs profiles of WT displayed the same pattern as E231Y profile but different in terms of principal CDs and the amount of product obtained. For longer incubation time (24 hr), when 0.1 U and 0.15 U of E231Y *Cg*AMs were used, CD16 to CD23 were significantly produced. When compared to the WT profile at 24 hr, E231Y *Cg*AM produced a higher amount of total CDs. E231Y *Cg*AM could produce smaller CDs faster than WT *Cg*AM under longer incubation time and higher unit of enzyme.

(A)

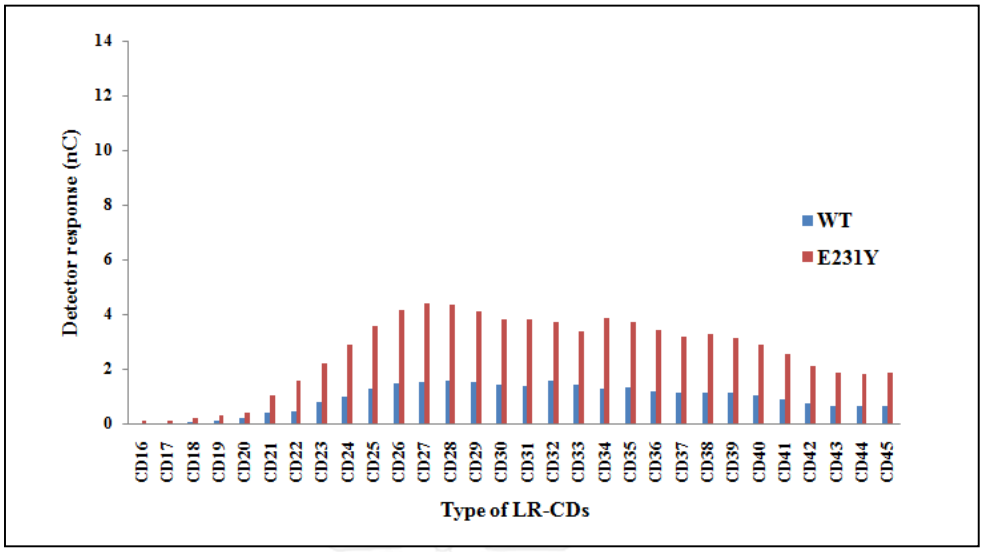

(B)

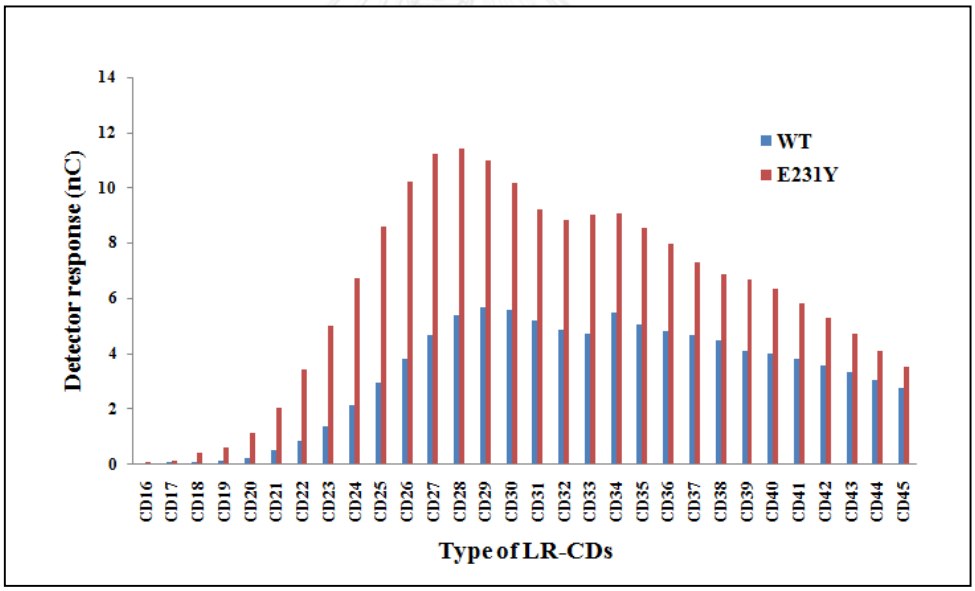

Figure 40 HPAEC analysis of LR-CDs profiles at different incubation times. *Cg*AMs carrying 0.05 U starch degradation activity were incubated with 0.2% (w/v) pea starch at 30°C. (A) Incubation of 1 hr (B) Incubation time of 3 hr

(C)

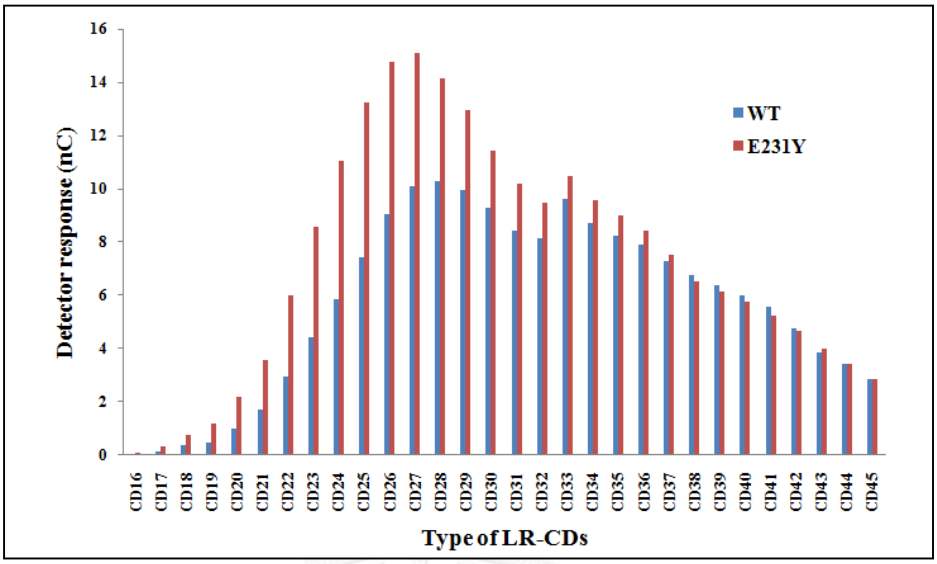

(D)

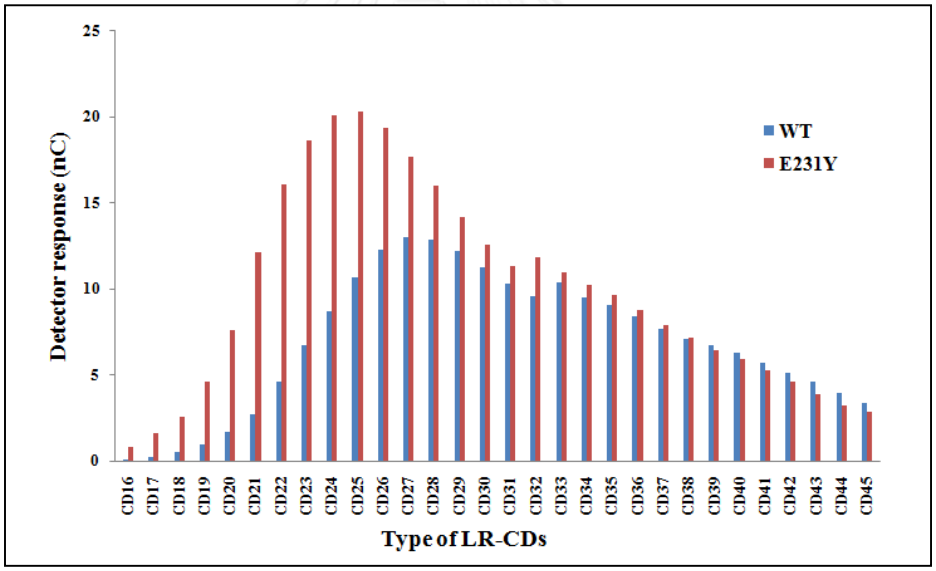

Figure 40 (continue) HPAEC analysis of LR-CDs profiles at different incubation times. *Cg*AMs carrying 0.05 U starch degradation activity were incubated with 0.2% (w/v) pea starch at 30°C. (C) Incubation of 6 hr (D) Incubation time of 12 hr

(E)

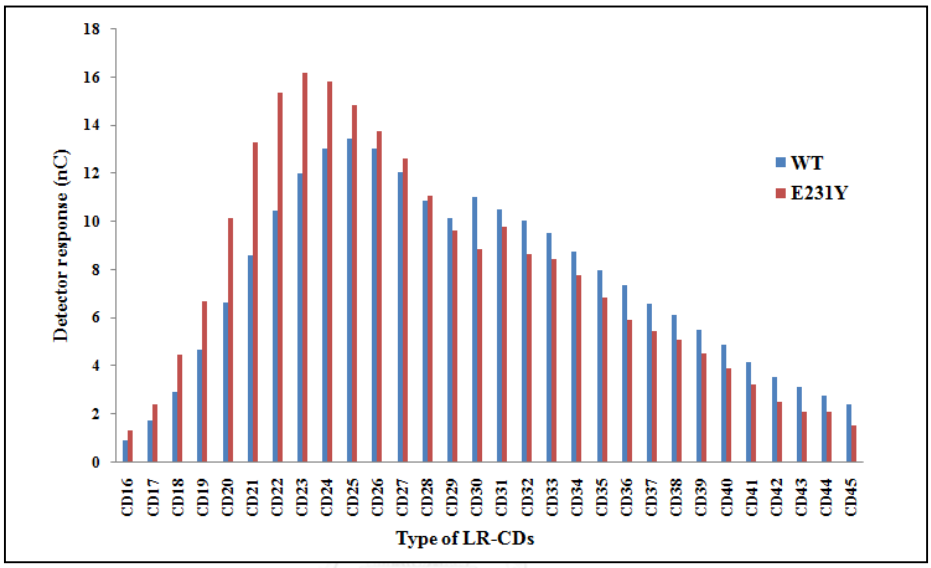

Figure 40 (continue) HPAEC analysis of LR-CDs profiles at different incubation times. *Cg*AMs carrying 0.05 U starch degradation activity were incubated with 0.2% (w/v) pea starch at 30°C. (E) Incubation time of 24 hr

(A)

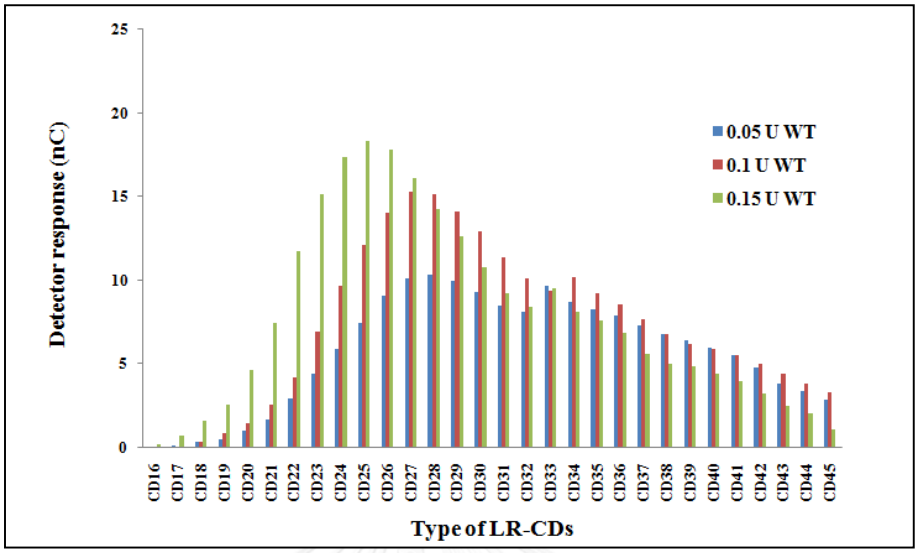

(B)

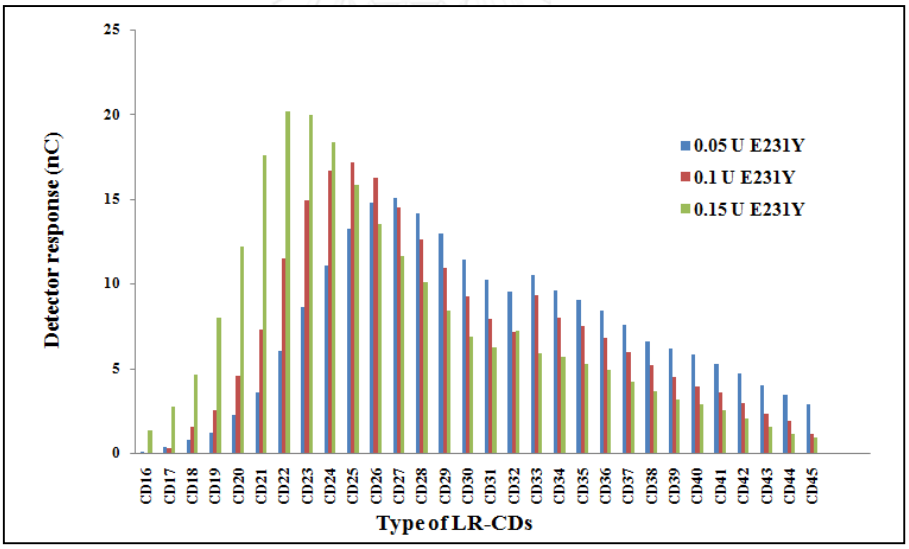

Figure 41 HPAEC analysis of LR-CDs profiles obtained by *Cg*AMs with 0.05, 0.1 and 0.15U of starch degradation activity. *Cg*AMs were incubated with 0.2% (w/v) pea starch at 30°C. (A) Incubation time of 6 hr (B) Incubation time of 6 hr

(C)

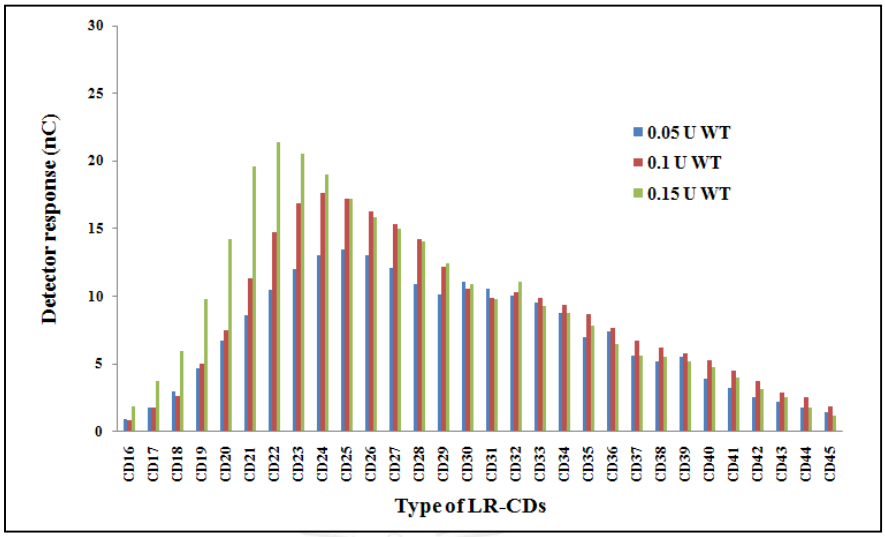

(D)

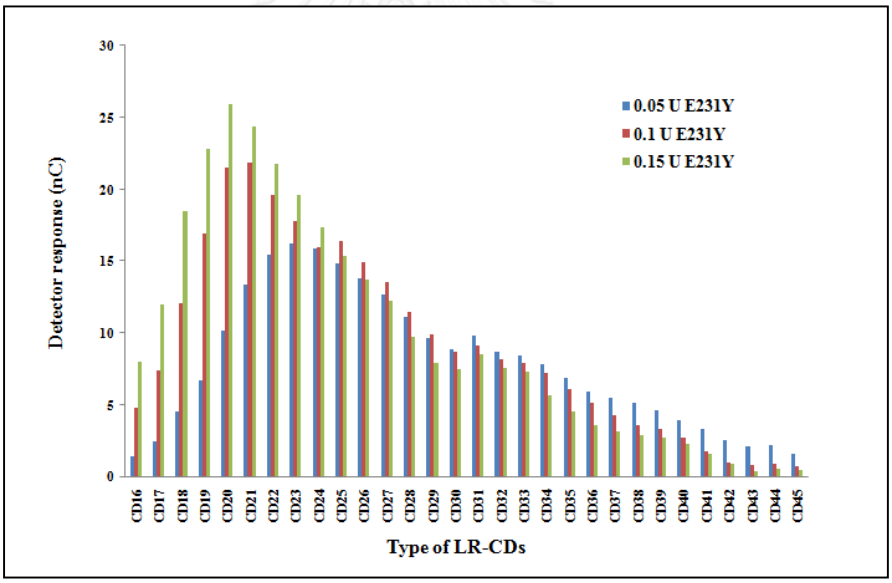

Figure 41 (continue) HPAEC analysis of LR-CDs profiles obtained by *Cg*AMs with 0.05, 0.1 and 0.15U of starch degradation activity. *Cg*AMs were incubated with 0.2% (w/v) pea starch at 30°C. (C) Incubation time of 24 hr (D) Incubation time of 24 hr

Table 10 Summary of principal CDs obtained under varying incubation times by *Cg*AMs carrying 0.05 U starch degradation activity

Incubation time (hr)	Principal CDs	
	WT	E231Y
1	CD27 to CD29	CD27 to CD29
3	CD27 to CD29	CD27 to CD29
6	CD27 to CD29	CD26 to CD28
12	CD26 to CD28	CD24 to CD26
24	CD24 to CD26	CD22 to CD24

Table 11 Summary of principal CDs obtained under varying the amount of enzyme

Incubation time (hr)	Amount of enzyme* (U)	Principal CDs	
		WT	E231Y
6	0.05	CD27 to CD29	CD26 to CD28
	0.1	CD27 to CD29	CD24 to CD26
	0.15	CD24 to CD26	CD22 to CD24
24	0.05	CD24 to CD26	CD24 to CD26
	0.1	CD23 to CD25	CD20 to CD22
	0.15	CD21 to CD23	CD19 to CD21

**unit of starch degradation activity*

3.4.8 Secondary structure analysis by Circular dichroism (CD) spectrometry

In order to investigate the effect of E231Y mutation on secondary structure and folding property on *Cg*AM, circular dichroism (CD) analysis was performed. Purified WT and E231Y *Cg*AMs with 0.2 mg/ml concentration were subjected to wavelength scanning in the range of 190 to 250 nm. The overlay of *Cg*AMs' CD spectra was shown in Figure 42. The result revealed that the CD spectra of WT and E231Y *Cg*AM were closely overlaid. The ratio of α-helix, β-sheet and random coil, estimated by K2D3 program, was 35%, 16% and 49% in WT and 32%, 19% and 49% in E231Y *Cg*AM.

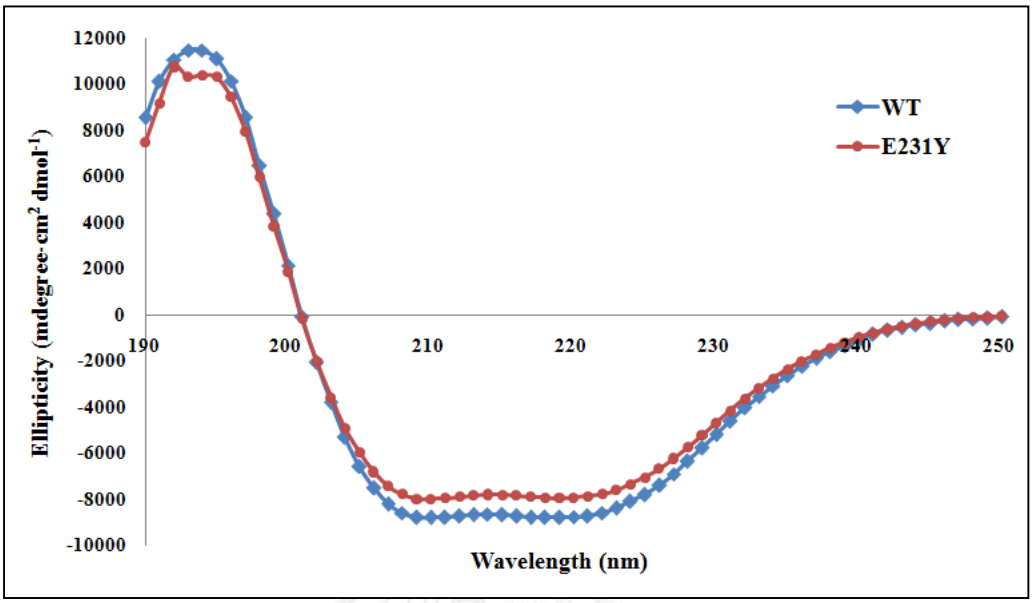

Figure 42 Circular dichroism (CD) spectra of WT and E231Y *Cg*AMs. *Cg*AMs with 0.2 mg/ml were analyzed by CD spectrometer (J-815, Jasco, Japan) under wavelength scanning from 190 to 250 nm at 25°C.

Table 12 Estimation of *Cg*AMs' secondary structure composition, calculated by K2D3 program.

*Cg*AM	Percentage of secondary structure composition		
	α-helix	β-sheet	Random coil
WT	35%	16%	49%
E231Y	32%	19%	49%

CHAPTER IV

DISCUSSION

In Starch and Cyclodextrin Research Unit, AM from *C. glutamicum* was successfully cloned with an ORF of 2,121 bps which could be deduced into 706 amino acids, and expressed in *E. coli* BL21 (DE3) (Srisimarat *et al*., 2012). *Cg*AM catalyzes four main reactions comprising disproportionation, cyclization, coupling and hydrolysis activity (Takaha and Smith, 1999). The catalytic mechanism of *Cg*AM, however, has not yet been elucidated. The intriguing property of AMs is to produce large-ring cyclodextrins (LR-CDs) with a DP of 19 and higher. Nowadays, LR-CDs have considerably interested to be used in several applications such as pharmaceuticals, food science and protein refolding kit etc (Machida *et al*., 2000, Sasaki and Akiyoshi, 2010). Due to the fact that LR-CDs are just becoming an alternative choice to study, in depth investigation on LR-CDs formation of AMs is required. This research aims to identify a key residue of *Cg*AM that play a vital role in determining the LR-CDs product pattern. When the knowledge is gained, it would be better to improve LR-CDs production or selectively produce a range of LR-CDs size of interest (Penninga *et al*., 1995). In this work, mutant with altered LR-CDs profile was screened and selected to characterization in order to obtain the effects of mutation on *Cg*AM characteristic and to extend the knowledge on structure-function relationship.

4.1 Screening for mutant with altered LR-CDs profile from random mutagenesis library

4.1.1 Screening by disproportionation activity assay

Random mutagenesis library is supported by Asst. Prof. Kuakarun Krusong, Ph.D. in the aim to screen for a mutated *Cg*AM that possesses an altered LR-CDs profile. At first, those mutagenesis clones were randomly screened by disproportionation activity assay. Disproportionation activity along with cyclization activity is the main activities of *Cg*AM (Srisimarat *et al*., 2011). A clone that retained at least 80% of WT's activity was selected for further investigation while the others were neglected. The result indicated that there were numerous clones lowering in disproportionation activity. This might cause by mutations on *CgAM* gene at position that probably belonged to catalytic site or other vital part of *Cg*AM. Furthermore, those clones might be constructed by PCR-mediated random mutagenesis using high concentration of $MnCl_2$, leading to higher rate of base substitutions on *CgAM* gene (Fujii *et al*., 2005, Melzer *et al*., 2015, Pritchard *et al*., 2005). 1E5 and H5 mutants were purposeful candidates according to the selection criteria. They displayed over 100% disproportionation activity as compared to the WT.

4.1.2 Expression and partial purification of WT and selected *Cg*AMs

CgAM gene is inserted to the downstream region of T7 promoter of pET-17b. Based upon pET system, T7 RNA polymerase binds to the T7 promotor in order to initiate *CgAM* transcription. However, the operator site is blocked by *lac* repressor protein. Addition of IPTG can decrease the affinity of *lac* repressor towards the operator

site, allowing the transcription of *Cg*AM gene. In this work, the expression of *CgAM* gene was triggered by 0.4 mM IPTG induction. All *Cg*AMs in Starch and Cyclodextrin Research Unit were reported to be expressed as intracellular enzymes (Srisimarat *et al*., 2011, Tantanarat *et al*., 2014, Kaewpathomsri *et al*., 2015, Nimpiboon *et al*., 2016). The cells were harvested after 2 hr IPTG induction and then disrupted via sonication. The specific activity of crude *Cg*AMs was shown in Table 3. The optimum expression of WT *CgAM* gene was at 2 hr after IPTG induction (Srisimarat *et al*., 2012). Thus, this work followed the optimum expression as previously reported and the specific activity of crude *Cg*AM (about 2.2 U/mg) was not different from that of the precedent report. In case of mutated *Cg*AMs, the optimization will be performed for a selective mutant of which the altered LR-CDs profile was confirmed. At 2 hr after IPTG induction, fortunately, crude 1E5 and H5 *Cg*AMs contained a specific activity about 1.5 to 1.8 U/mg (Table 3). They would be then subjected to partial purification without considering the optimized expression condition by this time due to an enough enzyme activity for further experiment.

CgAM gene under pET-17b expression vector was expressed without His-tag. In the first step, DEAE FF™ column was used to purify *Cg*AM. DEAE FF™ column is a weak anion exchange chromatography so that the proteins with net negative charge are retained in a column matrix, and can be eluted by increasing the ionic strength of the elution buffer. SDS-PAGE of partially purified *Cg*AMs showed many protein bands as shown in Figure 15. This may be due to the fact that there are several proteins holding a net negative charge under pH 7.4 of 50 mM phosphate buffer. WT *Cg*AMs was successfully partially purified with a specific activity of about 15 U/mg with 30% yield while mutated *Cg*AMs contained specific activity of 8 U/mg with 20% yield. According

to previous report, partially purified WT *Cg*AM showed a specific activity of 13 U/mg with 36% recovery (Srisimarat *et al*., 2011).

4.1.3 Analysis of LR-CDs profiles

The other main activity of AM is cyclization activity, an intramolecular transglycosylation to form larger cyclic oligosaccharide called large-ring cyclodextrin (Takaha and Smith, 1999, Zheng *et al*., 2002b, Zheng *et al*., 2002a). Due to the fact that pea starch contained a high content of amylose, depending upon the variety of peas, it has been used as a substrate for LR-CDs production (Vilaplana *et al*., 2012). *Cg*AM shows higher affinity towards starch with high amylose content (Hilbert and Mac, 1946), investigated by iodine method (Vongpichayapaiboon *et al*., 2016). LR-CDs were synthesized and then analyzed by HPAEC-PAD. The LR-CDs product profiles of all *Cg*AMs were compared as shown by Figure 16. The result demonstrated that 1E5 *Cg*AM could produce higher amount of CD26 to CD35, but maintained the principal CDs (CD27 to CD29) as the WT's. Meanwhile, the principal CDs of H5 were CD30 to CD32 and CD34 to CD36. Both LR-CDs product profiles of 1E5 and H5 *Cg*AMs were different from that of WT enzyme. It is possible that 1E5 and H5 mutant carry mutated amino acid residues at substrate binding site.

4.2 Screening for mutant with altered LR-CDs profiles from site-directed mutagenesis clones

According to the structure of *Cg*AM obtained via x-ray crystallographic technique (Srisimarat *et al*., 2013) and prepared to publish, some mutants were constructed by site-directed mutagenesis based upon the fitting 3D structure. In this work, E231Y mutant was selected to study.

4.2.1 Expression and purification of E231Y *Cg*AM

E231Y *Cg*AM gene was also expressed under T7 promoter of pET-17b. The basic principle of pET-system expression has been discussed in section 4.1.2. In this work, the expression of *CgAM* gene was induced by 0.4 mM IPTG induction. The cells were harvested after 4 hr IPTG induction and then disrupted via sonication. The specific activity of crude *Cg*AMs was shown in Table 4.

E231Y *Cg*AM was achieved in partial purification by using the process discussed early in section 4.1.2. WT *Cg*AMs was successfully partially purified with a specific activity of about 12.3 U/mg with 27% yield whilst E231Y *Cg*AM contained specific activity of 4.84 U/mg with 20.5% yield.

4.2.2 Analysis of LR-CDs profile of E231Y *Cg*AM

Produced under controlling unit of enzyme (0.05 U of starch degradation) and 6 hr incubation time, WT and E231Y LR-CDs mixtures were analyzed by HPAEC-PAD. Merged *Cg*AMs' LR-CDs profiles were shown in Figure 20. The principal CDs of E231Y enzyme were dramatically shifted upward to CD42 to CD44 whereas the WT's was CD27 to CD29. This can be proposed that E231Y mutation may be located nearly the substrate binding site. The proposal of E231Y effect on *Cg*AM activity will be discussed in section 4.4.

4.3 Expression and purification of WT and E231Y *Cg*AM

4.3.1 Optimization of E231Y *CgAM* gene expression

As previously mentioned, *CgAM* gene expression was triggered by 0.4 mM IPTG induction. E231Y *Cg*AM was expressed in *E. coli* BL21 (DE3) using pET-17b expression vector. Aiming to obtain more intracellular expression, optimization of E231Y *CgAM* gene expression was carried out. The result indicated that *Cg*AM production at 37°C resulted in inclusion body formation after IPTG induction with little production (10 to 15%) as soluble protein (Figure 23). The formation of inclusion body is especially true under conditions of high level expression, leading to distort native state of the enzyme (Strandberg and Enfors, 1991). Although *Cg*AM became more expressed as soluble protein at 4 and 5 hr after IPTG induction, it did not contain higher starch transglycosylation activity. Recombinant *Cg*AM was overexpressed as inclusion body, aggregated forming in the interior of *E. coli* cells. Proteins recovered from inclusion bodies could sometimes be refolded into their native states, but, due to their

diverse physicochemical properties, a versatile refolding approach was still lacking (Kuroda, 2009). In this work, the expression condition was improved by cultivation at lower temperature (16°C) instead (Esposito and Chatterjee, 2006). The result showed that soluble *Cg*AM could be obtained at 2 hr after IPTG induction. The highest starch transglycosylation activity was found at 16 hr after IPTG induction (data not shown). It was also observed that the accumulation of inclusion bodies was clearly decreased. This might probably be due to decreasing of the rate of protein synthesis. Thus, this appropriate condition was used for the expression of E231Y *Cg*AM. There are several strategies that are available to decrease the inclusion body formation such as using weaker promoter, lowering the inducer concentration, changing the growth medium, using mild solubilizing agent etc. (Strandberg and Enfors, 1991, Esposito and Chatterjee, 2006, Fernandez *et al*., 2007, Singh *et al*., 2015)

4.3.2 Purification of WT and E231Y *Cg*AMs

To obtain purified WT and E231Y *Cg*AMs, two-step purification was performed by these following steps; DEAE FF™ and Phenyl FF™ column chromatography, respectively. The concept of purification using DEAE FF™ column has been previously discussed in section 4.1.2. Phenyl FF™ column is known as hydrophobic interaction chromatography (HIC). The separation is based upon the hydrophobic interactions of proteins and immobilized phenyl groups. As bound proteins differ in hydrophobicity, separation is based on the varying strength of the hydrophobic interactions. Binding is promoted by the presence of moderately high concentrations of anti-chaotropic salts and elution is improved by decreasing the affinity towards hydrophobic groups on the medium, usually by decreasing the ionic

strength of the elution buffer (Nelson and Cox., 2005). As previously mentioned, Phenyl FF™ column must be equilibrated with the buffer containing 1 M ammonium sulfate, and protein sample must contain 1 M ammonium sulfate as well in order to promote binding interaction. Bound *Cg*AMs were eluted by decreasing concentration of ammonium sulfate to 0 M.

SDS-PAGE analysis presented a single *Cg*AM band of 84 kDa (Figure 27). This indicated an achievement of *Cg*AM purification in two-step purification. The molecular mass of *Cg*AMs, expressed with no His-tag at N terminus, was close to previous report (Srisimarat *et al*., 2011). The size of *Cg*AM was closed to AM from *Thermococcus litoralis*, 79 kDa (Xavier *et al*., 1999); on the other hand, the size was obviously different to AMs from *Thermus* sp., 57 kDa of *T. aquaticus* (Terada *et al.*, 1999) and 55 kDa of *T. filiformis*, (Kaewpathomsri *et al*., 2015), and 72 kDa of AM from *E. coli* (Pugsley and Dubreuil, 1988). In addition, *Cg*AM was known to be a single polypeptide chain with no subunit (Srisimarat *et al*., 2011) However, some dimer AMs have been reported in *Pseudomonas stutzeri* (Terada *et al*., 1999) and pea chloroplast (Lu and Sharkey, 2004).

4.4 Characterization of E231Y *Cg*AM

4.4.1 Effect of temperature and pH on *Cg*AM activities

E231Y *Cg*AM displayed an increasing in optimum temperature by 5°C on both starch transglycosylation (35°C) and disproportionation activity (45°C) when compared to the WT. A slight increase of optimum pH (0.5 pH unit from WT optimum) was observed on both activities as well; pH 6.5 was the most suitable pH for E231Y *Cg*AM. This can be stated that E231Y mutation may play some effects on *Cg*AM, resulted in a change of these characteristics. Optimum temperature can be explained as a temperature at which the enzyme reaches its maximum catalyzing power with the simultaneous decrease in the amount of active enzyme through thermal irreversible inactivation (Daniel and Danson, 2010). Thus, it is possible that mutation at Glu-231shifts the most effective native state of the enzyme to higher temperature. Consequently, a change of optimum pH can also be described that the enzyme approaches its most favorable native state at that pH (Daniel and Danson, 2013).

4.4.2 Effect of temperature and pH on *Cg*AM stability

The temperature and pH stability of E231Y *Cg*AM on starch transglycosylation activity were studied. As could be seen in Figure 34, the activity was well maintained (nearly 100% up to 120 min) at 20°C and 30°C. At the optimum temperature, the activity could be maintained around 80% (up to 60 min) and 60% (up to 120 min). Higher temperature immensely decreased its stability. E231Y *Cg*AM shared the same pattern of temperature and pH stability as WT pattern (Srisimarat *et al*., 2012). This could be proposed that E231Y mutation did not alter the stability of the enzyme.

Although the optimum temperature of E231Y *Cg*AM was changed, it was not correlated with the stability of the enzyme. E231Y enzyme could maintain nearly 100% of activity at no more 10 min incubation time at the optimum temperature. This could be suggested that Glu-231 of *Cg*AM did not involve in thermal stability.

4.4.3 *Cg*AM activities

All *Cg*AM activities were examined and those specific activity values were shown in Table 6. In comparison to the WT *Cg*AM, E231Y *Cg*AM displayed higher specific activity of disproportionation activity (1.38-fold) and cyclization activity (2.75-fold), respectively. Conversely, lower specific activity was observed on starch transglycosylation activity (1.58-fold) of E231Y *Cg*AM. Meanwhile, starch degradation, hydrolysis and coupling activity of E231Y *Cg*AM were not different from the WT. Generally, *Cg*AM exhibits low hydrolysis and coupling activity as its common characteristic (Fujii *et al*., 2007, Hansen *et al*., 2009, Srisimarat *et al*., 2012)

The result of structural superimposition of *Cg*AM and *Thermus aquaticus* amylomaltase (*Ta*AM) revealed that Glu-231 residue of *Cg*AM was closely corresponded with Tyr-54 of *Ta*AM (Figure 43). Previously, Tyr-54 is reported as one of the key residues, apart from Ser-470, mainly located at a secondary glucan binding site. It functions in curving an amylose chain during cycloamylose formation. In spite of the fact that the second binding glucan site is unique in AM, the conserved amino acids of this site are ambiguous (Przylas *et al*., 2000a). Tyr-54, in conjunction with Tyr-101, of *Ta*AM contributes to help stabilize the binding of amylose via hydrophobic interaction as shown by Figure 44 (Przylas *et al*., 2000b). Glu-231 residue of *Cg*AM is therefore proposed to be a part of this second glucan binding site. The increase in

cyclization activity of E231Y *Cg*AM may result from a change in this glycan binding site which leads to promote affinity towards pea starch. By comparing to previous report, mutation at Tyr-54 in *Ta*AM resulted in the increment of cyclization activity, but decrease in hydrolysis and coupling activities (Fujii *et al*., 2005, Fujii *et al*., 2007). In addition, this mutation may help promote disproportionation activity, but not for starch transglycosylation activity. A discrepancy between these two reactions may be caused by a change in substrate affinity; decrease of affinity towards soluble starch and increased of affinity towards maltotriose (G3).

4.4.4 Substrate specificity on disproportionation activity

An affinity towards oligosaccharide substrates (G2 to G7) was observed on disproportionation activity. Maltotriose (G3) was found to be the best substrate for *Cg*AMs as indicated by Figure 36. Several publications on AMs' substrate specificity reported that G3 was the best substrate for disproportionation activity (Kaper *et al*., 2007, Srisimarat *et al*., 2012, Nimpiboon *et al*., 2016). The order of preferable substrate of E231Y *Cg*AM was G3 >> G4 > G5 > G6 ~ G7 > G2 whereas the order of the WT was G3 >> G4 > G5 > G6 > G7 ~ G2. The order of WT *Cg*AM was similar to previous study (Srisimarat *et al*., 2012) and AM from *Thermus thermophilus* HB8 (Kaper *et al*., 2007). E231Y *Cg*AM seemed to catalyze G7 substrate as well as G6 substrate. This might be due to the effect of E231Y mutation. A406V *Cg*AM in which Ala (A) at residue 406 was substituted by Val (V) showed the same pattern as E231Y *Cg*AM (Nimpiboon *et al*., 2016). When compared to the WT enzyme, A406V enzyme also displayed higher disproportionation activity as well as E231Y *Cg*AM.

4.4.5 Kinetic studies on *Cg*AM activities

Kinetic study of three activities including starch transglycosylation, disproportionation and cyclization was investigated as described in section 2.11.6. All kinetic parameters of each activity were represented in Table 7 to 9. As compared to the WT *Cg*AM, E231Y showed higher substrate affinity towards glucose (starch transglycosylation) and pea starch (cyclization) but lower affinity for maltotriose (disproportiontion). K_m value of disproportionation reaction that has been reported was closed to this study (Srisimarat *et al*., 2012, Nimpiboon *et al*., 2016). Catalytic efficiency of all three activities, however, was higher than those of the WT. These were corresponded to the increase of cyclization and disproportionation activities. As mentioned earlier, Glu-231 residue might help binding of substrate at the second glucan binding site. Thus, it could be suggested that the enhancement in their catalytic powers were from this mutation. Mutation at second substrate binding site of enzymes in α-amylase family has been reported to affect the activity of enzyme (Cockburn *et al*., 2014, Fujii *et al*., 2007, Bozonnet *et al*., 2007, Robert *et al.*, 2003).

4.4.6 Secondary structure of *Cg*AMs

In the aim to examine whether the mutation affects enzyme conformation and stability, one of the alternative approaches is to investigate the secondary structure of the enzyme by Circular dichroism (CD) technique (Louis-Jeune *et al*., 2012). CD technique can determine a rapid secondary structure composition of the enzyme. Based upon different array alignments of polypeptide backbone, the optical transition of each secondary structure is shifted or split under wavelength excitation, resulting in a

distinctive CD spectrum of each structure. If a change in structure is detected, it results in a distorted CD spectrum in comparison to the reference spectrum (Greenfield and Fasman, 1969, Greenfield, 2006). The CD spectrum and secondary structure composition (shown in Table 12) of WT *Cg*AM were nearly similar to those previously reported (Rachadech *et al*., 2015, Nimpiboon *et al*., 2016). By comparing the CD spectra of E231Y *Cg*AM to CD spectra of WT *Cg*AM, the composition of secondary protein structure is estimated by implemented K2D3 program (Louis-Jeune *et al*., 2012). The superimposition of WT and E231Y *Cg*AMs spectra was closely overlaid. Thus, changing in E231Y *Cg*AM activities such as starch transglycosylation, disproportionation and cyclization activity did not derive from the alteration of secondary structure of the enzyme. This can be concluded that a mutation at Glu (E) position 231 to Tyr (Y) has an effect on *Cg*AM characteristic.

4.6.7 The influence of incubation time and unit of enzyme on LR-CDs production

When the purified E231Y *Cg*AM was used to synthesize LR-CDs at 30°C for 6 hr inubation time, the principal LR-CDs products were CD26 to CD28. These principal LR-CDs products were drastically shifted downward to smaller size when compared to those (CD42 to CD44) synthesized from partially purified E231Y *Cg*AM. This might probably due to the unit of starch degradation activity. Because of the impurity of the enzyme used during LR-CDs synthesis, the partially purified E231 *Cg*AM fraction might contain other starch degrading enzymes. Thus, the 0.05 U of starch degradation activity was not from E231 *Cg*AM solely, but could be from another starch degrading enzyme. This led to the shift of principal LR-CDs profiles between fully and partially

purified E231Y *Cg*AMs. Besides, it could be from an experimental error, or else human error. To confirm this incident, however, the experiment must be done separately at least three times.

To investigate the effect of incubation time on LR-CDs product profile, E231Y and WT *Cg*AM carrying equal unit of starch degradation were used to synthesize LR-CDs. Both *Cg*AMs tended to produce smaller LR-CDs at longer incubation throughout the time course of synthesis. The time-dependent attribute of AM has been reported in several species (Takaha *et al*., 1998, Takaha and Smith, 1999, Terada *et al*., 1999, Srisimarat *et al*., 2012). At 1 to 12 hr incubation time, the amount of LR-CDs products produced by E231Y *Cg*AM was significantly higher than the WT enzyme. It is suggested that E231Y CgAM carries higher cyclization activity because of the mutation at Glu-231. At 24 hr, E231Y *Cg*AM carrying 0.05 U starch degradation activity yielded CD22 as the smallest principal LR-CDs product whereas CD24 was the smallest CDs of WT. It can be stated that E231Y enzyme catalyzed a faster rate in changing larger to smaller CDs. The amount of larger CDs was significantly dropped under longer incubation time. This may cause by the effect of E231Y mutation towards LR-CDs hydrolysis and coupling at longer incubation time. Previously, Srisimarat *et al* have been studied time course hydrolysis of WT *Cg*AM. It was found that LR-CDs hydrolysis was gradually increased under longer incubation time. To confirm whether these activities gave a clearly effect on LR-CDs product pattern, time course hydrolysis and coupling should be done in comparison to the WT *Cg*AM in further works. Apart from incubation time, unit of enzyme is one of the most critical parameters on LR-CDs formation. The result indicated that higher amount of enzyme used significantly shifted the principal CDs to smaller with increasing in their amounts (Figure 3.30). When

enzymes with 0.15 U were employed, E231Y *Cg*AM could produce the smallest principal CDs as CD19. It can be pointed that higher unit of enzymes relates to the increase of smaller LR-CDs product. It seemed larger LR-CDs were declined under higher enzyme concentrations. However, E231Y also catalyzed a higher conversion rate of changing larger CDs to smaller CDs. Previously, mutation at Tyr-54 of *Ta*AM resulted in the decrease of hydrolysis and coupling activities. It was noted that Tyr-54 was required to maintain those activities (Fujii *et al*., 2007). Thus, it may be possible that mutation at Glu-231 tends to increase hydrolysis and coupling activities. To explain this incident, however, time course hydrolysis and coupling are needed as well.

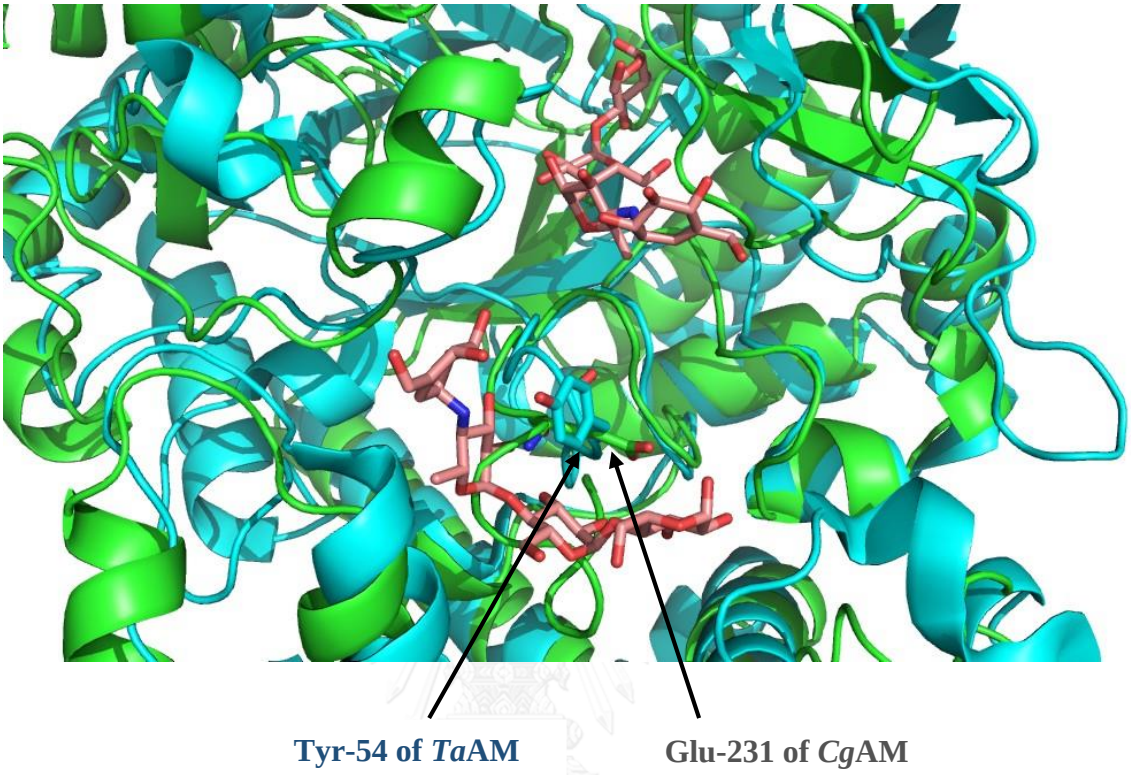

Figure 43 Superimposition of *C. glutamicum* (*Cg*AM) and *T. aquaticus* (*Ta*AM). *Cg*AM and *Ta*AM are represented in green and blue, respectively. Two bound acarboses, located in active site (upper) and second binding glucan site (lower), are shown in pink. Tyr-54 of *Ta*AM and Glu-231 of *Cg*AM are labeled. These two residues are closely superimposed and proposed to play the same role in stabilizing amylose during cycloamylose formation.

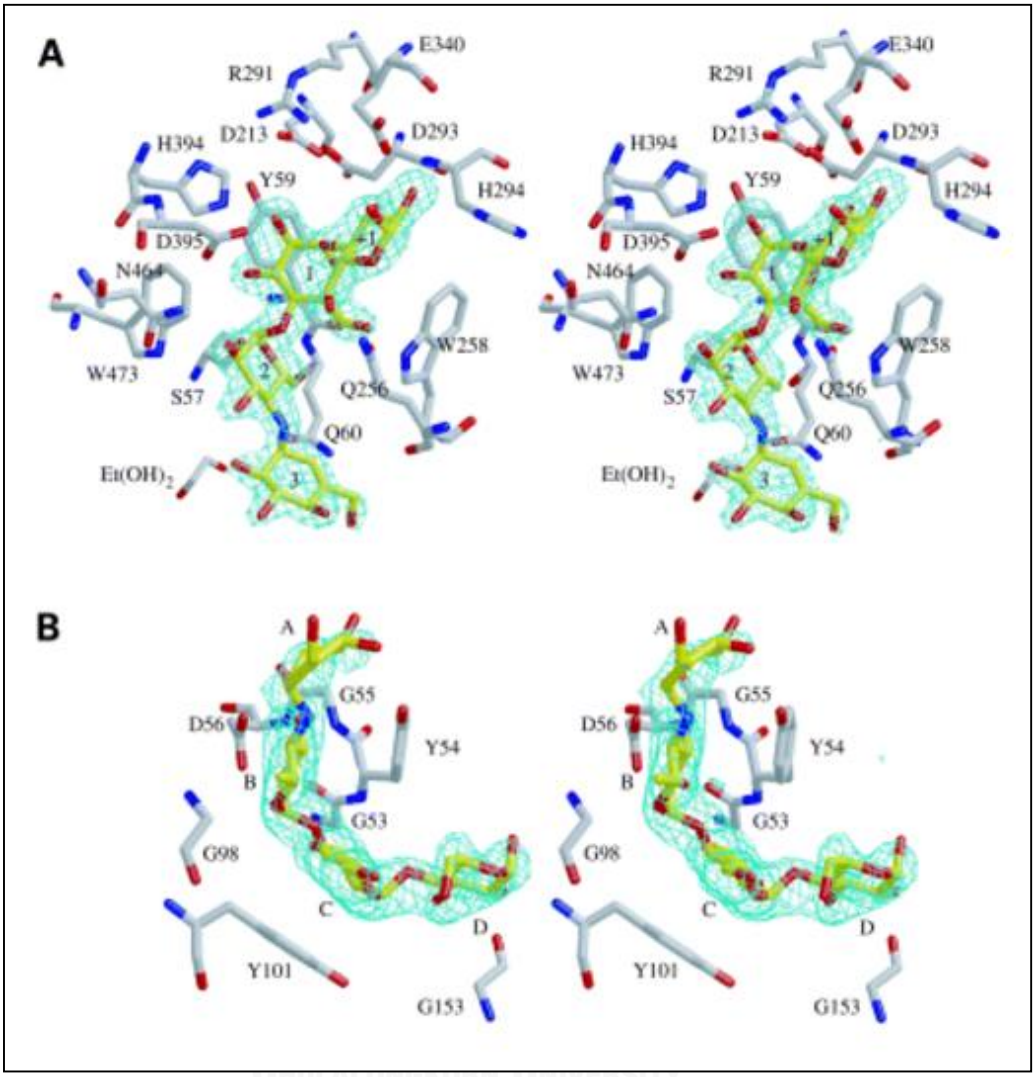

Figure 44 Stereo views of the amylomaltase–acarbose complexs (A) Acarbose bound to the active center. (B) Second acarbose molecule at second binding glucan. Tyr-54 and Tyr-101, hydrophobic residues, play a role in determining the conformation and binding of acarbose to this site. They interact with unit C of acarbose via hydrophobic interaction (Przylas *et al*., 2000a).

CHAPTER V

CONCLUSIONS

1. Screened from random mutagenesis clones, partially purified H5 and 1E5 *Cg*AM displayed an altered LR-CDs product profile from that of the WT *Cg*AM. 1E5 *Cg*AM maintained the principal CDs (CD27 to CD29) as the WT enzyme did but produced in higher amount. For H5 *Cg*AM, the principal CDs were shifted to larger CDs (CD30 to CD32 and CD34 to CD36).

2. Screened from site-directed mutagenesis clones, partially purified E231Y *Cg*AM by which amino acid residue 231 Glu (E) was substituted by Tyr (Y) displayed an altered LR-CDs product profile from that of the WT *Cg*AM. The principal CDs were shifted to CD42 to CD44. In this study, E231Y *Cg*AM was selected for further investigation.

3. The expression condition of soluble E231Y *Cg*AM was to induce with 0.4 mM IPTG at 16°C for 16 hr.

4. E231Y *Cg*AM was successfully purified by two-step purification using DEAE FF™ and Phenyl FF™ with the specific activity (starch transglycosylation) of 29.8 U/mg, 14.7 purification fold and 5.84% recovery.

5. The optimum temperatures of E231Y *Cg*AM of starch transglycosylation and disproportionation activity were 35°C and 45°C. By comparing to WT *Cg*AM, it showed the increase of 5°C for both activities. At 35°C, E231Y *Cg*AM could maintain 80% of starch transglycosylation activity up to 120 min.

6. The optimum pH of E231Y *Cg*AM of starch transglycosylation and disproportionation activity was at pH 6.5 of potassium phosphate buffer. By comparing to WT *Cg*AM, it showed the increase of 0.5 pH unit for both activities. Under this optimum pH, E231Y *Cg*AM could maintain nearly 100% of starch transglycosylation activity after pre-incubated at that pH for 1 hr.

7. E231Y *Cg*AM exhibited higher disproportionation and cyclization activity but lower starch transglycosylation activity when compared to the WT *Cg*AM. Meanwhile, starch degradation, hydrolysis and coupling activity were the same.

8. Maltotriose (G3) was found to be the best preferable substrate of both *Cg*AMs. The order was G3 >> G4 > G5 > G6 ~ G7 > G2 while WT *Cg*AM showed the order of G3 >> G4 > G5 > G6 > G7 ~ G2.

9. From overall kinetic studies, E231Y *Cg*AM showed lower substrate affiinity towards starch transglycosylation and cyclization activities. The catalytic efficiency values (k_{cat}/K_m) of E231Y *Cg*AM on starch transglycosylation, disproportionation and cyclization activities were higher than those of the WT.

10. CD analysis showed that there was no change in the secondary structure of E231Y *Cg*AM when compared to the WT *Cg*AM. The changes in *Cg*AM activities thus might cause by the effect of mutation.

11. Both higher amount of enzyme or longer incubation used during LR-CDs synthesis could significantly affect the LR-CDs product pattern by decrease the principal CDs to smaller size. A mutation at residue E231 resulted in higher rate to change the products from larger to smaller size.

12. In this study, residue E231 of *Cg*AM which was proposed to be a part of the secondary binding glucan site played a role in determining LR-CDs pattern by improving the cyclization activity.

REFERENCES

BARENDS, T. R., BULTEMA, J. B., KAPER, T., VAN DER MAAREL, M. J., DIJKHUIZEN, L. & DIJKSTRA, B. W. 2007. Three-way stabilization of the covalent intermediate in amylomaltase, an alpha-amylase-like transglycosylase. *The Journal of Biological Chemistry,* 282, 17242-9.

BERTOFT, E. 2015. Fine Structure of Amylopectin. *In:* NAKAMURA, Y. (ed.) *Starch: Metabolism and Structure.* Tokyo: Springer Japan.

BOZONNET, S., JENSEN, M. T., NIELSEN, M. M., AGHAJARI, N., JENSEN, M. H., KRAMHOFT, B., WILLEMOES, M., TRANIER, S., HASER, R. & SVENSSON, B. 2007. The 'pair of sugar tongs' site on the non-catalytic domain C of barley alpha-amylase participates in substrate binding and activity. *The FEBS Journal,* 274, 5055-67.

COCKBURN, D., WILKENS, C., RUZANSKI, C., ANDERSEN, S., WILLUM NIELSEN, J., SMITH, A. M., FIELD, R. A., WILLEMOëS, M., ABOU HACHEM, M. & SVENSSON, B. 2014. Analysis of surface binding sites (SBSs) in carbohydrate active enzymes with focus on glycoside hydrolase families 13 and 77 — a mini-review. *Biologia Plantarum,* 69, 705-712.

DANIEL, R. M. & DANSON, M. J. 2010. A new understanding of how temperature affects the catalytic activity of enzymes. *Trends in Biochemical Sciences,* 35, 584-591.

DANIEL, R. M. & DANSON, M. J. 2013. Temperature and the catalytic activity of enzymes: A fresh understanding. *FEBS Letters,* 587, 2738-2743.

DECKERT, G., WARREN, P. V., GAASTERLAND, T., YOUNG, W. G., LENOX, A. L., GRAHAM, D. E., OVERBEEK, R., SNEAD, M. A., KELLER, M., AUJAY, M., HUBER, R., FELDMAN, R. A., SHORT, J. M., OLSEN, G. J. & SWANSON, R. V. 1998. The complete genome of the hyperthermophilic bacterium *Aquifex aeolicus*. *Nature*, 392, 353-358.

DIPPEL, R. & BOOS, W. 2005. The maltodextrin system of *Escherichia coli*: metabolism and transport. *Journal of Bacteriology*, 187, 8322-31.

ENDO, T., UEDA, H., KOBAYASHI, S. & NAGAI, T. 1995. Isolation, purification, and characterization of cyclomaltododecaose (ν-cyclodextrin). *Carbohydrate Research*, 269, 369-373.

ESPOSITO, D. & CHATTERJEE, D. K. 2006. Enhancement of soluble protein expression through the use of fusion tags. *Current Opinion in Biotechnology*, 17, 353-8.

FERNANDEZ, A., CHEN, J. & CRESPO, A. 2007. Solvent-exposed backbone loosens the hydration shell of soluble folded proteins. *The Journal of Chemical Physics*, 126, 245103.

FLEISCHMANN, R. D., ADAMS, M. D., WHITE, O., CLAYTON, R. A., KIRKNESS, E. F., KERLAVAGE, A. R., BULT, C. J., TOMB, J. F., DOUGHERTY, B. A., MERRICK, J. M. & ET AL. 1995. Whole-genome random sequencing and assembly of *Haemophilus influenzae* Rd. *Science*, 269, 496-512.

FUJII, K., MINAGAWA, H., TERADA, Y., TAKAHA, T., KURIKI, T., SHIMADA, J. & KANEKO, H. 2005. Use of Random and Saturation Mutageneses To Improve the Properties of *Thermus aquaticus* Amylomaltase for Efficient Production of Cycloamyloses. *Applied and Environmental Microbiology,* 71, 5823-7.

FUJII, K., MINAGAWA, H., TERADA, Y., TAKAHA, T., KURIKI, T., SHIMADA, J. & KANEKO, H. 2007. Function of second glucan binding site including tyrosines 54 and 101 in *Thermus aquaticus* amylomaltase. *Journal of Bioscience and Bioengineering,* 103, 167-73.

GODA, S. K., EISSA, O., AKHTAR, M. & MINTON, N. P. 1997. Molecular analysis of a *Clostridium butyricum* NCIMB 7423 gene encoding 4-alpha-glucanotransferase and characterization of the recombinant enzyme produced in *Escherichia coli*. *Microbiology,* 143 (Pt 10), 3287-94.

GREENFIELD, N. & FASMAN, G. D. 1969. Computed circular dichroism spectra for the evaluation of protein conformation. *Biochemistry,* 8, 4108-16.

GREENFIELD, N. J. 2006. Using circular dichroism spectra to estimate protein secondary structure. *Nature Protocols,* 1, 2876-90.

HAGA, K., KANAI, R., SAKAMOTO, O., AOYAGI, M., HARATA, K. & YAMANE, K. 2003. Effects of essential carbohydrate/aromatic stacking interaction with Tyr100 and Phe259 on substrate binding of cyclodextrin glycosyltransferase from alkalophilic *Bacillus* sp. 1011. *The Journal of Biochemistry,* 134, 881-91.

HANSEN, M. R., BLENNOW, A., PEDERSEN, S. & ENGELSEN, S. B. 2009. Enzyme modification of starch with amylomaltase results in increasing gel melting point. *Carbohydrate Polymers,* 78, 72-79.

HENRISSAT, B. 1991. A classification of glycosyl hydrolases based on amino acid sequence similarities. *Biochemical Journal,* 280 (Pt 2), 309-16.

HENRISSAT, B., CALLEBAUT, I., FABREGA, S., LEHN, P., MORNON, J. P. & DAVIES, G. 1995. Conserved catalytic machinery and the prediction of a common fold for several families of glycosyl hydrolases. *Proceedings of the National Academy of Sciences of the United States of America,* 92, 7090-4.

HILBERT, G. E. & MAC, M. M. 1946. Pea starch, a starch of high amylose content. *The Journal of Biological Chemistry,* 162, 229-38.

HORVATHOVA, V., JANECEK, S. & STURDIK, E. 2001. Amylolytic enzymes: molecular aspects of their properties. *General Physiology and Biophysics,* 20, 7-32.

HWANG, S., CHOI, K. H., KIM, J. & CHA, J. 2013. Biochemical characterization of 4-alpha-glucanotransferase from Saccharophagus degradans 2-40 and its potential role in glycogen degradation. *FEMS Microbiology Letters,* 344, 145-51.

IVANOV, P. M. & JAIME, C. 2004. Insights into the Structure of Large-Ring Cyclodextrins through Molecular Dynamics Simulations in Solution. *The Journal of Physical Chemistry B,* 108, 6261-74.

JESPERSEN, H. M., MACGREGOR, E. A., HENRISSAT, B., SIERKS, M. R. & SVENSSON, B. 1993. Starch- and glycogen-debranching and branching enzymes: prediction of structural features of the catalytic (beta/alpha)8-barrel domain and evolutionary relationship to other amylolytic enzymes. *Journal of Protein Chemistry,* 12, 791-805.

JUNG, J. H., JUNG, T. Y., SEO, D. H., YOON, S. M., CHOI, H. C., PARK, B. C., PARK, C. S. & WOO, E. J. 2011. Structural and functional analysis of substrate recognition by the 250s loop in amylomaltase from *Thermus brockianus*. *Proteins,* 79, 633-44.

KAEWPATHOMSRI, P., TAKAHASHI, Y., NAKAMURA, S., KAULPIBOON, J., KIDOKORO, S.-I., MURAKAMI, S., KRUSONG, K. & PONGSAWASDI, P. 2015. Characterization of amylomaltase from *Thermus filiformis* and the increase in alkaline and thermo-stability by E27R substitution. *Process Biochemistry,* 50, 1814-1824.

KAPER, T., LEEMHUIS, H., UITDEHAAG, J. C., VAN DER VEEN, B. A., DIJKSTRA, B. W., VAN DER MAAREL, M. J. & DIJKHUIZEN, L. 2007. Identification of acceptor substrate binding subsites +2 and +3 in the amylomaltase from *Thermus thermophilus* HB8. *Biochemistry,* 46, 5261-9.

KAPER, T., TALIK, B., ETTEMA, T. J., BOS, H., VAN DER MAAREL, M. J. & DIJKHUIZEN, L. 2005. Amylomaltase of *Pyrobaculum aerophilum* IM2 produces thermoreversible starch gels. *Applied and Environmental Microbiology*, 71, 5098-106.

KAPER, T., VAN DER MAAREL, M. J., EUVERINK, G. J. & DIJKHUIZEN, L. 2004. Exploring and exploiting starch-modifying amylomaltases from thermophiles. *Biochemical Society Transactions,* 32, 279-82.

KEELING, P. L. & MYERS, A. M. 2010. Biochemistry and genetics of starch synthesis. *Annual Review of Food Science and Technology,* 1, 271-303.

KOBAYASHI, S. 1993. Fundamental Study and Application of Cyclodextrins. *Journal of the Japanese Society of Starch Science,* 40, 103-116.

KOIZUMI, K., SANBE, H., KUBOTA, Y., TERADA, Y. & TAKAHA, T. 1999. Isolation and characterization of cyclic alpha-(1-->4)-glucans having degrees of polymerization 9-31 and their quantitative analysis by high-performance anion-exchange chromatography with pulsed amperometric detection. *Journal of Chromatography A,* 852, 407-16.

KORNACKER, M. G., BOYD, A., PUGSLEY, A. P. & PLASTOW, G. S. 1989. A new regulatory locus of the maltose regulon in *Klebsiella pneumoniae* strain K21 identified by the study of pullulanase secretion mutants. *Journal of General Microbiology* 135, 397-408.

KURIKI, T. & IMANAKA, T. 1999. The concept of the alpha-amylase family: structural similarity and common catalytic mechanism. *Journal of Bioscience and Bioengineering,* 87, 557-65.

LARSEN, K. L. 2002. Large Cyclodextrins. *Journal of Inclusion Phenomena and Macrocyclic Chemistry,* 43, 1-13.

LOUIS-JEUNE, C., ANDRADE-NAVARRO, M. A. & PEREZ-IRATXETA, C. 2012. Prediction of protein secondary structure from circular dichroism using theoretically derived spectra. *Proteins,* 80, 374-81.

LU, Y. & SHARKEY, T. D. 2004. The role of amylomaltase in maltose metabolism in the cytosol of photosynthetic cells. *Planta,* 218, 466-73.

MACHIDA, S., OGAWA, S., XIAOHUA, S., TAKAHA, T., FUJII, K. & HAYASHI, K. 2000. Cycloamylose as an efficient artificial chaperone for protein refolding. *FEBS Letters,* 486, 131-5.

MELZER, S., SONNENDECKER, C., FOLLNER, C. & ZIMMERMANN, W. 2015. Stepwise error-prone PCR and DNA shuffling changed the pH activity range and product specificity of the cyclodextrin glucanotransferase from an alkaliphilic *Bacillus* sp. *FEBS Open Bio,* 5, 528-34.

MIYAZAWA, I., UEDA, H., NAGASE, H., ENDO, T., KOBAYASHI, S. & NAGAI, T. 1995. Physicochemical properties and inclusion complex formation of δ-cyclodextrin. *European Journal of Pharmaceutical Sciences,* 3, 153-162.

MONOD, J. & TORRIANI, A. M. 1950. [Amylomaltase of *Escherichia coli*]. *Annales de L'Institut Pasteur,* 78, 65-77.

MORA, M. M. M., SáNCHEZ, K. H., SANTANA, R. V., ROJAS, A. P., RAMíREZ, H. L. & TORRES-LABANDEIRA, J. J. 2012. Partial purification and properties of cyclodextrin glycosiltransferase (CGTase) from alkalophilic *Bacillus* species. *SpringerPlus,* 1, 61.

NAKAMURA, A., HAGA, K. & YAMANE, K. 1994. Four aromatic residues in the active center of cyclodextrin glucanotransferase from alkalophilic *Bacillus* sp. 1011: effects of replacements on substrate binding and cyclization characteristics. *Biochemistry,* 33, 9929-36.

NIETO, C., ESPINOSA, M. & PUYET, A. 1997. The maltose/maltodextrin regulon of *Streptococcus pneumoniae*. Differential promoter regulation by the transcriptional repressor MalR. *The Journal of Biological Chemistry,* 272, 30860-5.

NIMPIBOON, P., KAULPIBOON, J., KRUSONG, K., NAKAMURA, S., KIDOKORO, S. & PONGSAWASDI, P. 2016. Mutagenesis for improvement of activity and thermostability of amylomaltase from *Corynebacterium glutamicum*. *International Journal of Biological Macromolecules,* 86, 820-8.

NORISUYE, T. 1994. Viscosity Behavior and Conformation of Amylose in Various Solvents. *Polym J,* 26, 1303-1307.

PALMER, T. N., RYMAN, B. E. & WHELAN, W. J. 1976. The action pattern of amylomaltase from *Escherichia coli*. *European Journal of Biochemistry,* 69, 105-15.

PENNINGA, D., STROKOPYTOV, B., ROZEBOOM, H. J., LAWSON, C. L., DIJKSTRA, B. W., BERGSMA, J. & DIJKHUIZEN, L. 1995. Site-directed mutations in tyrosine 195 of cyclodextrin glycosyltransferase from *Bacillus circulans* strain 251 affect activity and product specificity. *Biochemistry,* 34, 3368-76.

PRITCHARD, L., CORNE, D., KELL, D., ROWLAND, J. & WINSON, M. 2005. A general model of error-prone PCR. *Journal of Theoretical Biology,* 234, 497-509.

PRZYLAS, I., TERADA, Y., FUJII, K., TAKAHA, T., SAENGER, W. & STRATER, N. 2000a. X-ray structure of acarbose bound to amylomaltase from *Thermus aquaticus*. Implications for the synthesis of large cyclic glucans. *European Journal of Biochemistry,* 267, 6903-13.

PRZYLAS, I., TOMOO, K., TERADA, Y., TAKAHA, T., FUJII, K., SAENGER, W. & STRATER, N. 2000b. Crystal structure of amylomaltase from *thermus aquaticus*, a glycosyltransferase catalysing the production of large cyclic glucans. *Journal of Molecular Biology*, 296, 873-86.

PUGSLEY, A. P. & DUBREUIL, C. 1988. Molecular characterization of malQ, the structural gene for the *Escherichia coli* enzyme amylomaltase. *Molecular Microbiology*, 2, 473-9.

RACHADECH, W., NIMPIBOON, P., NAUMTHONG, W., NAKAPONG, S., KRUSONG, K. & PONGSAWASDI, P. 2015. Identification of essential tryptophan in amylomaltase from *Corynebacterium glutamicum*. *International Journal of Biological Macromolecules*, 76, 230-5.

ROBERT, X., HASER, R., GOTTSCHALK, T. E., RATAJCZAK, F., DRIGUEZ, H., SVENSSON, B. & AGHAJARI, N. 2003. The structure of barley alpha-amylase isozyme 1 reveals a novel role of domain C in substrate recognition and binding: a pair of sugar tongs. *Structure*, 11, 973-84.

SASAKI, Y. & AKIYOSHI, K. 2010. Development of an artificial chaperone system based on cyclodextrin. *Current Pharmaceutical Biotechnology*, 11, 300-5.

SINGH, A., UPADHYAY, V., UPADHYAY, A. K., SINGH, S. M. & PANDA, A. K. 2015. Protein recovery from inclusion bodies of *Escherichia coli* using mild solubilization process. *Microbial Cell Factories*, 14.

SOLS, A. & DE LA FUENTE, G. 1957. [Glucose oxidase as an analytic reagent]. *Revista Española de Fisiología*, 13, 231-45.

SOLS, A. & DE LA FUENTE, G. 1958. [Glucose oxidase analysis]. *Laboratorio*, 25, 15-30.

SRISIMARAT, W., KAULPIBOON, J., KRUSONG, K., ZIMMERMANN, W. & PONGSAWASDI, P. 2012. Altered large-ring cyclodextrin product profile due to a mutation at Tyr-172 in the amylomaltase of *Corynebacterium glutamicum*. *Applied and Environmental Microbiology,* 78, 7223-8.

SRISIMARAT, W., MURAKAMI, S., PONGSAWASDI, P. & KRUSONG, K. 2013. Crystallization and preliminary X-ray crystallographic analysis of the amylomaltase from *Corynebacterium glutamicum*. *Acta Crystallographica. Section F, Structural Biology Communications,* 69, 1004-6.

SRISIMARAT, W., POWVIRIYAKUL, A., KAULPIBOON, J., KRUSONG, K., ZIMMERMANN, W. & PONGSAWASDI, P. 2011. A novel amylomaltase from *Corynebacterium glutamicum* and analysis of the large-ring cyclodextrin products. *Journal of Inclusion Phenomena and Macrocyclic Chemistry,* 70, 369-375.

STRANDBERG, L. & ENFORS, S. O. 1991. Factors influencing inclusion body formation in the production of a fused protein in *Escherichia coli*. *Applied and Environmental Microbiology,* 57, 1669-74.

TAIRA, H., NAGASE, H., ENDO, T. & UEDA, H. 2006. Isolation, Purification and Characterization of Large-Ring Cyclodextrins (CD36~~CD39). *Journal of Inclusion Phenomena and Macrocyclic Chemistry,* 56, 23-28.

TAKAHA, T. & SMITH, S. M. 1999. The functions of 4-alpha-glucanotransferases and their use for the production of cyclic glucans. *Biotechnology & Genetic Engineering Reviews,* 16, 257-80.

TAKAHA, T., YANASE, M., TAKATA, H., OKADA, S. & SMITH, S. M. 1998. Cyclic glucans produced by the intramolecular transglycosylation activity of potato D-enzyme on amylopectin. *Biochemical and Biophysical Research Communications,* 247, 493-7.

TANTANARAT, K., O'NEILL, E. C., REJZEK, M., FIELD, R. A. & LIMPASENI, T. 2014. Expression and characterization of 4-α-glucanotransferase genes from *Manihot esculenta* Crantz and *Arabidopsis thaliana* and their use for the production of cycloamyloses. *Process Biochemistry,* 49, 84-89.

TERADA, Y., FUJII, K., TAKAHA, T. & OKADA, S. 1999. *Thermus aquaticus* ATCC 33923 Amylomaltase Gene Cloning and Expression and Enzyme Characterization: Production of Cycloamylose. *Applied and Environmental Microbiology,* 65, 910-5.

TERADA, Y., YANASE, M., TAKATA, H., TAKAHA, T. & OKADA, S. 1997. Cyclodextrins are not the major cyclic alpha-1,4-glucans produced by the initial action of cyclodextrin glucanotransferase on amylose. *The Journal of Biological Chemistry,* 272, 15729-33.

TOMONO, K., MUGISHIMA, A., SUZUKI, T., GOTO, H., UEDA, H., NAGAI, T. & WATANABE, J. 2002. Interaction between Cycloamylose and Various Drugs. *Journal of Inclusion Phenomena and Macrocyclic Chemistry,* 44, 267-270.

UITDEHAAG, J. C., KALK, K. H., VAN DER VEEN, B. A., DIJKHUIZEN, L. & DIJKSTRA, B. W. 1999. The cyclization mechanism of cyclodextrin glycosyltransferase (CGTase) as revealed by a gamma-cyclodextrin-CGTase complex at 1.8-A resolution. *The Journal of Biological Chemistry,* 274, 34868-76.

VAN DER MAAREL, M. J., VAN DER VEEN, B., UITDEHAAG, J. C., LEEMHUIS, H. & DIJKHUIZEN, L. 2002. Properties and applications of starch-converting enzymes of the alpha-amylase family. *Journal of Biotechnology,* 94, 137-55.

VAN DER VEEN, B. A., VAN ALEBEEK, G. J., UITDEHAAG, J. C., DIJKSTRA, B. W. & DIJKHUIZEN, L. 2000. The three transglycosylation reactions catalyzed by cyclodextrin glycosyltransferase from *Bacillus circulans* (strain 251) proceed via different kinetic mechanisms. *European Journal of Biochemistry,* 267, 658-65.

VILAPLANA, F., HASJIM, J. & GILBERT, R. G. 2012. Amylose content in starches: Toward optimal definition and validating experimental methods. *Carbohydrate Polymers,* 88, 103-111.

VONGPICHAYAPAIBOON, T., PONGSAWASDI, P. & KRUSONG, K. 2016. Optimization of large-ring cyclodextrin production from starch by amylomaltase from *Corynebacterium glutamicum* and effect of organic solvent on product size. *Journal of Applied Microbiology,* 120, 912-20.

WALKER, G. J. & WHELAN, W. J. 1959. Synthesis of Amylose by Potato D-Enzyme. *Nature,* 183, 46-46.

WATANASATITARPA, S., RUDEEKULTHAMRONG, P., KRUSONG, K., SRISIMARAT, W., ZIMMERMANN, W., PONGSAWASDI, P. & KAULPIBOON, J. 2014. Molecular mutagenesis at Tyr-101 of the amylomaltase transcribed from a gene isolated from soil DNA. *Prikl Biokhim Mikrobiol,* 50, 273-82.

XAVIER, K. B., PEIST, R., KOSSMANN, M., BOOS, W. & SANTOS, H. 1999. Maltose metabolism in the hyperthermophilic archaeon *Thermococcus litoralis*: purification and characterization of key enzymes. *Journal of Bacteriology,* 181, 3358-67.

ZHENG, M., ENDO, T. & ZIMMERMANN, W. 2002a. Enzymatic Synthesis and Analysis of Large-Ring Cyclodextrins. *Australian Journal of Chemistry,* 55, 39-48.

ZHENG, M., ENDO, T. & ZIMMERMANN, W. 2002b. Synthesis of Large-Ring Cyclodextrins by Cyclodextrin Glucanotransferases from Bacterial Isolates. *Journal of Inclusion Phenomena and Macrocyclic Chemistry,* 44, 387-390.

APPENDICES

APPENDIX 1

Preparation of SDS-polyacrylamide gel electrophoresis (SDS-PAGE)

1) Stock reagents

2 M Tris-HCl pH 8.8

Tris (Hydroxymethyl)-aminomethane 24.2 g

Adjusted pH to 8.8 with 1 NHCl and adjusted volume to 100 ml with distilled water

1 M Tris-HCl pH 6.8

Tris (Hydroxymethyl)-aminomethane 12.1 g

Adjusted pH to 6.8 with 1 NHCl and adjusted volume to 100 ml with distilled water

10% (w/v) SDS

Sodium dodecyl sulfate 10 g

Adjusted volume to 100 ml with distilled water

50% (v/v) glycerol

100% glycerol 50 ml

Adjusted volume to 100 ml by adding 50 ml of distilled water

1% (w/v) bromophenol blue

Bromophenol blue 100 mg

Adding 10 ml of distilled water and stir the solution overnight. The solution was filtered to remove aggregated dye prior to use

2) Working solutions

Solution A

30% acrylamide, 0.8% bis-acrylamide, 100 ml

Acrylamide	29.2 g
N,N'-methylene-bis-acrylamide	0.8 g

Adjusted volume to 100 ml with distilled water

Solution B

4x separating gel buffer

2 M Tris-HCl pH 8.8	75 ml
10% SDS	4 ml
Distilled water	21 ml

Solution C

4x stacking gel buffer

1 M Tris-HCl pH 6.8	50 ml
10% SDS	4 ml
Distilled water	46 ml

10% ammonium persulfate (APS)

Ammonium persulfate	0.5 g
Distilled water	5 ml

Electrophoresis buffer

Tris (Hydroxymethyl)-aminomethane	3 g
Glycine	14.4 g
Sodium dodecyl sulfate	1 g

Adjusted volume to 1 litre with distilled water

5x sample buffer

1 M Tris-HCl pH 6.8	0.6 ml
50% glycerol	5 ml
10% SDS	2 ml
2-β-mercaptoethanol	0.5 ml
1% bromophenol blue	1 ml
Distilled water	0.9 ml

Coomassie gel staining solution

Coomassie blue R-250	1 g
Methanol	450 ml
Distilled water	450 ml
Glacial acetic acid	100 ml

Coomassie gel destaining solution

Methanol	100 ml
Glacial acetic acid	100 ml
Distilled water	800 ml

APPENDIX 2

Preparation of buffer for crude enzyme preparation

1) Stock solution

0.5 M potassium phosphate buffer pH 7.4

Component 1

0.5 M dipotassium hydrogen phosphate

Dipotassium hydrogen phosphate	26.127	g

Adjusted volume to 300 ml with distilled water

Component 2

0.5 M potassium dihydrogen phosphate

Potassium dihydrogen phosphate	6.814	g

Adjusted volume to 100 ml with distilled water

Component 2 was added to component 1 until the pH of the solution was 7.4

2) Extraction buffer

0.5 M potassium phosphate buffer	50	ml
0.1 mM PMSF in absolute ethanol	100	µl
2-β-mercaptoethanol	20	µl
0.5 M EDTA	50	µl

Adjusted the volume to 500 ml with distilled water

3) 0.85% (w/v) NaCl

Sodium chloride	0.85	g

Adjusted the volume to 100 ml with distilled water

APPENDIX 3

Preparation of purification buffer

1) Buffer for DEAE FF™ column purification

50 mM phosphate buffer pH 7.4

0.5 M phosphate buffer pH 7.4	50	ml
2-β-mercaptoethanol	50	µl
Adjusted the volume to 500 ml with distilled water		

50 mM phosphate buffer pH 7.4 with 1 M NaCl

0.5 M phosphate buffer pH 7.4	50	ml
2-β-mercaptoethanol	50	µl
Sodium chloride	29.22	g
Adjusted the volume to 500 ml with distilled water		

2) Buffer for Phenyl FF™ column purification

50 mM phosphate buffer pH 7.4

0.5 M phosphate buffer pH 7.4	50	ml
2-β-mercaptoethanol	50	µl
Adjusted the volume to 500 ml with distilled water		

50 mM phosphate buffer pH 7.4 with 1 M $(NH_4)_2SO_4$

0.5 M phosphate buffer pH 7.4	50	ml
2-β-mercaptoethanol	50	µl
Ammonium sulfate	66.07	g

Adjusted the volume to 500 ml with distilled water

APPENDIX 4

Preparation of iodine solution

10x stock solution

0.2% (w/v) I_2 in 2.0% (w/v) KI

Potassium iodide	2	g
Iodine	0.2	g

Adjusted volume to 100 ml with distilled water and stir the solution overnight prior to use

1x iodine solution

0.2% (w/v) I_2 in 2.0% (w/v) KI	10	ml
Distilled water	90	ml

APPENDIX 5

Preparation of Bradford's solution

1) Stock solution

Ethanol	100	ml
Phosphoric acid	200	ml
Coomassie blue G-250	350	mg

2) Working solution

Ethanol	15	ml
Phosphoric acid	30	ml
Stock solution	30	ml
Distilled water	425	ml

Filtered through Whatman paper No.1 prior to use.

APPENDIX 6

Preparation of bicinchoninic acid reagent

Solution A

4,4'-dicarboxy-2,2'-biquinoline	0.1302	g
Dissolved in 85 ml of distilled water		
$NaCO_3$	6.2211	g
Adjusted to 100 ml with distilled water		

Solution B

Component 1

L-aspartic acid	0.642	g
$NaCO_3$	0.8681	g
Dissolved in 15 ml of distilled water		

Component 2

$CuSO_4$	0.1736	g
Dissolved in 5 ml of distilled water		

Component 1 and 2 were mixed and adjusted the volume to 25 ml with distilled water

*In the assay, 24 ml of Solution A was mixed with 1 ml of solution B prior to use

APPENDIX 7

Preparation of DNS reagent

DNS reagent

2-hydroxyy-3,5-dinitrobenzoic acid	5	g
2 N NaOH	100	ml
Potassium sodium tartrate	150	g

Adjusted volume to 500 ml with distilled water

APPENDIX 8

Restriction map of pET-17b vector

pET-17b sequence landmarks	
T7 promoter	333-349
T7 transcription start	332
T7•Tag coding sequence	237-269
Multiple cloning sites	
(*Hin*d III - *Xho* I)	141-228
T7 terminator	28-74
pBR322 origin	1480
bla coding sequence	2241-3098

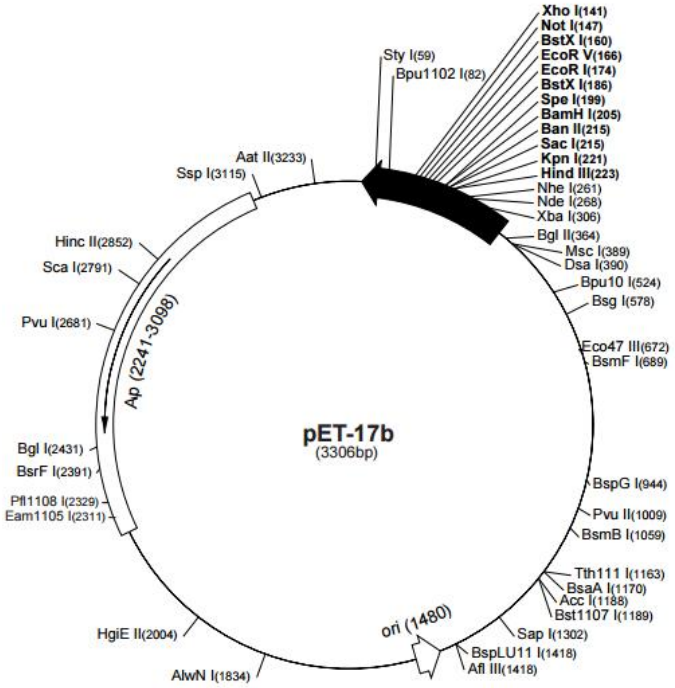

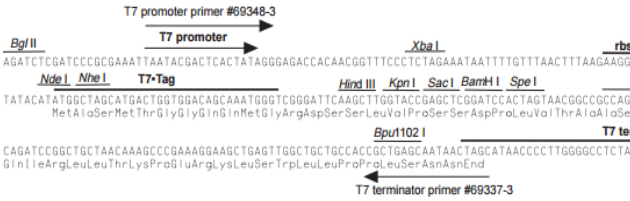

pET-17b cloning/expression region

APPENDIX 9

Standard curve for protein determination by Bradford's assay

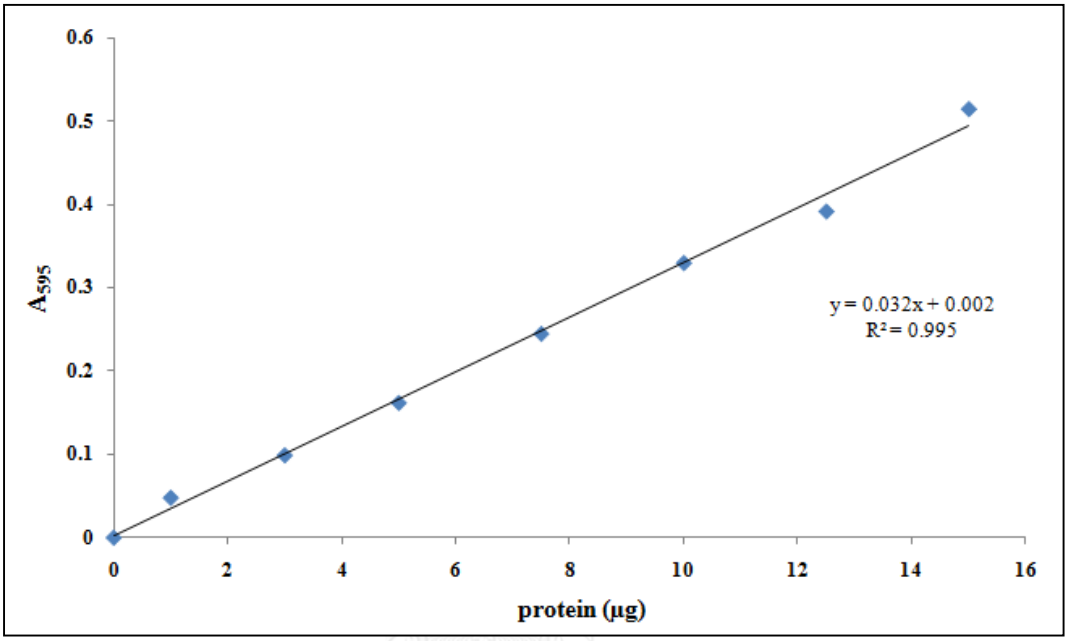

APPENDIX 10

Standard curve for starch degradation activity assay

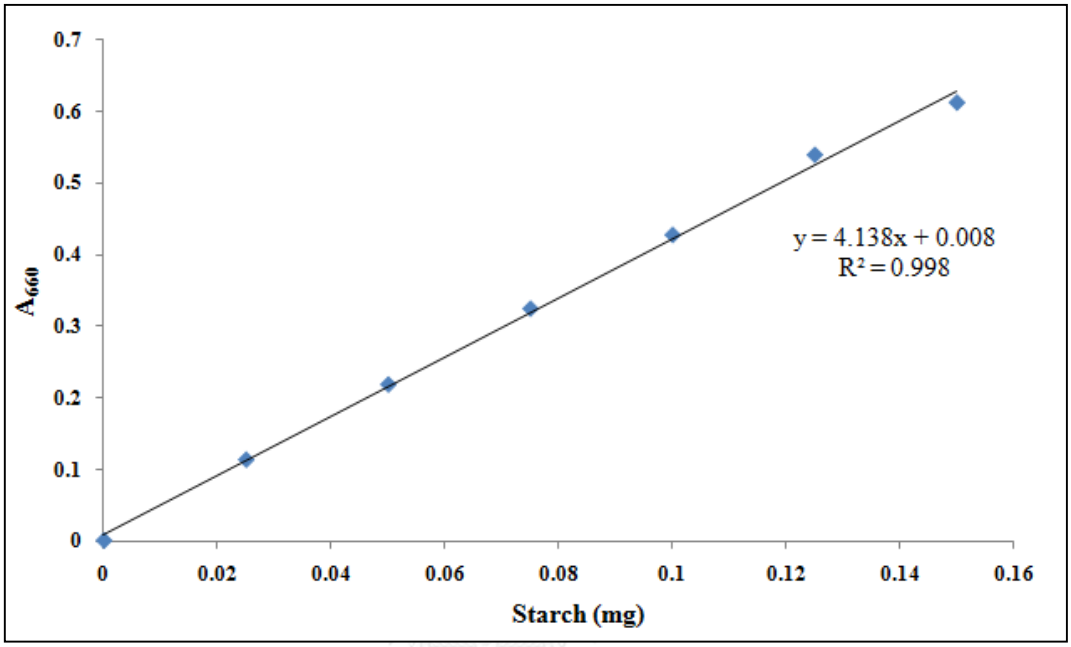

APPENDIX 11

Standard curve for glucose determination by glucose oxidase assay

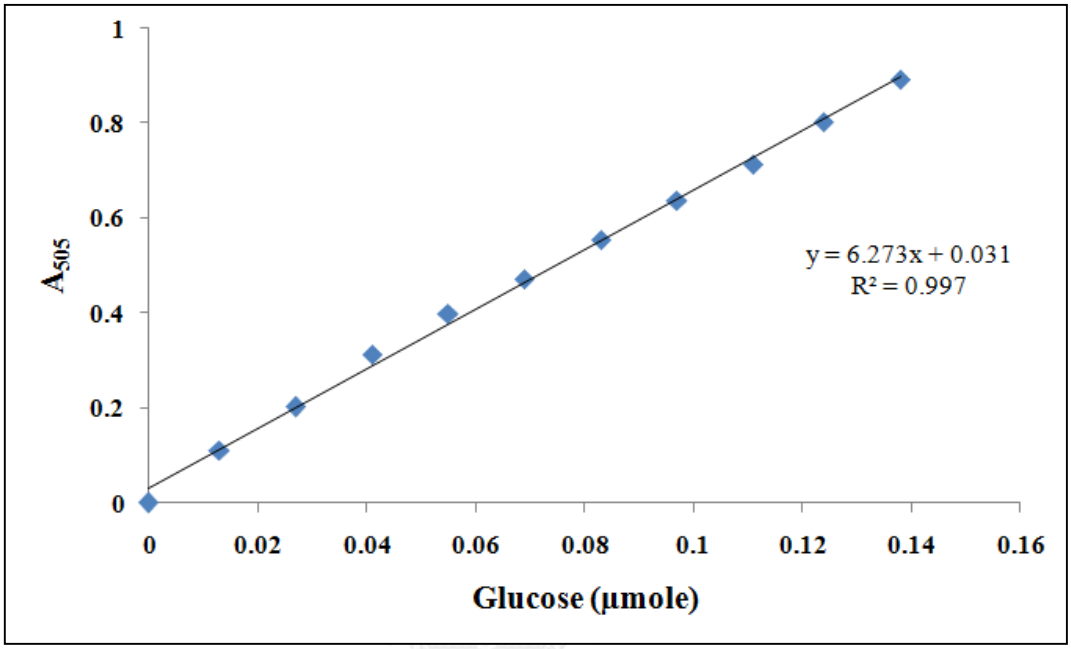

APPENDIX 12

Standard curve for glucose determination by bicinchoninic acid assay

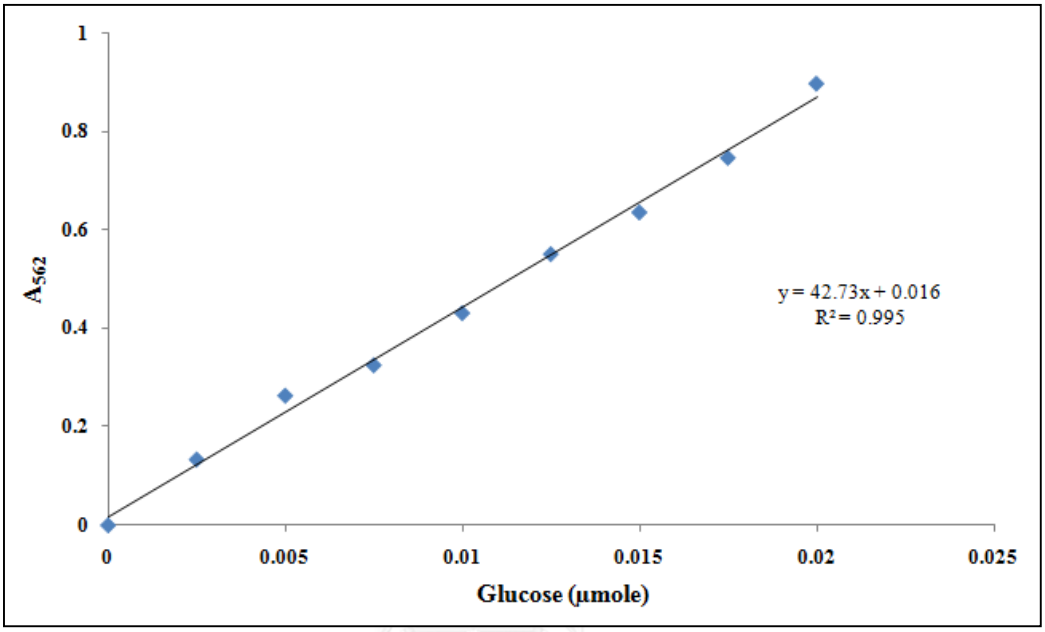

APPENDIX 13

Abbreviations (three letters and one letter) of amino acid residues found in protein

Alanine	Ala	A	Leucine	Leu	L
Arginine	Arg	R	Lysine	Lys	K
Asparagine	Asn	N	Methionine	Met	M
Aspartate	Asp	D	Phenylalanine	Phe	F
Cysteine	Cys	C	Proline	Pro	P
Glutamic acid	Glu	E	Serine	Ser	S
Glutamine	Gln	Q	Threonine	Thr	T
Glycine	Gly	G	Tryptophan	Trp	W
Histidine	His	H	Tyrosine	Tyr	Y
Isoleucine	Ile	I	Valine	Val	V

APPENDIX 14

Example of typical HPAEC profile

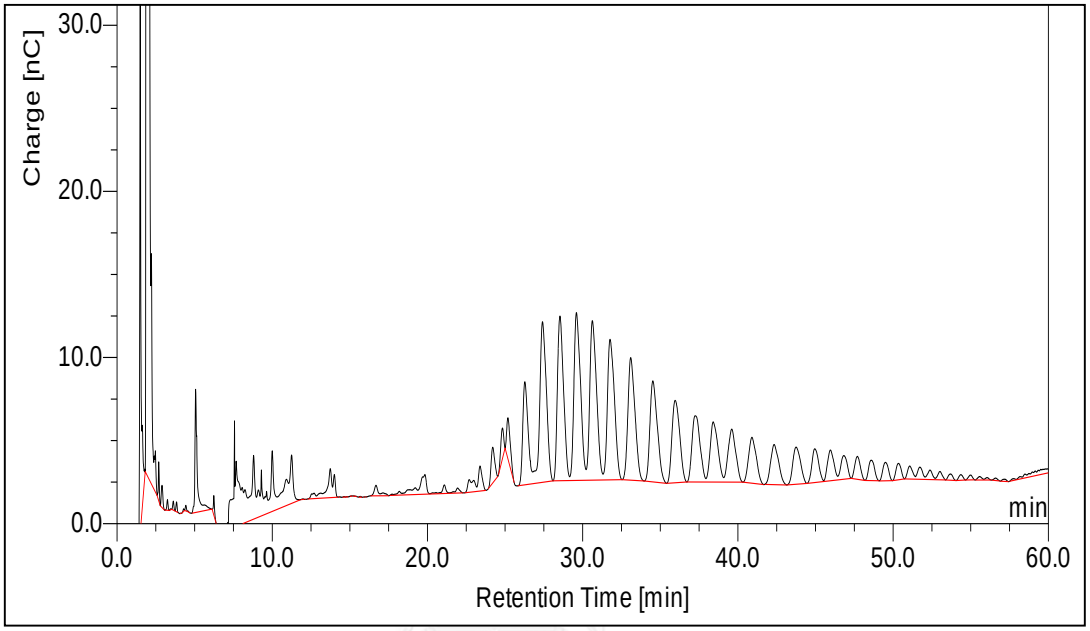

*each peak represents different CD size

VITA

Mr. Thanarat Pathomsoonthornchai was born on February 27th, 1990. He graduated with the Bachelor's degree from the Department of Biochemistry, Faculty of Science, Chulalongkorn University in 2009. Then, he continued studying Master degree in Biochemistry and Molecular Biology program, Faculty of Science at Chulalongkorn University.

He attended the 26th Annual Meeting of the Thai Society for Biotechnology and International Conference (TSB2014) at Mae Fah Luang University (School of Science) and his proceeding was published in the title of 'Screening for Corynebacterium glutamicum Amylomaltase Mutant to Altered Large-ring Cyclodextrin Production Profiles'. He also joined the 8th Asian Cyclodextrin Conference, held at Chulalongkorn University, for which the 2nd rank prize was awarded to him.